



REVIEW

Function, mechanism and drug discovery of ubiquitin and ubiquitin-like modification with multiomics profiling for cancer therapy



Yanyu Jiang[†], Shuaishuai Ni[†], Biying Xiao, Lijun Jia*

Cancer Institute, Longhua Hospital, Shanghai University of Traditional Chinese Medicine, Shanghai 200032, China

Received 16 January 2023; received in revised form 21 May 2023; accepted 17 July 2023

KEY WORDS

Ub and Ubl modifications;
Ub-activating enzyme;
Ub-conjugating enzyme;
Ub ligase;
Multiomics analyses;
Drug discovery;
Small molecule inhibitor;
Molecular glue

Abstract Ubiquitin (Ub) and ubiquitin-like (Ubl) pathways are critical post-translational modifications that determine whether functional proteins are degraded or activated/inactivated. To date, >600 associated enzymes have been reported that comprise a hierarchical task network (*e.g.*, E1–E2–E3 cascade enzymatic reaction and deubiquitination) to modulate substrates, including enormous oncoproteins and tumor-suppressive proteins. Several strategies, such as classical biochemical approaches, multiomics, and clinical sample analysis, were combined to elucidate the functional relations between these enzymes and tumors. In this regard, the fundamental advances and follow-on drug discoveries have been crucial in providing vital information concerning contemporary translational efforts to tailor individualized treatment by targeting Ub and Ubl pathways. Correspondingly, emphasizing the current progress of Ub-related pathways as therapeutic targets in cancer is deemed essential. In the present review, we summarize and discuss the functions, clinical significance, and regulatory mechanisms of Ub and Ubl pathways in tumorigenesis as well as the current progress of small-molecular drug discovery. In particular, multiomics analyses were integrated to delineate the complexity of Ub and Ubl modifications for cancer therapy. The present review will provide a focused and up-to-date overview for the researchers to pursue further studies regarding the Ub and Ubl pathways targeted anticancer strategies.

© 2023 Chinese Pharmaceutical Association and Institute of Materia Medica, Chinese Academy of Medical Sciences. Production and hosting by Elsevier B.V. This is an open access article under the CC BY-NC-ND license (<http://creativecommons.org/licenses/by-nc-nd/4.0/>).

*Corresponding author.

E-mail address: ljia@shutcm.edu.cn (Lijun Jia).

[†]These authors made equal contributions to this work.

Peer review under responsibility of Chinese Pharmaceutical Association and Institute of Materia Medica, Chinese Academy of Medical Sciences.

1. Introduction

Ubiquitination (or ubiquitylation) is a common and essential post-translational modification that regulates several biological processes by degrading or activating/inactivating numerous proteins. In the 1980s, Hershko et al.^{1,2} described ubiquitination as an ATP-dependent enzymatic reaction cascade that induced the conjugation of a highly conserved 76-residue Ub to substrates. For their contribution to the field of ubiquitination-mediated proteolysis, they were awarded the Nobel Prize in 2004. The ubiquitination reaction is sequentially catalyzed by three enzymes: Ub-activating enzyme (E1), Ub-conjugating enzyme (E2) and Ub ligase (E3)^{3,4}. The first step of ubiquitination involves the ATP-dependent activation of Ub by an E1. Subsequently, the activated Ub is transferred to an E2 via a transthiolesterification reaction. Finally, a specific E3 delivers the activated Ub to the substrate via covalent attachment (Fig. 1A). To date, 2 E1s, 33 E2s, and >600 E3s have been identified in the Ub pathway. Furthermore, several Ubl proteins

have been identified as post-translational modifiers, such as neural precursor cell expressed, developmentally down-regulated gene 8 (NEDD8), and small ubiquitin like modifier (SUMO)⁴. These proteins share a similar Ub-fold domain and the ability to conjugate to substrates *via* a cascade reaction driven by three evolutionarily related enzymes⁴.

Accumulating studies have revealed that Ub and Ubl modifications are related to the development of distinct human diseases, especially in the onset and progression of cancer. More than 90,000 references to Ub in PubMed highlight the significance of Ub and Ubl modifications for cellular homeostasis by 2022, August. Over 10,000 studies have shown that Ub and Ubl modifications play a crucial role in regulating tumor growth, proliferation, differentiation, metabolism, and the formation of tumor microenvironment³ (Fig. 1B). Furthermore, they are also involved in almost all cell death processes, such as apoptosis, autophagy, senescence, necrosis, lysosome-dependent cell death, necroptosis, and ferroptosis (Fig. 1B). These findings suggest the importance

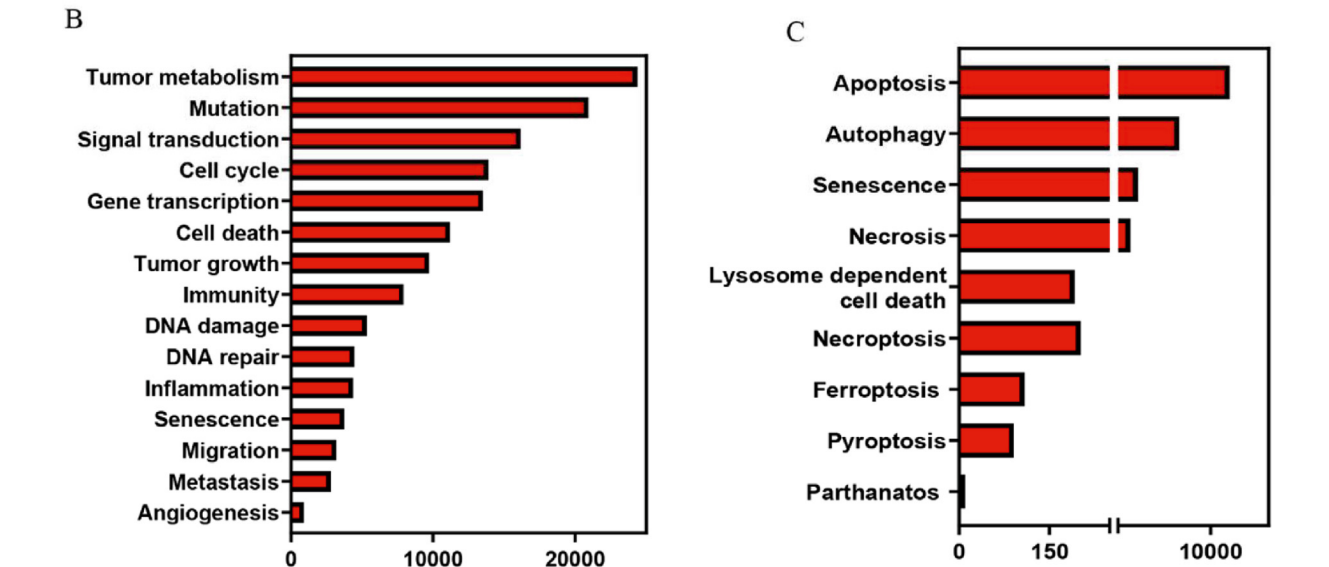
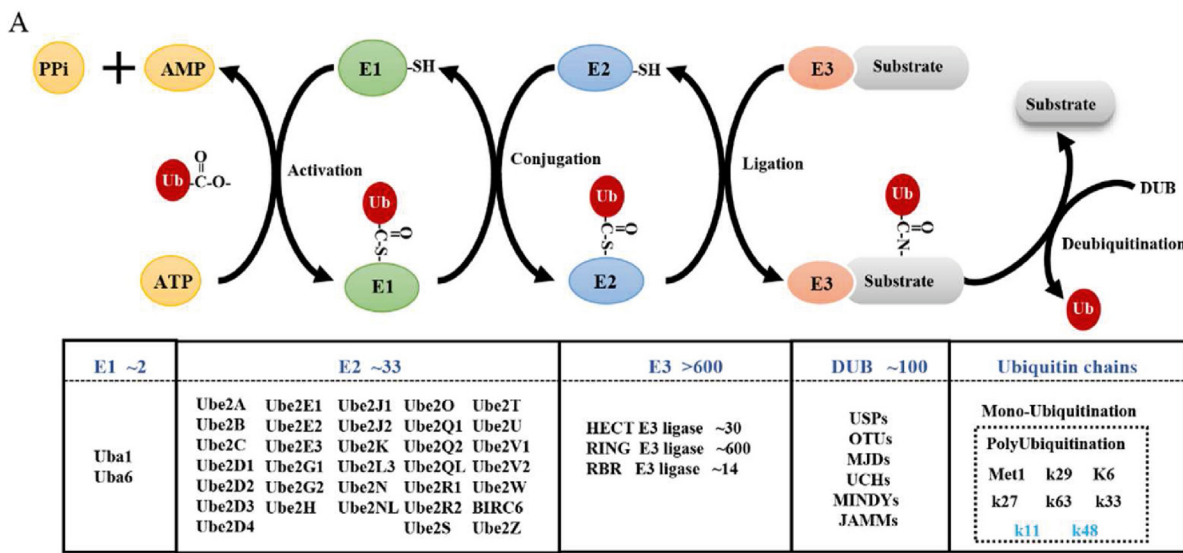


Figure 1 Process of ubiquitination and its associated functions. (A) Schematic diagram of the ubiquitination and deubiquitination process and their related enzymes. (B, C) Ubiquitination involves in almost all tumor associated pathways and cell death pathways.

of Ub or Ubl pathways for tumorigenesis. In the present review, we have summarized the current efforts and prospects of the Ub and Ubl pathways in tumors, including oncogenic or tumor-suppressive functions, clinical significance, regulatory mechanisms, and targeted drugs. Moreover, we have summarized some important challenges that are faced by current targeting Ub or Ubl studies, and how advances in multiomics profiles can help us to deeply understand and address these challenges.

2. Advancements in the studies of Ub and Ubl-associated enzymes in cancer

Abnormality of Ub and Ubl pathways in tumors is closely related to the dysregulation of their catalytic enzymes, including E1s, E2s, E3s and deubiquitinases^{3,5–8}. These anomalies are regulated at various layers, including overexpression, depletion, or mutation. Given that the best characterized function of Ub and Ubl pathways is to maintain cellular homeostasis, these pathways have been identified as attractive targets for cancer therapy. Therefore, a comprehensive overview of the anomalies and their roles of Ub- and Ubl-associated enzymes, including E1s, E2s, E3s and deubiquitination enzymes, in tumorigenesis is essential. In the following sections, we have summarized the latest advancements in the studies of Ub and Ubl-associated enzymes in tumors. We also discussed neddylation, a representative Ubl pathway *via* adding NEDD8 to substrates, to provide insight into the feature of the Ubl conjugation machinery in cancer.

2.1. Targeting E1s suppresses tumor initiation or progression

Two Ub-activating enzymes UBA1 (also known as UBE1) and UBA6 have been identified so far. In 1981, UBA1 was identified as the first E1, which catalyzes Ub activation in 99% cellular ubiquitination reactions^{9,10}. It was not until 2007 that UBA6 was identified as an alternative E1, which activated Ub with the same efficiency as that of UBA1 in approximately 1% cellular ubiquitination reactions¹¹. UBA1 and UBA6 possess three common domains, the adenylation domain that binds with ATP, catalytic cysteine domain that forms the thioester bond with Ub, and Ub-fold domain (UFD) that interacts with E2¹⁰ (Fig. 2). The difference in UFD determines the specificity of the E1–E2 pairs. UBA1 favors pairing with UBE2A, UBE2B, UBE2C, UBE2D_{1–4}, UBE2G_{1–2}, UBE2H, UBE2J_{1–2}, UBE2K, UBE2L3, UBE2Q2, UBE2R_{1–2}, UBE2S, and UBE2T, whereas UBA6 specificity activates UBE2Z (also known as Use1). Additionally, UBA6 also pairs with other UBA1 paired E2 enzymes, including UBE2G2, UBE2S, UBE2D_{1–4}, UBE2E3, UBE2T, and UBE2L3¹² (Fig. 2). Recently, a genome-wide pan-cancer CRISPR/Cas9 screening was conducted to investigate the difference between UBA1 and UBA6 in suppressing tumor cell growth¹⁰. The screening results revealed that UBA1 depletion inhibited the growth of the analyzed cancer cell lines ($n = 582$), whereas UBA6 knockdown suppressed the growth of only 10.9% of the analyzed cancer cell lines¹⁰, thereby

indicating that UBA1 is more essential than UBA6 for tumor growth.

As for Ubl E1, NEDD8 activating enzyme E1 (NAE), a heterodimer of NAE1 and UBA3, is significantly up-regulated in a myriad of tumor tissues. The overexpression of NAE promotes the tumorigenesis and tumor progression, while its inhibition *via* pharmacological (e.g., MLN4924) or genetic approaches (e.g., siRNA) suppresses tumor growth^{13–15}. In mechanism, targeting NAE to the inhibition of neddylation 1) induces apoptosis *via* inhibiting the degradation of ATF4, I κ B α and NOXA^{13,16–21}; 2) promotes senescence *via* inducing the accumulation of p21 and p27^{22–24}; 3) facilitates cell cycle arrest *via* suppressing the degradation of p21, p27 and Wee1^{25–27}; 4) induces the re-initiation of DNA replication (re-replication) by increasing the levels of CDT1 and ORC1^{28,29}; 5) inhibits the inflammation *via* inducing the accumulation of I κ B α or RHBO^{30,31}. 6) suppresses the infiltration of immune suppressive cells (e.g., MDSCs and TAMs) *via* NF κ B–CCL2/CXCL1 axis^{32–34}; 7) inhibits tumor angiogenesis *via* inducing the accumulation of RhoA³⁵; and 8) suppresses the extravasation of cancer cells *via* disrupting actin cytoskeleton formation²⁵. Furthermore, the inactivation of neddylation also induces protective autophagy in tumor cells *via* 1) inducing the accumulation of DEPTOR (a well-known inhibitor of mTORCs)³⁶; 2) inhibiting the degradation of HIF1 α to activate REDD1–TSC1 pathway³⁷; and 3) blocking the degradation of I κ B α to activate the ROS–ATF3 pathway³⁸ (Fig. 3).

2.2. Functions and regulatory mechanisms of E2s in cancer

Up to 33 Ub-associated E2s have been identified, which share the common catalytic ubiquitin-conjugating (UBC) domain³⁹. Through the UBC domain, a free E2 interacts with E1 to afford an activated Ub from the E1–Ub adduct. After coupling with a specific E3, E2–Ub transfers Ub to the target substrates to form Ub chains³⁹. Notably, the type of Ub chains is determined by E2. For example, UBE2C and UBE2S are specific Lys11-linked ubiquitin-conjugating enzymes^{40–43}, whereas UBE2D and UBE2R1 catalyze the formation of Lys48-linked polyubiquitin chain^{44,45}.

UBE2C, also known as UbcH10, delivers Ub to the substrate, which is followed by UBE2S-driven Ub extension to form the Lys11-polyubiquitination chain^{40–43}. Both UBE2C and UBE2S are overexpressed in various cancer cell lines and tumor tissues^{46,47} and facilitate malignant transformation of the cells or tumor growth by promoting the degradation of tumor-suppressing substrates (e.g., p27 and p53)^{40–43,48–51}. UBE2C transgenic mice is susceptible to developing spontaneous tumors when exposed to certain carcinogens (e.g., anthracene derivatives)⁴⁶. UBE2C and UBE2S are also activated by certain oncogenes, such as estrogen receptor 1 and androgen receptor (AR)^{50,52}, AKT1⁵³, APC/CCDH1, and Emi1^{42,54}, whereas they are suppressed by the tumor suppressor p53^{50,52}. Interestingly, there appears to be some divergence in the tumor-promoting functions of UBE2S and

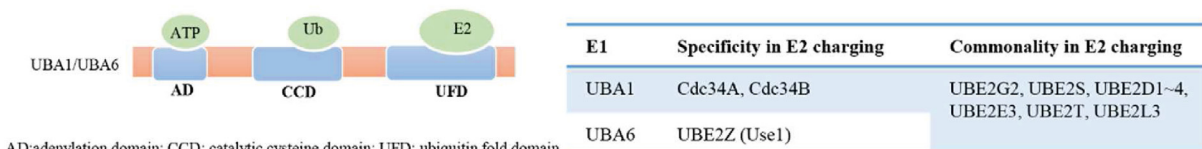


Figure 2 Schematic structure of E1s (UBA1 and UBA6), and the specificity of the E1–E2 pairs.

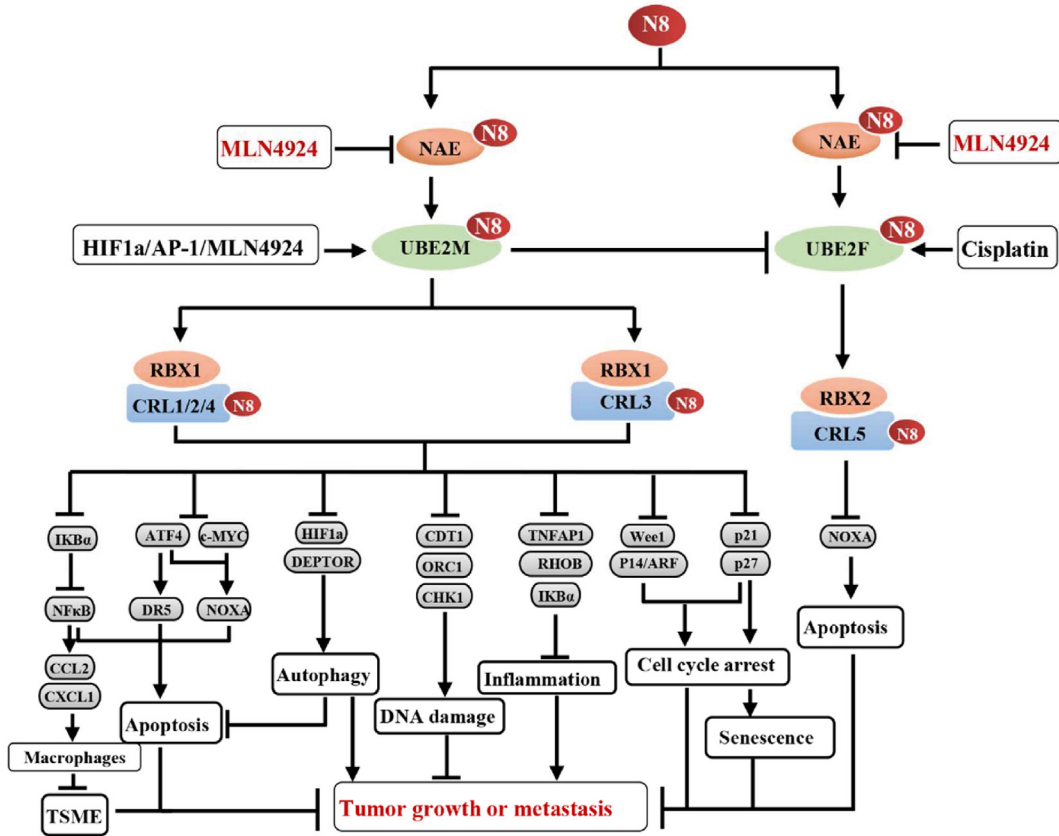


Figure 3 Regulatory and pro-tumoral mechanisms of neddylation pathway. N8: NEDD8, neural precursor cell expressed, developmentally down-regulated gene 8; TSME: tumor suppressive microenvironment.

UBE2C in cancers. For instance, it has been observed that the deletion of UBE2C, but not UBE2S, regulates the degradation of DEPTOR, which in turn suppresses lung cancer cell growth⁵⁵.

UBE2D (also known as UBCH5) efficiently delivers Ub to the substrate, while UBE2R1 (also known as Cdc34) promotes the extension of the Lys48-linked polyubiquitin chain^{44,45}. According to clinical tumor sample analysis, UBE2D and UBE2R1 are overexpressed in numerous tumor tissues, such as lung cancer^{56,57}, hepatocellular carcinoma^{58,59} and multiple myeloma⁶⁰, and regulate the ubiquitination and degradation of several essential tumor-suppressive substrates, including IKB α , cyclin-dependent kinase inhibitor p21 and p27^{45,61-63}. Additionally, UBE2R1 stabilizes the epidermal growth factor receptor by competing with UBE2D-matched Casitas B-lineage lymphoma (c-Cbl), thereby promoting the proliferation of lung cancer cells⁵⁶. This research reveals a previously unknown function of E2s, describing that they can directly stabilize substrates instead of acting as Ub carriers to promote the ubiquitination and degradation of substrates.

In contrast to the Ub pathway, neddylation involves only two E2 enzymes, UBE2M and UBE2F. In general, UBE2M pairs with RBX1 to promote the neddylation of cullin 1, 2, 3, 4A and 4B, while UBE2F pairs with RBX2 to enhance the neddylation of cullin 5. Our studies, as well as other studies, have demonstrated that UBE2M and UBE2F are up-regulated in various tumors^{17,64,65}. Consequently, the overexpression of UBE2M primarily leads to the accumulation of substrates on the cullin 1, 2, 3, 4A or 4B (e.g., ATF4, p21, p27, CDT1 and ORC1), whereas the overexpression of UBE2F promotes the accumulation of cullin5 substrates (e.g., NOXA) (Fig. 3). Interestingly, there is a cross-talk

between these two independent E2s. The activated UBE2M serves as a dual E2 to induce the proteolysis degradation of UBE2F, thereby inducing the accumulation of pro-apoptosis protein NOXA, which promotes apoptosis in lung cancer cells⁶⁶.

2.3. Functions and regulatory mechanisms of E3s in cancer

More than 600 E3 ligases have been identified in humans so far, which contribute to the functional diversity and substrate specificity of ubiquitination. According to their structures and functions, E3 ligases are grouped into three main categories: really interesting new gene (RING), homologous to E6-associated protein C-terminus (HECT), and RING-in-between-RING (RBR) E3 ligases (Fig. 4). Especially, RING E3 ligases, the largest E3 ligases with more than 600 members, were summarized in details in this section.

2.3.1. Representative RING E3s in cancer

RING E3 ligases share a common RING domain or U-box domain for binding with E2–Ub thioester. RING E3s typically transfer Ub directly from E2 to the targeted substrates. All RING E3 ligases have an E2 binding domain, but not every RING E3 ligase possesses the substrate recognition domain. Therefore, RING E3 ligases are divided into two groups: single-subunit RING E3 ligases (e.g., c-Cbl, MDM2, and IAP) and multi-subunit RING E3 ligases (e.g., Cullin–RING ligases [CRLs])⁶⁷ (Fig. 4). CRLs, also known as the largest RING E3 ligases, comprise several subunits, including RING, cullin, adaptor, and/or substrate receptor proteins⁶⁸ (Fig. 4). RBX1 and RBX2, also known as the two classical

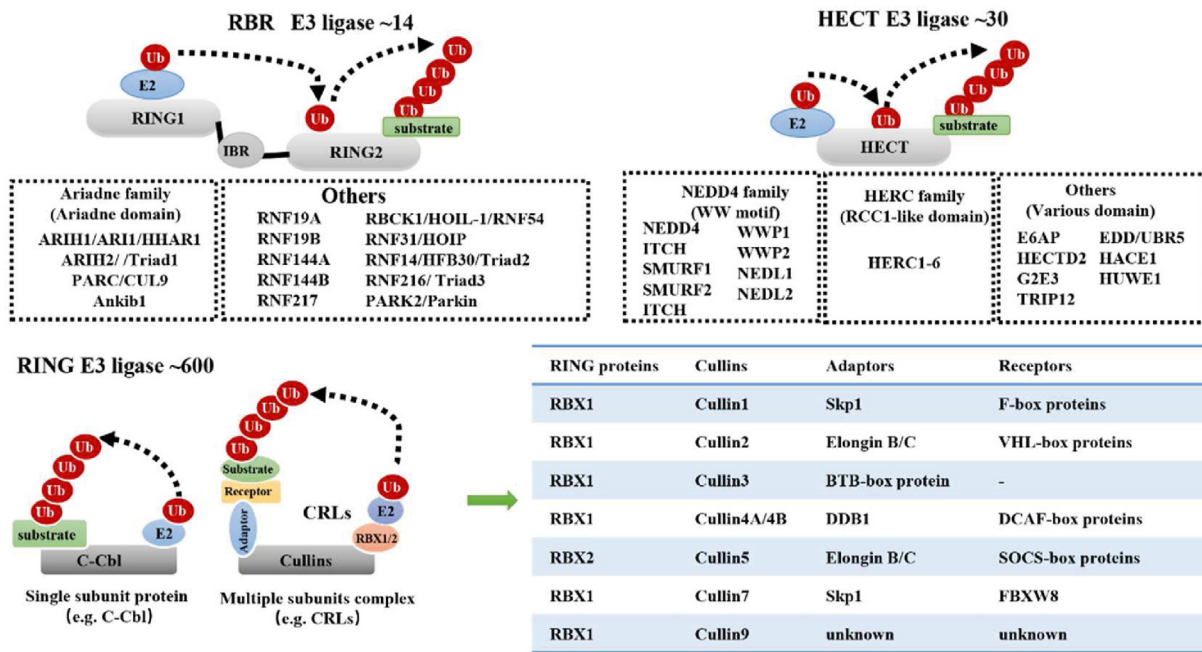


Figure 4 Structures and components of RING, HECT and RBR E3 ligases. According to the active form, RING E3s are divided into 2 groups, including the single-subunit RING E3 ligases and multiple subunit E3 ligases.

RING proteins of CRLs, deliver Ub or Ubl from the E2–Ub or E2–Ubl complex to the substrate⁶⁸. Cullins constitute the skeletal proteins of CRLs that assemble the RING, adaptor, and/or receptor proteins to deliver Ub to the recruited substrates⁶⁸. Eight distinct cullins paired with RBX1 or RBX2 form CRL1, CRL2, CRL3, CRL4A, CRL4B, CRL5, CRL7, and CRL9⁶⁸, which are primarily involved in regulating certain specialized cellular functions during tumor initiation and progression.

2.3.1.1. CRL1 E3 ligases. CRL1, also known as SKP1-Cullin1-F-box protein (SCF), comprises four subunits: RBX1, cullin1, adaptor protein Skp1, and substrate receptor F-box proteins. F-box proteins have two essential functional domains, the F-box motif for Skp1-mediated cullin1 recruitment and the C-terminal domain for substrate recognition. Based on the latter, F-box proteins are divided into three categories: 10 members of FBXWs with WD40 repeats, 22 members of FBXLs with leucine-rich repeats (LRR), and 37 members of FBXOs with a different domain or no recognizable motifs^{69,70}. Among them, S-phase kinase-associated protein 2 (Skp2), F-box and WD repeat domain-containing 7 (FBXW7), and β -transducin repeat-containing E3 ubiquitin protein ligase (β -TRCP) are well-characterized F-box proteins in cancer studies (Fig. 5).

In 1995, Skp2 (also known as FBXL1, FBL1, and p45) was identified as an essential cytokinetic regulator of the cyclin A–CDK2 complex for S-phase entry⁷¹. In the past 26 years, Skp2 has been established as an oncogene that promotes the progression of various tumors, such as those of lung cancer⁷², nasopharyngeal carcinoma⁷³, hepatocellular carcinoma⁷⁴ and gastric carcinoma⁷⁵. Mechanistically, Skp2 recognizes substrates *via* its LRR domain in a phosphorylation kinase-dependent manner, subsequently promoting the formation of a Lys48-linked polyubiquitin chain for substrate degradation *via* the 26S proteasome or the formation of a Lys63-linked polyubiquitin chain for protein–protein interaction (PPI) and activation⁷. Therefore, Skp2 substrates are divided into

two categories: proteolytic substrates, including p21⁷⁶, p27⁷⁷, p57⁷⁸, CDT1⁷⁹, ORC1⁸⁰ and FOXO1⁸¹ and nonproteolytic substrates, including AKT^{73,82}, YAP⁸³, MTH1⁸⁴, LKB1⁸⁵, NBS1⁸⁶ and Twist⁸⁷. Notably, proteolytic Skp2 substrates primarily exhibit tumor-suppressive activity, inhibiting tumor growth or promoting cell death pathways (*e.g.*, apoptosis or senescence), whereas the nonproteolytic Skp2 substrates primarily promote tumor growth or metastasis⁷. Thus, Skp2 constitutes a promising pharmacological target in cancer therapy owing to its essential role in facilitating tumor initiation and progression.

FBXW7, also known as FBW7, CDC4, and SEL-10, is widely regarded as a tumor suppressor. Numerous FBXW7 substrates have been identified as oncoproteins that promote tumor growth, including Aurora A^{88,89}, BRAF⁹⁰, c-Jun^{91,92}, c-Myc^{93,94}, GFI1⁹⁵, HIF1 α ^{96,97}, SHOC2⁹⁸, KLF5^{99,100}, MCL1^{101,102}, NOTCH1^{103–105} and ZNF322A¹⁰⁶, further highlighting the tumor-suppressive property of FBXW7. FBXW7 encodes three isoforms, namely FBXW7 α , FBXW7 β , and FBXW7 γ , which display distinct subcellular distributions. FBXW7 α is a major isoform in human tissues and cells, located in the nucleoplasm; FBXW7 β resides in the cytoplasm, whereas FBXW7 γ is primarily found in the nucleolus^{107,108}. Therefore, different FBXW7 isoforms may cooperatively promote the ubiquitination of oncogenic proteins. Loss-of-function *FBXW7* mutations have been frequently observed in tumors where they intensify tumor progression, chemoresistance, and radiation tolerance^{90,95,101,107,109,110}. Additionally, *FBXW7* is activated by p53¹¹¹ and suppressed by some microRNA, such as miR-24¹¹², miR-27¹¹³, miR-32¹¹⁴, miR-223¹¹⁵ and miR-367¹¹⁶. Thus, targeting the negative regulators or substrates of FBXW7 can serve as an effective anticancer strategy.

β -TRCP1 (also known as FBXW1, FBXW1A, and FWD1) and β -TRCP2 (also known as FBXW11, FBXW1B, and HOS) are subordinate members of the β -TRCP family that exert context-dependent oncogenic or tumor-suppressive effects. For example, β -TRCP targets numerous tumor suppressors, including I κ B α ^{117,118},

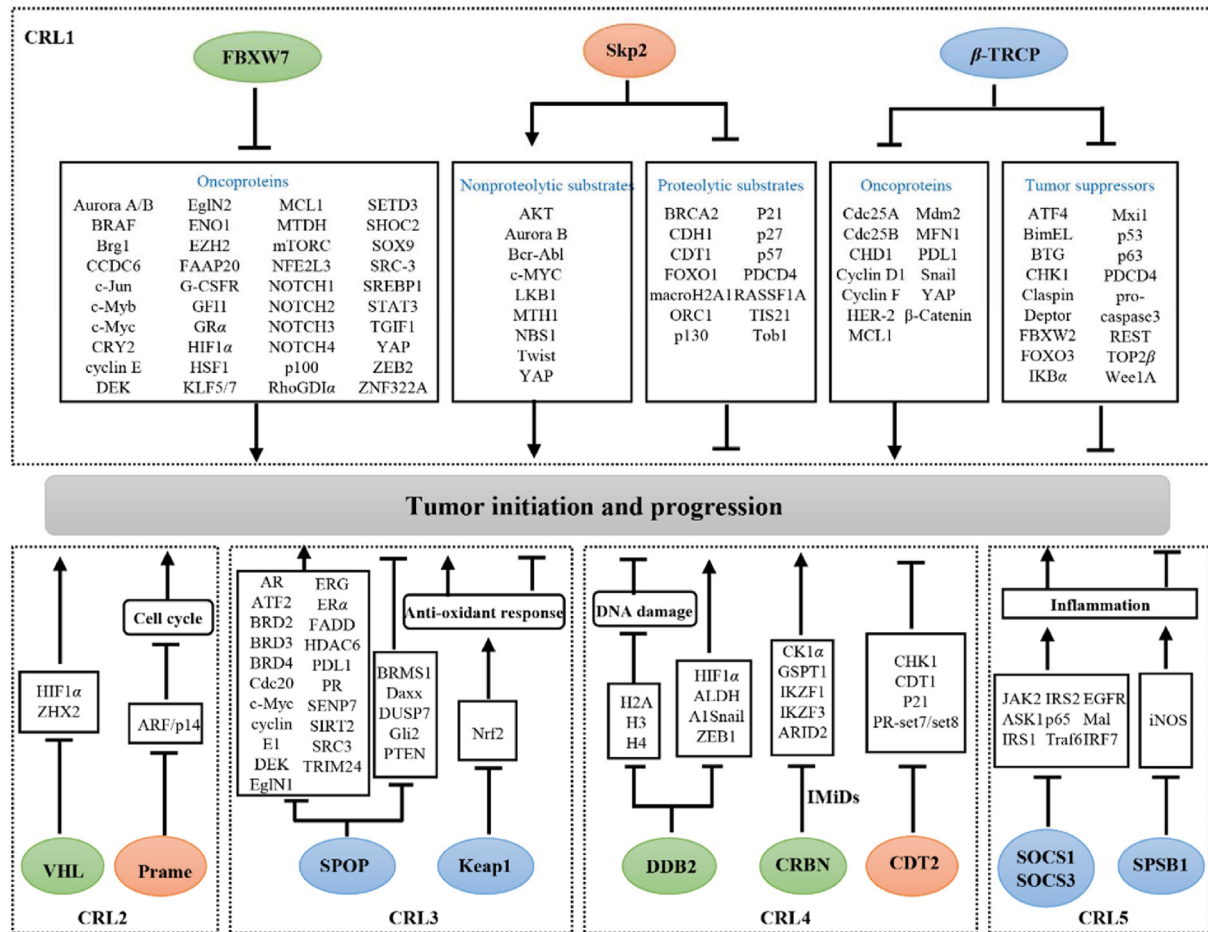


Figure 5 Representative receptors or adaptors of CRL E3 ligases and their role in tumor initiation and progression. Green: tumor suppressive role; Orange: tumor promoting role; Blue: dual roles in a context-dependent manner.

Wee1¹¹⁹, p53¹²⁰, DEPTOR¹²¹, FBXW2¹²², BimEL¹²³, Mxi1¹²⁴, PDCD4¹²⁵, and pro-caspase3¹²⁶, for degradation to facilitate tumor growth, whereas β -TRCP ubiquitinates certain important oncogene proteins, including HER2¹²⁷, YAP¹²⁸, MDM2¹²⁹, PD-L1¹³⁰ and MCL1¹³¹, to suppress tumor initiation or progression (Fig. 5). Clinical tissue analysis revealed that β -TRCP is upregulated in various tumors (*e.g.*, colorectal cancer and hepatoblastomas) and is associated with decreased overall survival in patients with tumor^{132,133}, whereas somatic mutations of β -TRCP promote the progression of certain tumors (*e.g.*, gastric and prostate cancers)^{134,135}.

2.3.1.2. CRL2 E3 ligases. CRL2 comprises RBX1, cullin2, adaptor protein Elongin B/C, and substrate recognition subunit¹³⁶. The most characteristic substrate recognition subunit of CRL2 is the Von Hippel-Lindau tumor suppressor (VHL). VHL was initially cloned in 1993¹³⁷, and subsequently its mutations were identified in most ccRCC cases in 1994¹³⁸. The classical substrates of VHL include hypoxia-inducible factors (HIFs)¹³⁶. Loss-of-function VHL mutations induce HIF accumulation, which further facilitates tumor angiogenesis by promoting HIF-mediated transcription of essential oncogenes, including VEGF and EPO¹³⁹. Loss-of-function VHL mutations and elevated HIF and VEGF levels have been frequently observed in tumors, especially in those of ccRCC^{140–142}. Hence, targeting the VHL–HIF–VEGF axis constitutes a major

therapeutic intervention strategy for ccRCC^{142,143}. In addition to HIFs, VHL substrates include Zinc fingers and homeoboxes 2 (ZHX2)¹⁴⁴, protein kinase C¹⁴⁵, β -adrenergic receptor¹⁴⁶, and the RNA polymerase II subunit hsRPB7¹⁴⁷. ZHX2, an NF- κ B transcriptional activator, offers an additional therapeutic option for patients with HIF-insensitive or -resistant ccRCC¹⁴⁴.

2.3.1.3. CRL3 E3 ligases. Unlike other CRLs, CRL3 comprises RBX1, cullin3, and broad-complex-tramtrack-bric- α -brac (BTB) adaptor protein. BTB proteins not only directly bind to cullin3 but also recognize substrates via their BTB domain (also known as the POZ domain). Functionally, BTB proteins facilitate the 26S proteasome-mediated substrate degradation by promoting the formation of Lys48-linked polyubiquitin chains. Conversely, BTB proteins catalyze Lys63- and Lys33-linked ubiquitination, affecting PPI and subcellular localization¹⁴⁸. To date, 188 putative BTB proteins have been identified in the human genome, which are grouped into five subfamilies: the BTB-kelch ($n = 55$), BTB-Zn finger ($n = 49$), K^+ voltage-gated channel ($n = 27$), and KCTD ($n = 25$) subfamilies and others ($n = 32$)¹⁴⁸. Kelch-like ECH-associated protein 1 (Keap1) and speckle-type BTB/POZ protein (SPOP) constitute two classical substrate adaptor proteins of CRL3 (Fig. 5).

Keap1 was identified as a nuclear factor erythroid 2-related factor 2 (Nrf2) inhibitor. Nrf2 is a key regulator of cellular anti-oxidant response that stimulates the transcription of >200

antioxidant genes, including HO1 and NQO1¹⁴⁹. Previous studies have reported that Nrf2 is ubiquitinated by cytoplasmic Keap1 under normal conditions. Conversely, the oxidation of Keap1 by reactive oxygen species or electrophiles failed to ubiquitinate Nrf2, inducing its accumulation. The accumulated Nrf2 translocated into the nucleus, thereby increasing the transcription of antioxidant genes and preventing oxidative damage to normal cells and tissues. Thus, Nrf2-knockout mice are susceptible to spontaneous tumors^{150,151}. However, numerous studies have shown that Nrf2 hyperactivation protects cancer cells from chemotherapeutic agents or radiotherapy-induced oxidative stress¹⁴⁹.

SPOP regulates substrate ubiquitination and affects the progression of several human cancers, including lung cancer¹⁵², prostate cancer^{153–156}, RCC^{157,158}, endometrial cancer^{155,159} and breast cancer¹⁶⁰. Generally, SPOP acts as a tumor suppressor in multiple cancers (*e.g.*, lung and prostate cancers) by mediating the degradation of several oncproteins, including ERG¹⁵⁶, PD-L1¹⁶¹, cyclin E1¹⁶², ATF2¹⁶³, c-Myc¹⁶⁴, AR¹⁶⁵, steroid receptor coactivator 3¹⁶⁶, BRD2, BRD3 and BRD4^{153–155}. However, SPOP exhibits an oncogenic function in RCC by mediating the degradation of phosphatase and tensin homologue (PTEN), proapoptotic molecule Daxx, Gli2, DUSP6, and DUSP7¹⁵⁷. The subcellular localization of SPOP primarily affects its dual functions. SPOP accumulates in the nucleolus of cells to mediate oncprotein degradation^{154,167,168}. Conversely, SPOP demonstrates predominantly cytoplasmic localization in ccRCC due to the VHL mutations and hypoxic conditions in ccRCC, consequently promoting the degradation of cytoplasmic tumor suppressors (*e.g.*, PTEN, Daxx, Gli2, DUSP6, and DUSP7)¹⁵⁷.

2.3.1.4. CRL4 E3 ligases. CRL4 is subdivided into CRL4A and CRL4B based on the skeleton proteins of cullin 4A and cullin 4B, respectively. Damage-specific DNA-binding protein 1 (DDB1) is an essential adaptor protein of CRL4 that detects and repairs damaged DNA. Meanwhile, DDB1-cullin4 associated factors (DCAF_is) serve as substrate receptors^{169,170}. Three representative DCAF_is in anticancer therapy are damage-specific DNA-binding protein 2 (DDB2), denticleless E3 ubiquitin protein ligase homolog (DTL), and cereblon (CRBN) (Fig. 5).

DDB2 is a WD40 repeat-containing protein that heterodimerizes with DDB1 to repair DNA damage or inhibit the transcription of certain oncogenes. When DDB2 is directly linked to damaged DNA, it assembles the CRL4 complex to ubiquitylate histones H2A¹⁷¹, H3, or H4¹⁷², thereby facilitating DNA repair by weakening the histone–DNA interaction. Furthermore, DDB2 was ubiquitinated by CRL4A at the lesion site^{173,174}, thus inducing the accumulation of damage recognition factor XPC to remove damaged pyrimidine dimers^{174,175}. Therefore, DDB2 knockout mice are susceptible to skin carcinogenesis, and the upregulation of DDB2 suppresses the onset and progression of UV-induced squamous cell carcinoma^{176–178}. In addition, DDB2 inhibits the transcription of HIF1 α ¹⁷⁹, ALDHA1¹⁸⁰, Snail and ZEB1¹⁸¹, thus inhibiting tumor growth or epithelial-to-mesenchymal transition.

As a potential oncprotein, DTL (also known as CDT2, DCAF2, RAMP, and L2DTL) recognizes and ubiquitinates its substrates to master genome stability^{182,183}. Inducing the accumulation of CDT1¹⁸⁴, p21¹⁸⁵ and PR-set7/set8¹⁸⁶ in the S phase in a proliferating cell nuclear antigen (PCNA)-dependent manner, CDT2 knockdown inhibits DNA replication. Knockdown of CDT2

triggers G2 cell cycle arrest by preventing the degradation of CHK1 in a PCNA-independent manner¹⁸⁷. In contrast, overexpression of CDT2 accelerates the degradation of the substrate, CDT1, subsequently promoting cancer cell re-plication and impairing senescence or apoptosis¹⁸⁸.

CRBN, an important substrate recognition receptor of the CRL4, is the primary target of immunomodulatory drugs (IMiDs), such as thalidomide and its derivatives (*e.g.*, pomalidomide, lenalidomide, CC-885) for hematological malignancy treatment. CRBN facilitates the ubiquitination and degradation of the Ikaros family (IKZF1 and IKZF3) in a lenalidomide-dependent manner^{189–191} and that of ARID domain-containing protein 2 (ARID2) in a pomalidomide-dependent manner to suppress the survival and proliferation of multiple myeloma cells¹⁹². In acute myeloid leukemia cells, CRBN promotes the degradation of G1 to S-phase transition protein 1 to exert a broad-spectrum anticancer effect in a CC-885-dependent manner¹⁸⁹. Furthermore, CRBN stabilizes CD147 and monocarboxylate transporter 1 (MCT1) to promote angiogenesis, tumor growth, or lactate export, whereas IMiDs interact with CRBN to disrupt the CD147–MCT1 complex and exert antitumor and teratogenic effects¹⁹³. Interestingly, CRBN also functions as a transmembrane protein-specific co-chaperone molecule of HSP90 to modulate HSP90–AHA1 activity, whereas IMiDs inhibit their interaction to suppress multiple myeloma cell growth¹⁹⁴.

2.3.1.5. CRL5 E3 ligases. CRL5 comprises the scaffold protein cullin 5, RING protein RBX2, adaptor protein Elongin B/C, and substrate recognition receptor protein SOCS. The primary substrate receptors of CRL5 include 37 members, categorized into 5 types: SOCS, ASB, SPSB, and WSB subfamilies and others (such as Rab40 and MUF1)¹⁹⁵.

Suppressor of cytokine signaling 1 (SOCS1, also known as SSI1) and SOCS3 (also known as SSI3) are two extensively studied SOCS proteins of CRL5 that suppress inflammatory reaction and exert context-dependent effects in tumorigenesis¹⁹⁵. SOCS1 depletion in macrophages¹⁹⁶ or dendritic cells¹⁹⁷ in conditional knockout mice enhances antitumor inflammation or antigen-specific antitumor immunity. Conversely, SOCS3 or cullin 5 depletion inhibits integrin β 1 degradation, subsequently activating the focal adhesion kinase/SRC (FAK/SRC) signaling pathway, thereby promoting small-cell lung cancer metastasis¹⁹⁸. Similarly, SOCS1 inhibits STAT3 phosphorylation and limits granulocyte–macrophage colony-stimulating factor and interleukin-6 production, thus inhibiting myeloid-derived suppressor cell differentiation and increasing antitumor immunity¹⁹⁹. Additionally, elevated SOCS3 levels improve the susceptibility of castration-resistant prostate cancer cells toward natural killer cells²⁰⁰. Consistent with these findings, low SOCS1 and SOCS3 expression levels have been frequently observed and positively associated with poor prognosis in patients with small-cell lung¹⁹⁸ and breast cancer²⁰¹.

SplA/ryanodine receptor domain and SOCS box-containing 1 (SPSB1, also known as SSB1) ubiquitinates a key inflammatory effector, inducible NO synthase (iNOS)^{202,203}. iNOS has multiple cellular origins and harbors both tumor prosurvival and suppressive functions²⁰⁴. In addition to iNOS, SPSB1 promotes p21 proteasomal degradation to increase the viability and migration of ovarian cancer cells²⁰⁵. Furthermore, SPSB1 promotes breast cancer recurrence by preventing chemotherapy- or HER2/neu inhibitor-induced apoptosis in tumor cells²⁰⁶.

2.3.2. HECT E3s in tumorigenesis

In contrast to RING E3s, HECT ligases ubiquitinate their substrates in two steps. They first load the activated Ub onto themselves to produce the E3–Ub intermediate *via* the HECT domain, and then they transfer Ub onto the substrates⁵ (Fig. 4). HECT E3s are divided into three subfamilies based on the N-terminal structure of the HECT domain: 1) Nedd4 subfamily, also known as C2–WW–HECT, whose structures contain two to four tryptophan–tryptophan (WW) domains; 2) HERC (HECT and RCC1-like domain) subfamily, which contains one or more RCC1-like domains; and 3) other HECT E3s, such as E6AP, HECTD2, G2E3, TRIP12, EDD, HACE1, and HUWE1⁵ (Fig. 4). NEDD4, one of the brain development regulators, is the first Nedd4 subfamily member to be identified²⁰⁷. In tumors, NEDD4 ubiquitylates and promotes degradation of PTEN, an essential tumor suppressor, to promote tumor growth²⁰⁸, whereas CK1α competitively antagonizes NEDD4-mediated PTEN ubiquitination to inhibit lung tumor growth²⁰⁹. In addition, NEDD4 promotes the formation of K63-linked polyubiquitination chains of MDM2 to stabilize MDM2, thus promoting the degradation of p53 and inhibiting the DNA damage response²¹⁰. Furthermore, NEDD4 promotes the proteasomal degradation of VDAC2/3, the voltage-dependent anion channel, to suppress erastin-induced ferroptosis²¹¹. On the contrary, the most prominent feature of NEDD4-null mice is delayed embryonic development and growth as a result of a decrease in insulin and insulin-like growth factor 1 (IGF-1)²¹². Meanwhile, knockout of NEDD4 upregulates PDL1 and inhibits CD8+ T cell infiltration in bladder cancer cells to avoid immune surveillance²¹³. Besides, NEDD4 inhibits RBX2 to sensitize etoposide-induced apoptosis²¹⁴. This dual function of NEDD4 in tumors justifies further research into NEDD4 for future anticancer therapy.

2.3.3. RBR E3s in tumorigenesis

RBR E3s, possessing the characteristics of both RING and HECT E3s, comprise a RING1 domain, an in-between-RING (IBR) domain, and a RING2 domain^{6,215}. RBR E3s catalyze the ubiquitination reaction in three steps. They first recognize the E2–Ub complex with the RING1 domain, then transfer Ub onto RING2 to form the E3–Ub intermediate, and finally transfer Ub onto the substrates^{6,215} (Fig. 4). Herein, 14 RBR E3s, including Parkinson protein 2 (also known as Parkin), RNF19A, RNF19B, RNF144A, RNF144B, RNF216, RNF217, RBCK1, RNF31 (also known as HOIP), RNF14, ARIH1, ARIH2, PARC, and Ankib1, identified in humans (Fig. 4)⁶.

Parkin is a well-known RBR E3 ligase with neuroprotective function²¹⁶. Parkin is often downregulated in various tumors and demonstrates tumor-suppressive activity^{217–219}. Parkin downregulation is typically associated with poor overall survival of patients with tumors^{217,218}. Parkin null mice are susceptible to developing carcinoma²²⁰. In mechanism, Parkin facilitates apoptosis *via* promoting the degradation of the antiapoptosis protein MCL1 during mitochondrial depolarization²²¹, whereas Parkin depletion promotes the activation of PI3K–AKT pathway in a PTEN-dependent manner to facilitate tumorigenesis²¹⁸. In addition, Parkin suppresses Kras-driven pancreatic tumorigenesis and HIF1α-mediated Warburg effect by promoting the degradation of SLC25A37 and SLC25A28²²². Furthermore, Parkin promotes the degradation of phosphoglycerate dehydrogenase (PHGDH), the first rate-limiting enzyme of serine synthesis, to inhibit serine synthesis and tumor progression²²³. Additionally, Parkin promotes the formation of the K33-linked polyubiquitination chain of

RIPK3 to inhibit necosome assembly, hence preventing necroptosis and tumorigenesis²²⁴.

2.4. Functions of representative deubiquitinases (DUBs) in cancer

Protein deubiquitination is a reversal of ubiquitination that uses deubiquitinases (DUBs) to remove Ub from substrates. Based on their sequence and domain conservation, ~100 identified DUBs have been classified into six families⁸. Five families of cysteine proteases include USPs, OTUs, UCHs, MJDs, and MINDYs^{8,225}. In addition, the JAB1/MPN/MOV34-domain-containing metalloproteases (JAMMs) comprise 16 zinc metallopeptidases^{8,225}. DUBs primarily remove Ub from substrates to modulate protein stability, enzymatic activity, and subcellular localization^{8,225}. Therefore, DUB disruption contributes to tumor initiation and progression by interfering with the dynamic equilibrium of ubiquitination.

Based on their roles in tumorigenesis, DUBs are classified into three types. The first type is prosurvival DUBs, such as USP2 and USP7 in the USP family and CSN5 in the Jamm family. USP2 is overexpressed in several human tumor tissues and is crucial for tumor growth as it inhibits the ubiquitination and degradation of oncoproteins, including Skp2²²⁶, Twist²²⁷, MDM2^{228,229}, TGFBR1²³⁰, fatty acid synthase (FAS)²³¹, PD-L1²³², and cyclin D1²³³. USP7 activation is associated with poor overall patient survival in multiple tumors. USP7 overexpression stabilizes numerous oncoproteins, such as EZH2²³⁴, PHF8²³⁵, MDM2²³⁶, LSD1²³⁷, β-Catenin²³⁸ and DNMT1^{239,240}, thereby stimulating tumor growth or drug resistance. CSN5 facilitates tumor growth by inhibiting the degradation of Snail²⁴¹, ZEB1²⁴², surviving²⁴³ and FOXM1²⁴⁴, whereas curcumin-induced CSN5 depletion decreases PD-L1 expression and enhances the anticancer efficacy of anti-CTLA4 drugs²⁴⁵.

Tumor-suppressive DUB families, CYLD lysine 63 deubiquitinase (CYLD) in the USP family and OTU deubiquitinase 1 (OTUD1) in the OTU family, constitute the second type of DUBs. CYLD inhibits the Wnt/β-catenin and TGF-β signaling pathways by regulating the Lys63-linked ubiquitination of ALK5, thereby suppressing tumor growth and cell invasion^{246,247}. OTUD1 deubiquitinates the TGF-β inhibitor SMAD7 and inhibits p53, thereby increasing the cleavage of caspase-3 and PARP-dependent apoptosis and enhancing tumor suppression^{248,249}.

Context-dependent DUBs, such as OTUD3 and USP10, constitute the third type of DUBs that exhibit contradictory functions in various tumors. OTUD3 regulates PTEN stability to inhibit PI3K/AKT signaling transduction and tumorigenesis in breast cancer²⁵⁰. However, OTU3 stabilizes GRP78 and promotes lung cancer cell growth and migration²⁵¹, suggesting that the tumor-suppressive or -proliferative activity of OTU3 depends on the tissue specificity of the tumor²⁵¹. USP10 typically functions as a tumor suppressor in lung cancer, RCC, and colon cancer, and as a tumor promoter in acute and chronic myeloid leukemia; however, in hepatocellular carcinoma, USP10 exerts multiple activities: a) it reverses the MDM2-induced nuclear export and degradation of p53 and reduces the progression of RCC²⁵²; b) it blocks the degradation of the canonical tumor suppressor PTEN and KLF4 and inhibits lung cancer growth^{253,254}; c) it antagonizes the transcriptional activity of the oncogene c-Myc by stabilizing SIRT6 and p53, thereby promoting cell cycle arrest and inhibiting colon cancer cell proliferation²⁵⁵; d) it stabilizes the oncoproteins FLt3 and Skp2 to facilitate the growth of myeloid leukemia^{256,257};

and e) in hepatocellular carcinoma, it removes the Ub chains on YAP/TAZ to promote the growth of the HepG2, SNU387, and Li7 cell lines²⁵⁸, whereas it stabilizes PTEN and AMPK α to suppress the growth of the Huh7, HCCLM3, MHCC97L, and Bel7402 cell lines²⁵⁹.

3. Multiomics analyses empower anticancer target identification in Ub and Ubl pathways

As mentioned above, Ub and Ubl pathways are attractive anti-cancer targets. However, the complexity of these pathways, comprising hundreds of Ub-associated enzymes that form a hierarchical task network to modulate substrates, complicates our understanding of their significance in cancer. Thus, there remains a need for a comprehensive approach to identify potential anti-cancer targets within the Ub and Ubl pathways. With the advancements of high-throughput sequencing and computational tools, multiomics analyses have emerged as valuable resources for unraveling the complexity of cancer. In the following sections, we will delineate the role of Ub and Ubl-associated enzymes in tumorigenesis by multiomics analyses. Furthermore, we will outline their advance in the identification of potential anticancer targets and application for precise treatment. The narrative order and associated subtitle are expanded in the order of E1, E2 and E3.

3.1. Multiomics analyses of E1s reveals that overexpression of *UBA1* and *UBA6* represents poor overall survival of tumor patients

First, we investigated the association between E1s in tumors and in normal tissues alongside their prognostic value using the Cancer Genome Atlas (TCGA) and Clinical Proteomic Tumor Analysis Consortium (CPTAC) databases from the UALCAN website^{260,261}. Compared with normal tissues, >13 tumor types expressed high *UBA1* and *UBA6* mRNA levels, whereas only 3 tumor types exhibited low *UBA1* and *UBA6* mRNA levels (Fig. 6A and B). At the protein level, *UBA1* and *UBA6* were overexpressed in colon cancer and head and neck squamous cancer (Fig. 6C and D). These findings align with the protumoral functions of *UBA1* and *UBA6*, as evidenced by the following observations: 1) targeting *UBA1* via pharmacological and genetic approaches significantly inhibits tumor cell growth, including lung cancer, colon cancer, liver cancer, acute myeloid leukemia, non-Hodgkin lymphoma, melanoma^{11,262–265}; 2) inhibition of *UBA1* overcomes drug resistance by inducing ER stress or apoptosis in myeloma²⁶⁶; 3) overexpression of *UBA6* promotes tumor formation²⁶⁷. Kaplan–Meier analysis revealed that higher *UBA1* in patients was associated with poorer overall survival in prostate adenocarcinoma, hepatocellular carcinoma, and lung adenocarcinoma (LUAD) (Fig. 7A). Similarly, patients with LUAD, kidney chromophobe, and ccRCC exhibited worse prognoses in case of high tumoral *UBA6* levels (Fig. 7B).

3.2. Multiomics analyses of E2s reveals the potential of *UBE2C* as a broad-spectrum anticancer target in tumors

The expression levels and clinical importance of ubiquitination-related E2s were determined using transcriptomic, proteomic, and clinical data from patients with tumors^{260,261}. The mRNA levels of 27 E2s (81.81%) were significantly upregulated in the tumor tissues of patients with LUAD than that in normal tissues, whereas

the mRNA levels of 23 E2s (69.70%) were significantly upregulated in the tumor tissues of patients with lung squamous cell carcinoma ($P \leq 0.05$) (Fig. 8A and B). Conversely, less than six E2s were significantly downregulated in the tumor tissues of patients with LUAD and lung squamous cell carcinoma ($P \leq 0.05$, respectively) (Fig. 8A and B). Kaplan–Meier analysis revealed that higher *UBE2C*, *UBE2O*, *UBE2S*, *UBE2T*, *UBE2V2* and *UBE2Z* in patients was associated with poorer overall survival in LUAD (Fig. 8A and B).

The *UBE2C* mRNA levels were 18- and 30-fold higher in the tumor tissue of patients with LUAD than that in normal tissues and those with lung squamous cell carcinoma tissue, respectively. An overall survival analysis revealed that *UBE2C* (HR = 2.50) was risk factors for LUAD ($P \leq 0.05$), but not in lung squamous cell carcinoma through the analysis of the TCGA database (Fig. 9A and B). *UBE2C* has been identified as an essential factor in Kras^{G12D}-induced lung cancer⁵⁵. In addition, in our multiomics analyses, *UBE2C* was considerably and consistently upregulated in the tumor tissue of patients within the enrolled 10 tumors, including lung cancer, than in the normal tissues at protein levels (Fig. 9A). *UBE2C*, in conjunction with the APC/C E3 ligase, promotes ubiquitylation and degradation of tumor suppressive proteins (e.g., p27, DEPTOR and p53)^{40–43,48–51,55}. The mRNA levels of *UBE2S*, which cooperate with *UBE2C* for Lys11-polyubiquitination chain extension (as discussed in detail in the previous section), were significantly upregulated in the tumor tissue of patients with LUAD and lung squamous cell carcinoma tissue than that in normal tissues (Fig. 8A and B). An overall survival analysis showed that the hazard ratio of *UBE2S* was up to 2.71 in LUAD (Fig. 8A). Consistently, Zhang et al.⁵⁵ reported that overexpression of *UBE2C* or *UBE2S* is related with the poor overall survival over 400 LUAD cases. Further protein level analysis showed that *UBE2S* was significantly upregulated in the tumor tissue of patients than in the normal tissues in ovarian cancer, head and neck cancer and glioblastoma, but not in lung cancer (Fig. 9B). Knockdown of *UBE2C*, but not *UBE2S*, inhibits the growth of lung cancer cells and Kras^{G12D}-induced lung carcinoma⁵⁵. This intriguing pattern suggests that *UBE2C*, but not *UBE2S* might be an attractive target for lung cancer.

3.3. Multiomics analyses of representative E3s reveals their clinical significance and regulatory mechanisms

F-box proteins, serving as substrate-recognition subunits of CRL1 E3 ligases, play important roles in tumor initiation and progression^{69,70}. To comprehensively delineate the role of F-box proteins in tumorigenesis, multiomics analyses were performed, encompassing all F-box proteins ($n = 69$), with the aim of providing insight into the characteristics of RING E3 ligases in cancer. Transcriptomic analysis showed that thirty-three F-box proteins were upregulated and twelve F-box proteins were downregulated ($P < 0.05$) at mRNA levels in LUAD tissues compared to normal tissues (Fig. 10A). At the mRNA level, the extensively studied F-box protein *Skp2* showed a 2.72-fold increase in LUAD. This finding aligns with previous studies that have confirmed the upregulation of *Skp2* in LUAD^{72,268}. These consistent results between our omics analyses and published data further support the reliability of our findings. The expression of *FBXO45*, a potential oncogene that inhibits tumor cell death by degrading tumor suppressor *FBXW7*²⁶⁹, was increased by 2.10-fold in LUAD (Fig. 10A). Similarly, the expression of *FBXW5*, an underlying oncogene that targets kinesin-13 and LATS1/2 for

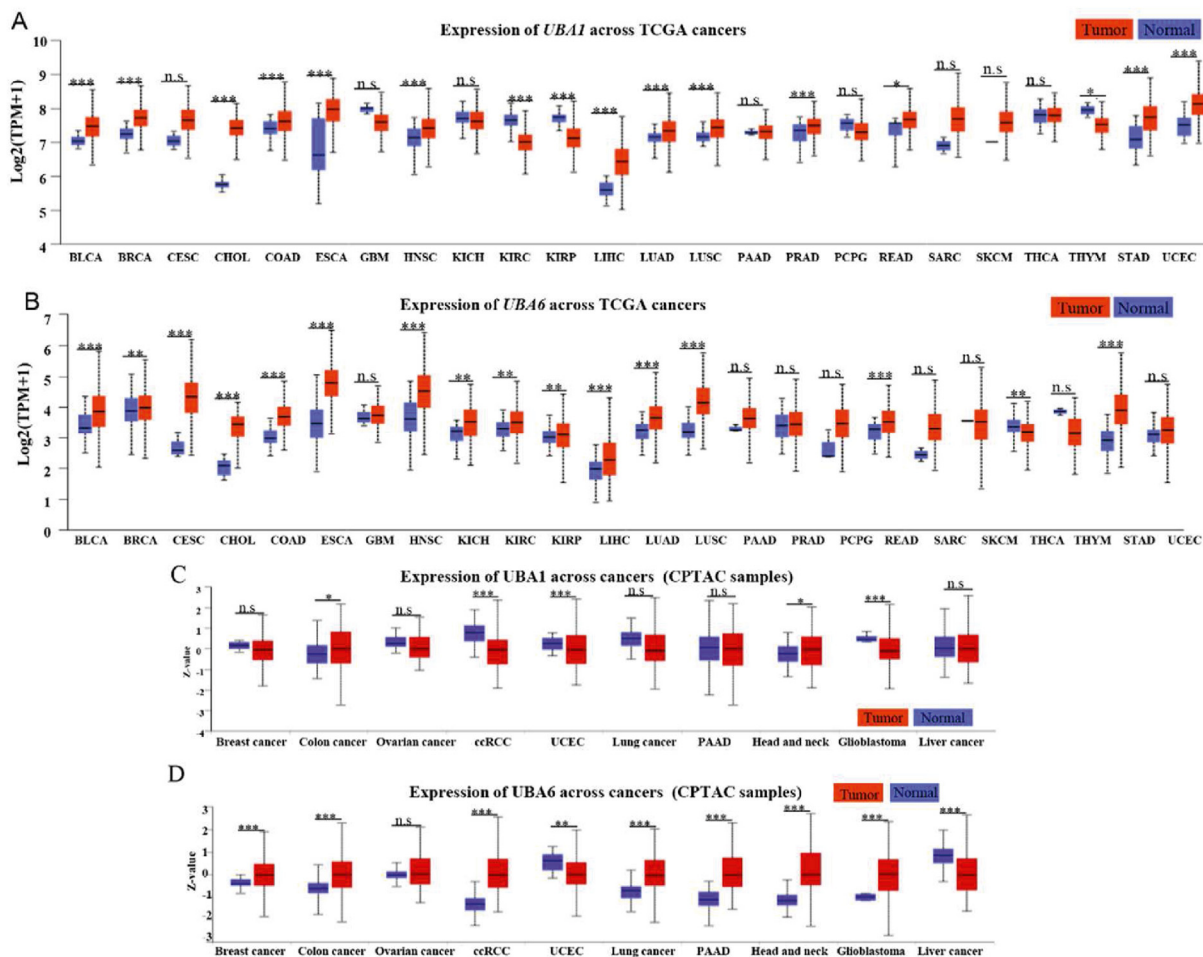


Figure 6 Multiomics analyses of E1s. (A–D) Gene expression levels of *UBA1* and *UBA6* in 24 tumors and normal tissues using TCGA database and CPTAC database in UALCAN website. Statistical significance was determined by the Mann–Whitney test (two-tailed): * $P < 0.05$, ** $P < 0.01$, *** $P < 0.001$, n.s. indicates no significant difference.

proteasomal degradation^{270,271}, was increased by 1.36-fold (Fig. 10A). At the protein level, *FBXW5* was significantly increased in ccRCC and uterine corpus endometrial carcinoma compared to normal tissues, whereas *FBXO45* was predominantly upregulated in breast cancer, ccRCC, head and neck squamous cell carcinoma, and glioblastoma (Fig. 10B and C). Consistently, *FBXW5* and *FBXO45* are overexpressed in numerous tumors and exhibit oncogenic properties^{270,271}. There were lower mRNA and protein levels of *FBXW2* (Fig. 10D). The downregulation of *FBXW2* leads to the inhibition of ubiquitylation and degradation of β -catenin and Skp2, thereby promoting lung cancer cell migration and invasion^{122,272}. In addition, the mRNA level of *FBXL21* was 14.59-fold higher in LUAD tissues than in normal tissues, followed by *FBXO43* (6.05-fold), *FBXO32* (5.70-fold), *CCNF* (also known as *FBXO1*, 3.78-fold), *FBXO41* (2.99-fold), *FBXL13* (2.86-fold), and *FBXL6* (2.08-fold) (Fig. 10A). These analyses offered a comprehensive perspective on the mRNA levels of F-box proteins in LUAD tissues compared to normal tissues.

High protein levels are regulated at multiple layers, including genetic amplification, transcriptional, translational, and post-translational levels. Consequently, we examined genetic alterations of Skp2, *FBXW7*, β -TRCP1 (gene name: *BTRC*), β -TRCP2

(gene name: *FBXWII*), *FBXW5*, *FBXO45* and *FBXW2* in thirty-three tumor types using the cBioPortal website (Fig. 11). Among these six F-box proteins, *SKP2* and *FBXO45* showed a higher amplification rate, whereas *FBXW7* was the most frequently mutated gene (Fig. 11A). *FBXW7*, a well-known tumor suppressor that has been discussed in detail in the previous section, was exhibited the highest frequency of endometrial cancer (mutation rate of 19.97%), colorectal cancer (14.81%) and cervical cancer (11.78%) (Fig. 10B). These mutation patterns of *FBXW7* were consistent with previous studies²⁷³. The mutations primarily occurred in the F-box domain and the substrate recognition WD40-repeat domain, particularly at three arginine residues (R465 C/H/G/L/P, R479Q/*G/P/L, and R505 G/C/H/L) in the WD40-repeat domain (Fig. 11C), which are essential for recognizing and binding substrates¹⁰⁷. Additionally, *Skp2*, a well-established oncogene, was found to be amplified in non-small cell lung cancer (amplification rate of 9.12%), bladder cancer (6.81%), and esophagogastric cancer (6.27%) (Fig. 11D). *FBXO45* surpassed *Skp2* with an amplification rate of 15.75% in ovarian epithelial tumor, followed by non-small cell lung cancer (14.72%) and cervical cancer (14.14%) (Fig. 10A and E). These results suggest that the overexpression of *Skp2* and *FBXO45* may be attributed to genetic amplification.

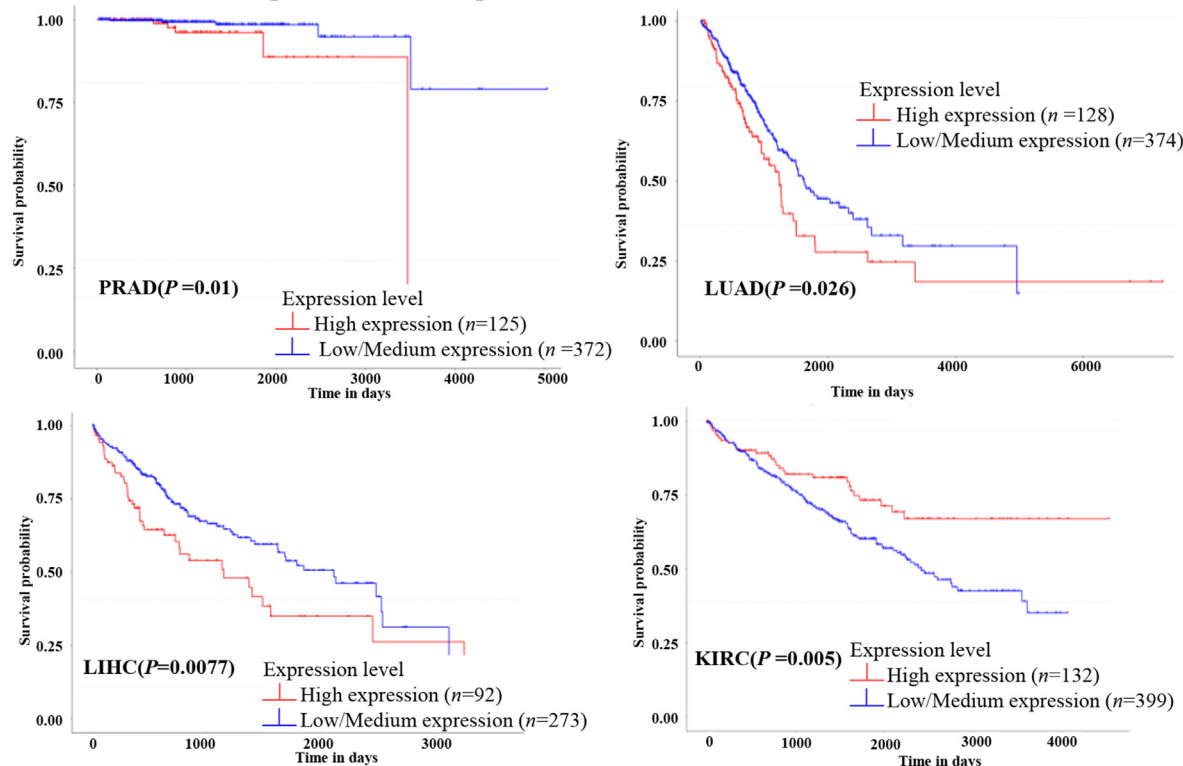
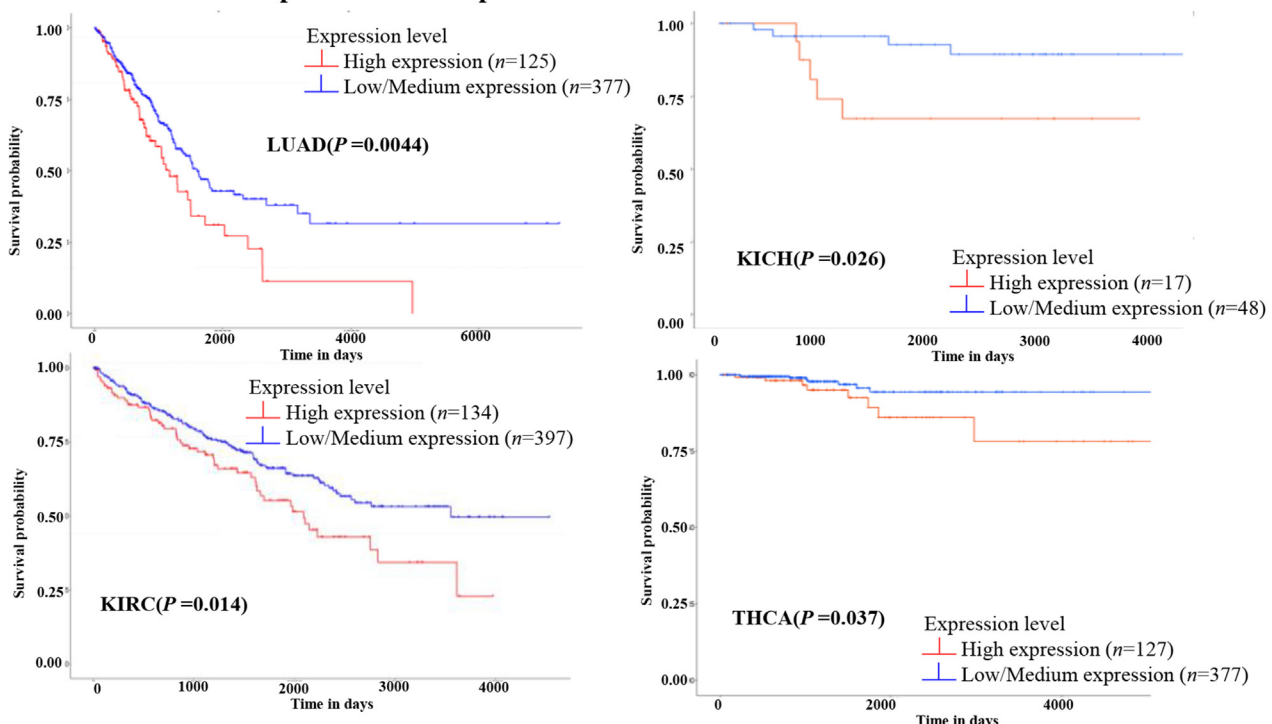
A Effect of *UBA1* expression level on patient survival**B Effect of *UBA6* expression level on patient survival**

Figure 7 Kaplan-Meier analyses of *UBA1* and *UBA6* using TCGA database in UALCAN website.

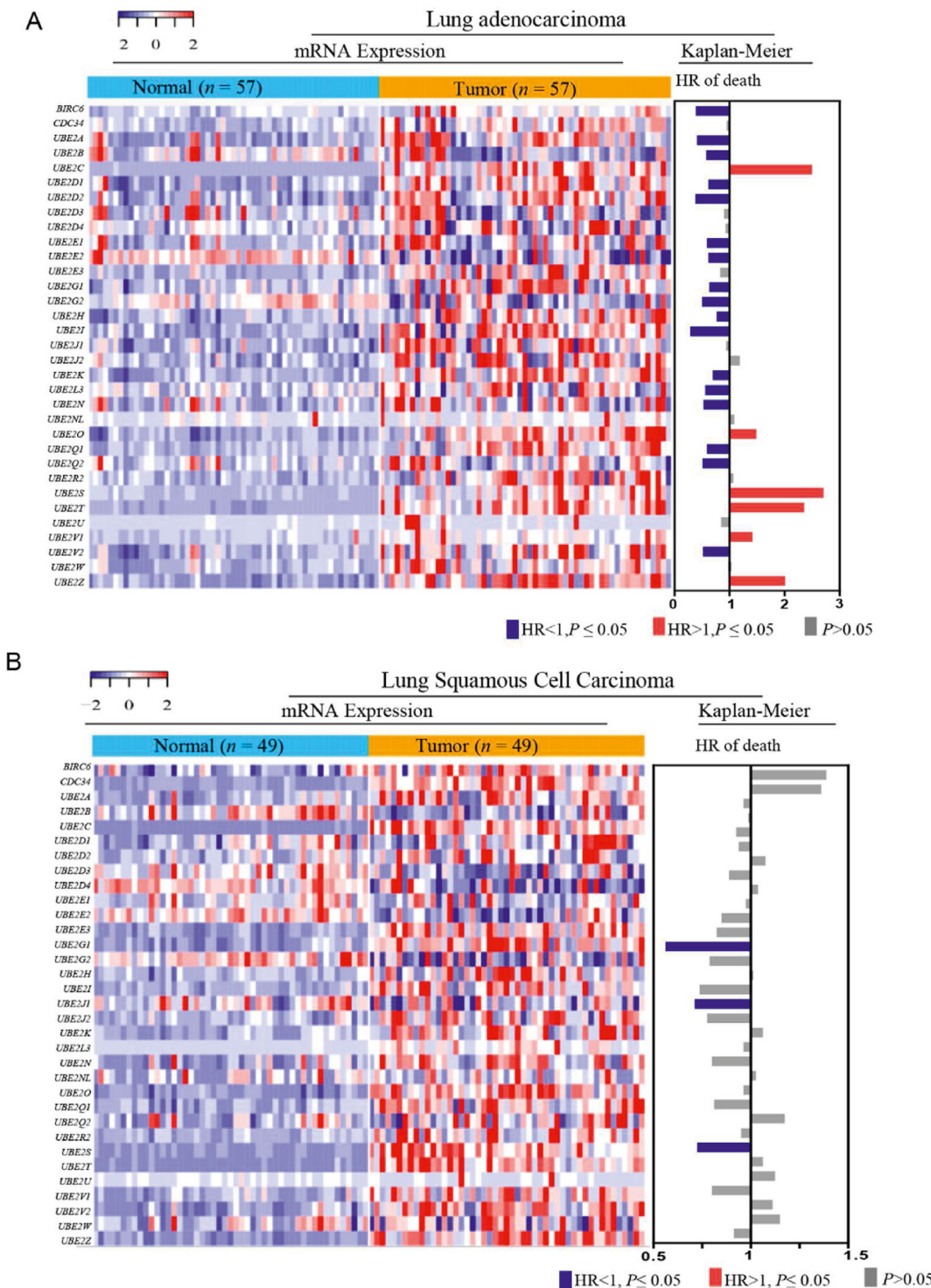


Figure 8 Multiomics analyses of E2s. (A, B) mRNA levels and Kaplan–Meier analyses of ubiquitination-associated E2s in lung adenocarcinoma and lung squamous cell carcinoma.

4. Overview of Ub and Ubl targeted drug discovery

The Ub and Ubl pathways are integral components of the ubiquitin–proteasome system (UPS) that is responsible for the degradation of over 80% of cellular proteins. In the past two decades, accumulated evidence confirmed that targeting 26S

proteasome (the downstream of UPS) had been viewed as a desirable outcome of anti-cancer therapeutics. This endeavor resulted in U.S. Food and Drug Administration (FDA) approval of the first proteasome inhibitor (PI) bortezomib (also called velcade) in 2003, for treatment of multiple myeloma and relapsed mantle cell lymphoma. Subsequently, other PIs, such as ixazomib,

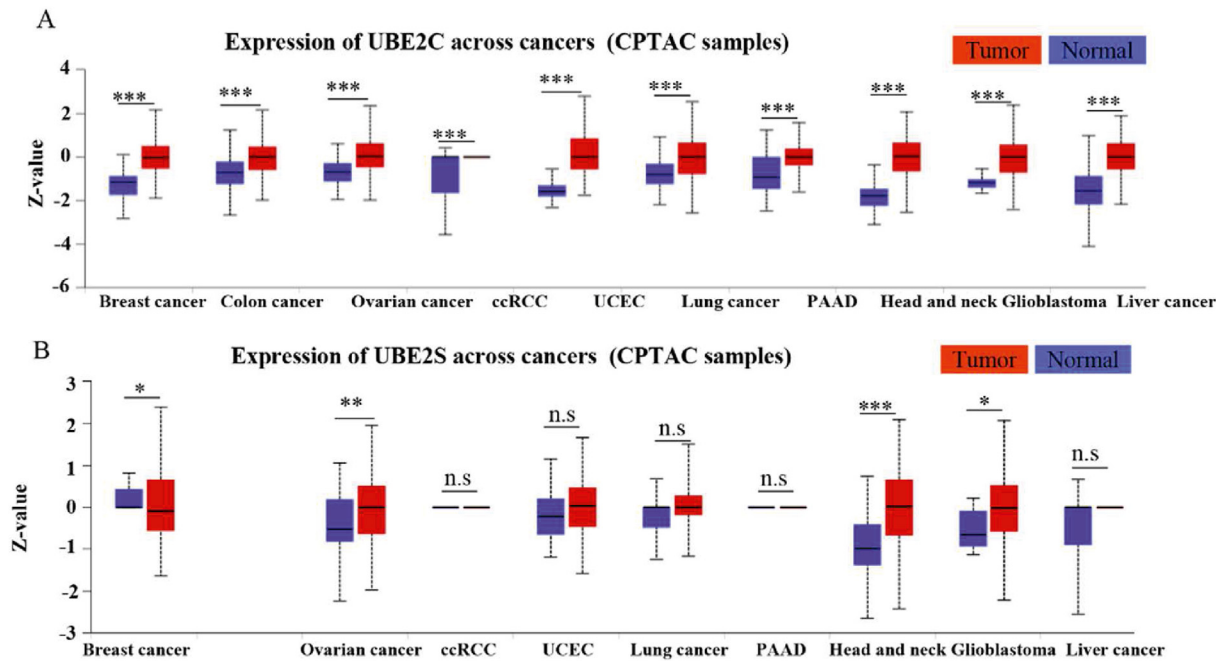


Figure 9 Gene expression levels of UBE2C and UBE2S in 10 tumors and normal tissues by exploring the CPTAC database in UALCAN website. Statistical significance was determined by the Mann–Whitney test (two-tailed): * $P < 0.05$, ** $P < 0.01$, *** $P < 0.001$, n.s. indicates no significant difference.

delanzomib, and carfilzomib, were approved, further validating anticancer reliability of UPS suppression in clinic. However, the application of PIs is hindered by limitations, including targeting specificity, oral stabilization, and low penetration into solid tumors, consistently constrain the application of PIs. For instance, PIs have shown limited effectiveness in solid tumors, even when combined with other antitumor agents. Recent rapid advances in the functions and mechanisms of Ub and Ubl pathway, offer potential solutions to address these challenges.

In this section, we categorized the current reported small molecule inhibitors targeting essential components of the Ub and Ubl pathways, including E1s, E2s, E3s, DUBs, as well as their structural characteristics, clinical research progress and limitations. We also discuss the application of E3s ligands in the studies of target protein degradation (TPD). Especially, molecular glue degraders (MGD), as a classical TPD type, are considered as a prospective therapeutic strategy in cancer therapies, to be summarized the current progress in this section. Recognizing the growing importance of bioinformatics approaches in the pharmaceutical industry, we also discussed the utilization of bioinformatics resources and methods to facilitate the TPD drug discovery based on the multiomic data.

4.1. Representative E1 and E2 inhibitors

As mentioned above, ubiquitination has two essential E1s, UAE1 (also known as UAE) and UBA6. The first successful attempt at UAE inhibition dates back to the 1990s. A nonhydrolyzable ATP analog, adenosyl-phospho-ubiquitinol, was designed and synthesized to evaluate the inhibitory activity of the UAE–Ub adduct in an ATP-competitive manner ($K_i = 50 \text{ nmol/L}$)²⁷⁴. This study first demonstrated the feasibility of selectively targeting the upstream of UPS, and developing small-molecular inhibitors of UAE. For a considerable amount of time, however, the majority of reported

UAE inhibitors lacked targeting specificity and potent inhibitory effects against UAE (half maximal inhibitory concentration $\text{IC}_{50} > 1 \mu\text{mol/L}$). Similar circumstances occurred during the development of Ubl inhibitors²⁷⁵. Not until 2009 did Soucy T.A. et al. develop the first NAE specific inhibitor, MLN4924 (also known as pevonedistat), with a new adenosine sulfamate (AdoS) skeleton (Fig. 12). MLN4924 is a potent and selective NAE inhibitor ($\text{IC}_{50} = 4 \text{ nmol/L}$) that is unrelated to other homologous enzymes, such as UAE, UBA6, and SUMO-activating enzyme (SAE) of SUMO ($\text{IC}_{50} = 1.50, 8.20, \text{ and } 1.80 \mu\text{mol/L}$, respectively)²⁷⁶. Furthermore, MLN4924 suppresses the growth of various cancer cell lines by inducing apoptosis, senescence, or sensitizing cancer cells to chemoradiation³³. The crystal structure of the MLN4924–NAE–NEDD8 ternary complex showed that MLN4924 not only binds with high affinity to the ATP-binding site of NAE but also forms a covalent cysteine thioester with NEDD8 via its terminal sulfamate moiety²⁷⁷.

The structure of MLN4924 inspired the researchers of Millennium Pharmaceuticals to successfully identify an AdoS analog, Compound 1, with potent UAE inhibiting activity²⁷⁸. Consistent with the mechanism of interaction between MLN4924 and the NAE complex, Compound 1 forms a covalent bond with Ub via its sulfamate group and then suppresses the formation of UAE–Ub thioester²⁷⁸. However, Compound 1 cannot be developed as a UAE inhibitor due to its nonselective effect on other E1 enzymes, including NAE and SAE. To develop highly selective UAE inhibitors, Hyer et al.¹¹ screened seven hundred small-molecular compounds and identified a potent, mechanism-based UAE inhibitor, TAK-243. Similar to Compound 1, the sulfamate moiety of TAK-243 blocks the covalent linkage between UAE and Ub. In contrast to Compound 1, TAK-243 not only inhibits UAE ($\text{IC}_{50} = 1 \text{ nmol/L}$), but also UBA6 ($\text{IC}_{50} = 7 \text{ nmol/L}$), NAE ($\text{IC}_{50} = 28 \text{ nmol/L}$), and SAE ($\text{IC}_{50} = 850 \text{ nmol/L}$)¹¹ at a lesser extent (Fig. 12). Accumulated evidence has shown that TAK-243

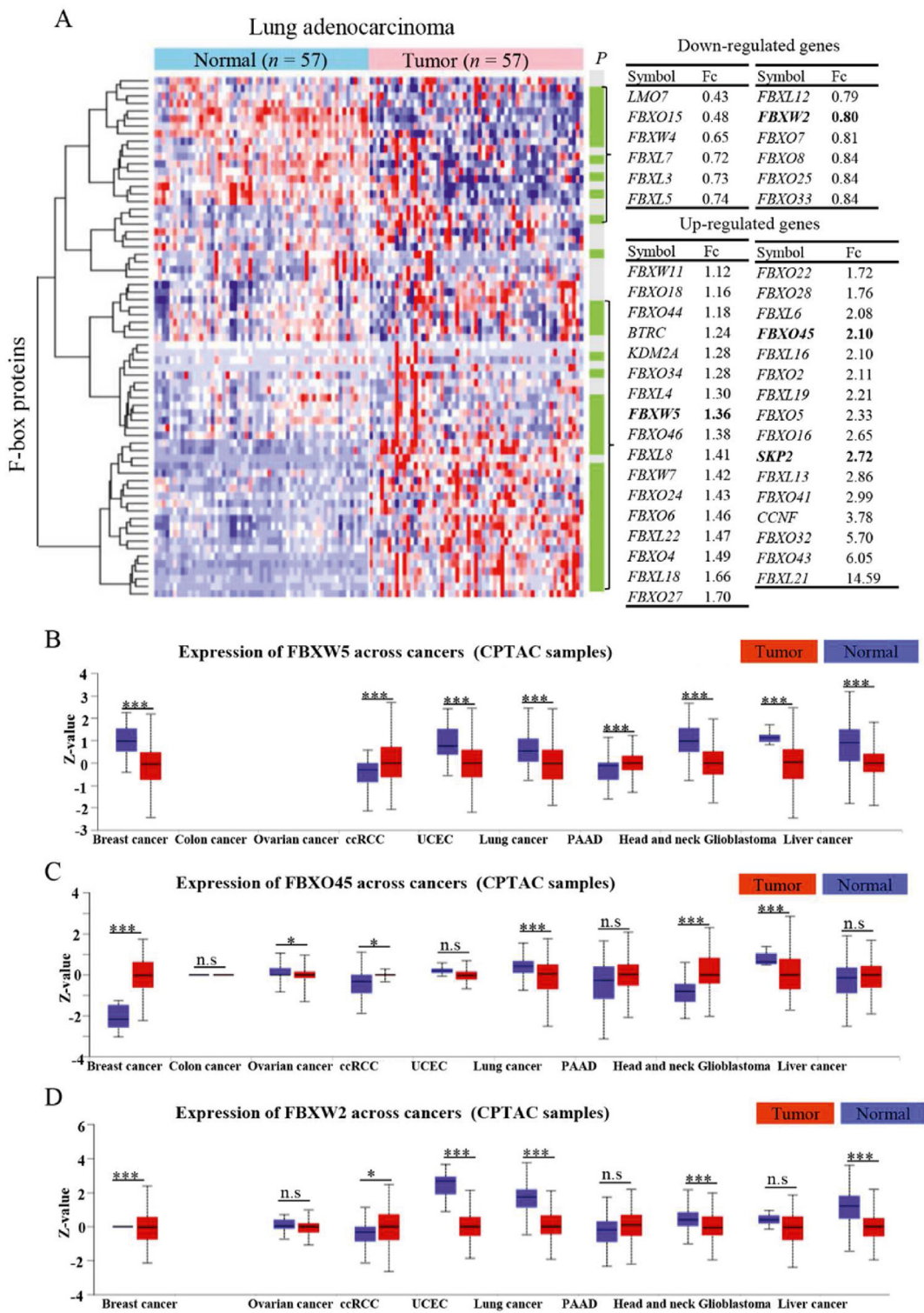


Figure 10 Multiomics analyses of F-box proteins ($n = 69$). (A) mRNA levels and prognostic values of F-box proteins in lung adenocarcinoma. (B–D) Protein expression levels of FBXW5, FBXO45 and FBXW2 in tumors and normal tissues by exploring the CPTAC database in UALCAN website.

completely suppresses the cellular ubiquitylation and induces ER stress-mediated apoptosis¹¹. According to the data from the ClinicalTrials website, TAK-243 has now entered the clinical phase for treating patients with acute/chronic myeloid leukemia or

myelodysplastic syndrome. Considering the potent SAE inhibition of Compound **1** and the high similarity between UAE and SAE, Langston et al.²⁷⁹ hypothesized that the sulfamate group of Compound **1** may also help covalently bind the SUMO–AdoS

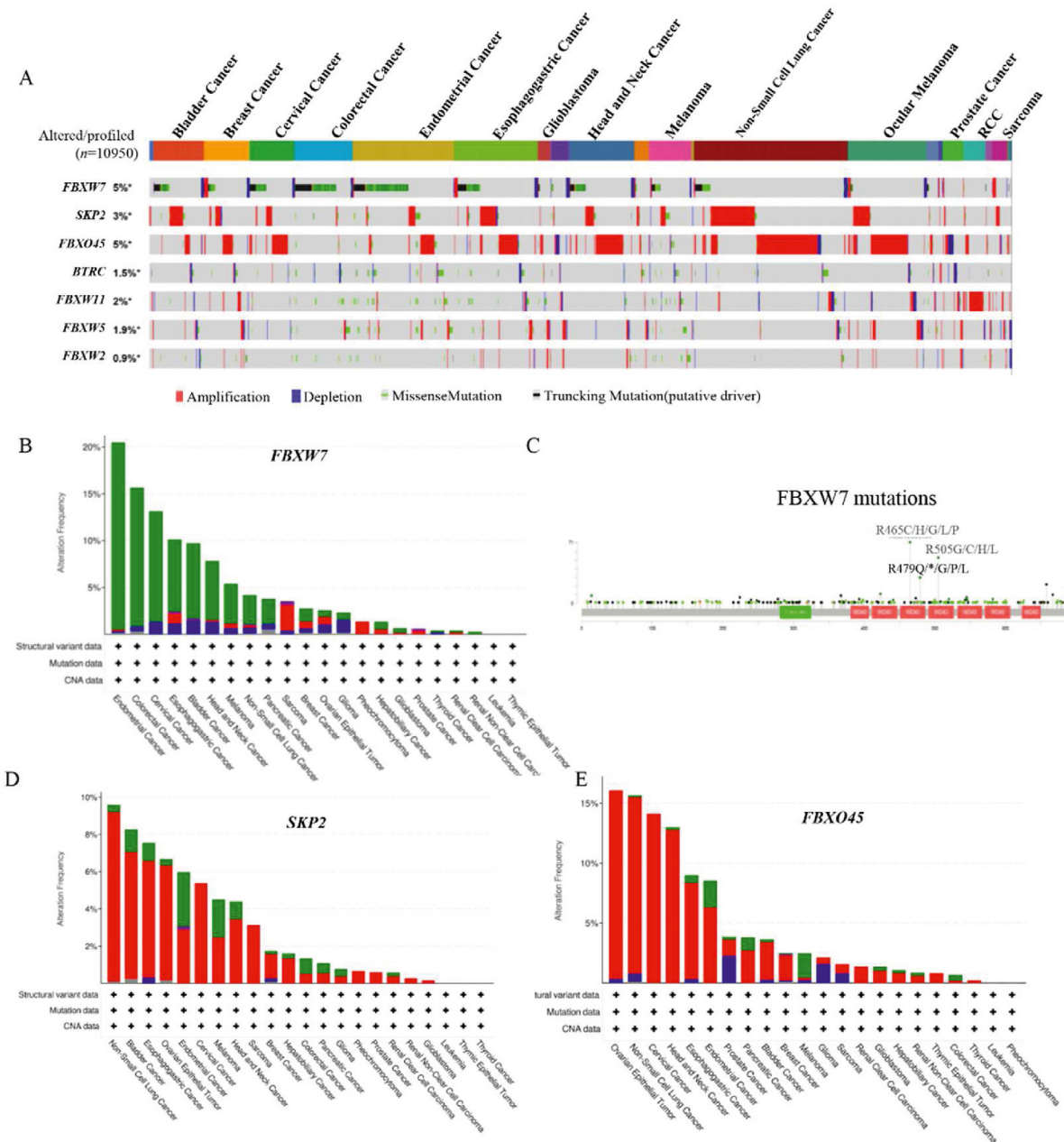


Figure 11 Multiomics analyses of F-box proteins. (A) Gene alterations of 7 F-box proteins were determined in 33 tumors via the exploration of cBioPortal website. (B) Cancer type summary about altered SKP2, FBXO45 and FBXW7. (C) Mutation site analysis of FBXW7 by exploring the cBioPortal website. (D, E) Cancer type summary about altered SKP2 and FBXO45.

adduct. Then, several Compound 1 analogs were synthesized, and their SAE inhibitory effects were investigated using the homogenous time-resolved fluorescence assay. TAK-981 was identified to specifically bind the enzyme SAE ($IC_{50} = 1$ nmol/L) more effectively than other E1 (IC_{50} , NAE = 0.96 μ mol/L, UAE > 1 μ mol/L). To date, TAK-981 has entered phase I clinical trials for patients with metastatic solid tumors in combination with pembrolizumab and non-Hodgkin's lymphoma in combination with rituximab (NCT03648372, NCT04074330, and NCT04381650)²⁷⁹.

Although E2s may constitute a promising target for anticancer therapeutics, comparatively fewer E2 small-molecular inhibitors have been reported than E1 inhibitors. Ceccarelli et al.²⁸⁰ screened

and identified a small molecule, CC0651 that selectively inhibits the E2 Ub-conjugating enzyme Cdc34. The crystal structure of the CC0651–Cdc34A–Ub complex revealed that CC0651 stabilizes a low-affinity interaction with a composite binding pocket generated by Cdc34A and Ub²⁸¹. Similar to TAK-243, CC0651 induces the accumulation of p27 by inhibiting its degradation ($IC_{50} = 1.7 \mu\text{mol/L}$) and suppresses the growth and proliferation of various cancer cell lines. Moreover, Tsukamoto et al.²⁸² identified leucettamol A ($IC_{50} = 105 \mu\text{mol/L}$) from the *Leucetta sponge* as the first Ubc13 inhibitor, and subsequently isolated two more Ubc13 inhibitors, Manadosterols A and B, which are derived from the marine sponge *Lissodendryx fibrosa* ($IC_{50} = 90 \text{ nmol/L}$ and 130 nmol/L , respectively). In contrast to several Ub- and

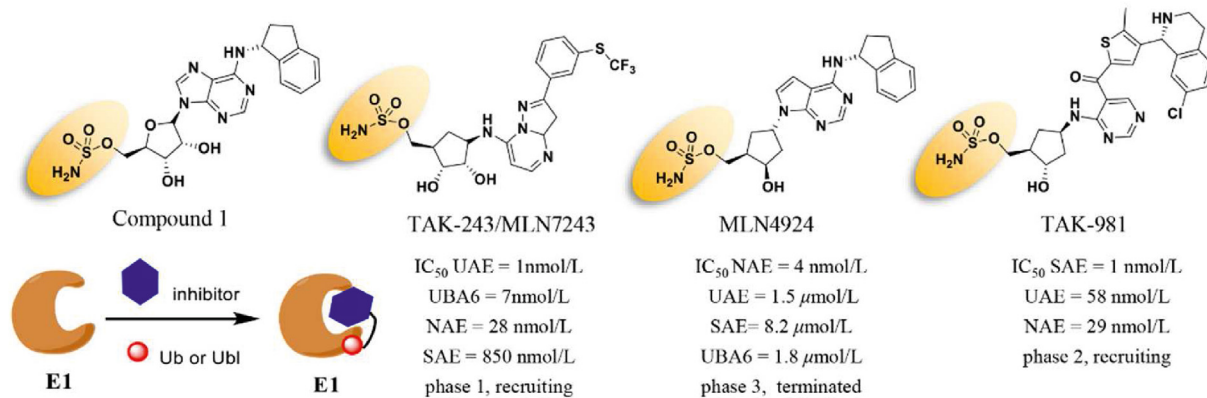


Figure 12 Chemical structures of AdoS-derived covalent inhibitors targeting E1 and their inhibitory mechanism.

NEDD8-related E2s, Ubc9 is the only E2 in the SUMOylation pathway. The submicromolar Ubc9 inhibitory activity of flavonoid analog 2D08 is utilized as a positive probe to identify other new Ubc9 inhibitors²⁸³.

4.2. Small-molecule ligands targeting RING E3 ligases

The Ub and Ubl pathways regulated the degradation of various substrates by establishing a PPI network involving human E3 ligase proteins as mentioned above. Over the past two decades, the development of PPI inhibitors has emerged as a viable and important technique for drug discovery targeting E3 ubiquitin ligases^{8,284}. However, these PPI inhibitors are still primarily based on the concept of “occupancy-driven” small-molecule modalities, also known as the inhibitor-centric approach. Unfortunately, only approximately 20% of the human proteome is druggable for an inhibitor-centric development approach. To address the critical limitations of the inhibitor-centric approach, the development of E3-associated modulators has introduced the concept of target protein degradation (TPD) as a novel pharmacologic modality²⁸⁵. Notably, proteolysis-targeting chimeras (PROTACs) have expanded the application of PPIs and provided insights into the degradation pathways for drug discovery^{286–289}. PROTACs are typically composed of an E3 small-molecule ligand, a connecting linker, and a target protein ligand²⁸⁷. The successful development of high-quality E3 small-molecule ligands is essential for PRO-TAC development. However, the lack of suitable E3 ligase ligands has been a major obstacle in the development of PROTAC degraders²⁹⁰. Fortunately, drug-like small-molecule ligands have been continuously developed to bind to the substrate receptor subunits of CRLs, such as CRL1^{Skp2}, CRL2^{VHL}, CRL3^{Keap1}, CRL3^{SPOP}, and CRL4^{CRBN}. Beyond that, ligands targeting other E3 ligases, such as MDM2 and cIAP, have been developed as E3 inhibitors or as part of PROTAC molecules^{290,291}. Among them, CRL4^{CRBN} and CRL2^{VHL} ligands have achieved notable success and are widely used in TPD studies and PROTAC design²⁹². In the following, we will highlight the recent progress in small-molecule ligands targeting RING E3 ligases.

4.2.1. Small-molecule ligands of cullin RING E3 ligases

Numerous studies have confirmed that CRL1^{Skp2} inhibits apoptosis and cell cycle arrest by regulating the degradation of cell cycle inhibitors p21 and p27, suggesting that Skp2 is a promising anticancer target. Chan et al. conducted a high-throughput virtual screening to identify several potential Skp2

inhibitors²⁹³ and found that Compound 25 displayed better Skp2 inhibitory activity than the other hit compounds and suppressed the survival of cancer cells and cancer stem cells. This study was the first to demonstrate that the pharmacological inactivation of Skp2 constitutes a promising approach for cancer treatment²⁹³. Although Wu et al.²⁹⁴ had previously identified a series of Skp2 probes *in silico*, including thiazolidinedione derivatives C1 and C2, there was insufficient evidence to support their anticancer effect.

As a CRL2 substrate receptor, VHL regulates the degradation of HIF-1 α and is involved in hypoxia adaptation. Previous studies have reported that residue hydroxy proline 564 (Hyp564) of HIF-1 α is essential to bind VHL, thereby targeting Hyp of HIF-1 α regulating its ubiquitin-mediated proteasomal degradation^{295,296}. Buckley et al.^{297,298} modified the structure of Hyp *in silico* to rationally design Hyp analogs, discovering the first small-molecule inhibitor that suppressed the PPI of VHL and HIF-1 α at submicromolar concentrations. Soares et al.²⁹⁹ further modified these Hyp analogs according to structure-guided and fragment-based drug design. Probe VH298 was identified as the first inhibitor with a double-digit nanomolar affinity for CRL2^{VHL} binding *in vitro* and *in vivo*²⁹⁹. Recently, a series of bifunctional small molecules containing two homologous VHL ligases, also known as Homo-PROTACs, were designed to dimerize the enzyme VHL and induce its self-degradation. The most active Homo-PROTAC, CM11, was designed as a selective and powerful VHL degrader at a concentration of 10 nmol/L³⁰⁰.

CRL3 possesses two primary E3 ubiquitin ligases, Keap1 and SPOP. CRL3^{Keap1} destabilizes its primary substrate Nrf2 to regulate the expression of antioxidant proteins and inflammatory regulators. Recently, CRL3^{Keap1} has steadily emerged as an attractive target for cancer therapy alongside various other diseases, such as diabetes, Alzheimer’s disease, and Parkinson’s disease, which involve oxidative stress and inflammation³⁰¹. According to prior research, in a phase 3 trial, the clinical candidate CDDO-Me inhibited the interaction between cullin3 and Keap1. Additional research demonstrated that CDDO-Me covalently binds to the BTB domain of Keap1³⁰². Biogene conducted a high-throughput screening to identify small molecules that directly inhibited the PPI of Keap1 and Nrf2³⁰². In a homogeneous fluorescence polarization assay, more than 300 thousand compounds were screened and evaluated. As the most active compound, ML334 exhibited a high affinity for Keap1 ($K_d = 1.00 \mu\text{mol/L}$)³⁰³. Additionally, Jiang et al.³⁰⁴ modified a potential Keap1 inhibitor by screening the commercial Evotec Lead Discovery library and

identified Compound **25** as an effective inhibitor of the interaction between Nrf2 and Keap1 with a half maximal effective concentration of 28.6 nmol/L. Recently, Astex Pharmaceuticals developed a series of novel oxathiazepin derivatives with potent affinity *via* fragment-based molecular modification and optimization. The analog KI-696 was inhibited the Keap1–Nrf2 interaction at a single nanomolar concentration ($K_d = 1.30$ nmol/L)³⁰⁵. SPOP with the BTB domain plays vital roles in the growth and progression of tumors by mediating the ubiquitination of several important substrates, such as PTEN and DUSP7^{157,306,307}. Jiang et al.^{308,309} identified a series of small-molecule SPOP inhibitors by integrating virtual screening, pharmacophore modeling, and molecular docking. They further found optimal Compound **6b** to inhibit SPOP-mediated PPI in ccRCC cells at a concentration of 10 μmol/L. Following optimization and SAR analyses, Compound **6c** was identified as having superior SPOP inhibition and ccRCC cytotoxicity to those of **6b**^{308,309}.

4.2.2. Small-molecule ligands of single-subunit RING E3s ligases IAPs and MDM2 ligands

Unlike CRLs, IAPs and MDM2 are two classical single-subunit protein RING E3 ubiquitin ligases. The IAP family, which consists of cIAP1/2 (cellular inhibitor of apoptosis) and XIAP (X-linked inhibitor of apoptosis), induces apoptosis by various mechanisms, including receptor-mediated, mitochondria-mediated, and TNF factor receptor 1 (TNFR1)-mediated apoptosis^{310,311}. The IAP family is typically composed of a ubiquitin-associated (UBA) domain, a RING domain, and multiple BIR domains (BIR1/2/3). Du et al.³¹² revealed that the second mitochondria-derived activator of caspase [SMACs, also known as direct IAP-binding protein with low pI (DIABLO)] has a promising endogenous antagonistic effect against IAPs *via* interacting with BIR2 and BIR3 domains. Extensive studies have shown that an N-terminal four peptide molecule (Ala1–Val2–Pro3–Ile4, AVPI) forms a similar binding model with SMAC (SMAC $K_d = 420$ nmol/L, AVPI $K_d = 580$ nmol/L)³¹³. The binding model showed that the amino group (–NH₂) and carbonyl group (–C=O) of AVPI form multiple hydrogen bonds with the corresponding residues Glu314, Gln319, Trp310, Trp323, and Thr308. Based on the SARs of AVPI–BIR3, several SMAC mimetics were designed to assess the IAP inhibitory activity (Fig. 13). Genentech had advanced GDC-0152 and GDC-0917, the first-generation IAP inhibitors, through phase 1 clinical trials. Compared to pan-IAP inhibition of GDC-0152, GDC-0917 displayed a 250-fold more selectivity for cIAP over XIAP^{314,315}. In addition to GDC-0152 and GDC-0917, Novartis has also developed the SMAC analog LCL161, a 1st generation peptidomimetic that recently passed phase 2 clinical trials for patients with relapsed or refractory multiple myeloma³¹⁶. Subsequently, a series of peptidomimetic BIR3 IAP antagonists with bicyclic lactam skeletons were published by Sun et al.³¹⁷, which advanced the research of second-generation IAP antagonists. Cyclization of valine and proline formed [8,5]-bicyclic Debio-1143 (also known as Xevipant), a 2nd generation IAP antagonist. Subsequent research showed that Debio-1143 possessed superior inhibitory selectivity (IC₅₀ XIAP and cIAP1/2 BIR3 = 66.4, 1.9, and 5.1 nmol/L, respectively) and pharmacokinetic properties than the majority of 1st generation inhibitors. Currently, a phase 3 clinical trial is recruiting patients with locally advanced squamous cell carcinoma of the head and neck treated with Debio-1143 in conjunction with platinum-based chemotherapy (NCT04459715).

As described above, the BIR3 domain of IAPs binds to caspase-9 whereas the BIR2 domain binds to caspase-3/7³¹⁸. Previously reported monovalent antagonists always bind to the BIR3 domains of XIAP and c-IAP1, and the majority exhibit higher selectivity than BIR2 selectivity. Li et al.³¹⁹ proposed a 3rd generation SMAC mimetic with a distinct dimer skeleton that more effectively induced apoptosis in human cancer cells (Fig. 13). In addition, the results demonstrated that the bivalent antagonists had superior inhibitory efficacy against caspase-3/7 and –9 by engaging both BIR2 and BIR3 domains of the IAP family. Inspired by the aforementioned discoveries, two representative bivalent IAP antagonists APG-1387³²⁰ and birinapant³²¹, were further developed by Ascension and TetraLogic, respectively. APG-1387 had been applied to patients recruited in phase 1 clinical trials to treat advanced solid tumors or hematologic malignancies (NCT03386526). However, various druggability problems, including physicochemical features (high MW, high TPSA) and poor oral bioavailability, limited the use of either APG-1387 or birinapant in the treatment of solid tumors. Using fragment-based drug discovery, nonalanine small molecules, as a new class of IAP antagonists have recently been developed³²². Tolipanapt (also known as ASTX660), a nonalanine and dual antagonist of XIAP and c-IAP1 (IC₅₀ = 2.80 and 0.22 nmol/L, respectively), was synthesized from a simple acetylamine fragment³²². Compared to previously reported antagonists, linapant exhibited reduced hERG inhibition (30% @ 30 μmol/L) and adequate oral efficacy.

MDM2 is another representative single protein RING E3 ligase³²³. MDM2 promotes p53 degradation to adversely regulate the tumor suppressor p53, thereby restraining p53-mediated cell cycle arrest and cell apoptosis (Fig. 14). In 2004, Roche reported the first selective MDM2 inhibitor, Nutlin-3a, that was identified from a series of *cis*-imidazoline-derived molecules³²⁴. Nutlin-3a inserts its two 4-chlorophenyl groups into the Trp23 and Leu26 pockets by mimicking the interaction of the p53 peptide, which directs its isopropoxy group toward the Phe19 pocket. Meanwhile, its *cis*-imidazoline scaffold replaces the helical backbone of the p53 peptide without polar hydrogen bonding interactions. According to the SARs, Roche further optimized the structure of Nutlin-3a to increase its potency and metabolic stability. As the first clinical MDM2 inhibitor, the analog molecule RG7112 had completed phase 1 clinical trials for patients with advanced solid tumors and hematologic neoplasms (NCT00623870, NCT00559533)³²⁵. According to a subsequent mechanistic investigation of the MDM2–p53 interaction, the indole ring of Trp23 residue in p53 is deeply inserted into a hydrophobic cavity on the surface of MDM2, and its NH group forms a hydrogen bond with residues in MDM2 (p53-Trp23/MDM2-Leu54)³²⁶. Inspired by this observational result, Ding et al.³²⁶ mimicked the structural interaction of Trp23 residue in p53 with MDM2 by deriving a unique spirooxindole alkaloids and subsequently identified a series of potent non-peptide MDM2 inhibitors³²⁷. Additionally, the optimal variant SAR405838 had completed phase 1 safety testing. In recent years, several analogs of SAR405838, such as RG7388103 from Roche³²⁸, APG-115 from Ascension³²⁷, and DS-3032b from Daiichi Sankyo³²⁹, have entered clinical trials.

Chiral drug design is important for the development of MDM2 inhibitors. In 2012, researchers at Amgen developed a series of novel piperidinone-derived MDM2 inhibitors *via de novo* design and chiral synthesis³³⁰. These chiral inhibitors maintain the binding model of previous molecules that occupy with the Trp23,

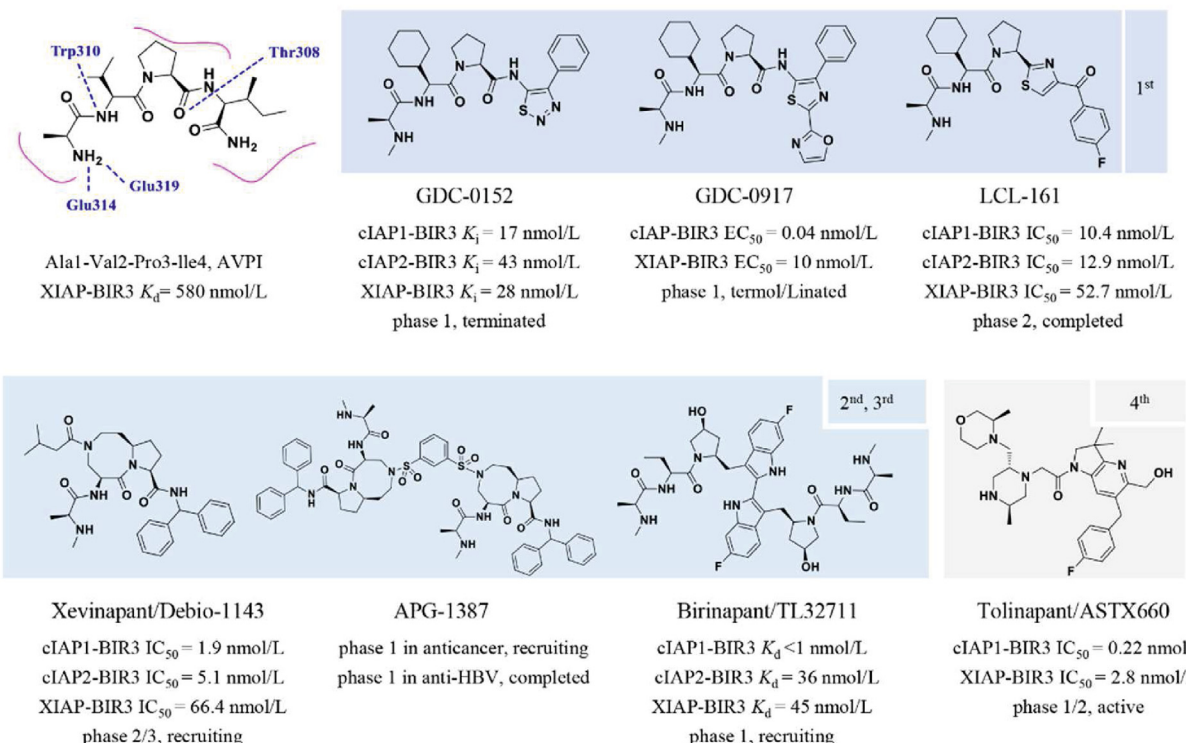


Figure 13 Various generations of IAP antagonists, 1st generation Smac peptidomimetic antagonist family, 2nd generation Smac peptidomimetic antagonist with bicyclic structure, 3rd generation Smac peptidomimetic antagonist family with bivalent structure, non-peptide IAP antagonists.

Leu26, and Phe19 pockets of MDM2, as well as generating an electrostatic interaction between the carbonyl linker and the imidazole side chain of His96 in MDM2³³⁰. AMG232, the preferred compound, exhibits significant MDM2 inhibitory

activity (surface plasmon resonance [SPR] K_D = 0.045 nmol/L, SJS-A1 EdU IC₅₀ = 9.10 nmol/L) as well as promising pharmacokinetics characteristics and antitumor activity in the SJS-A1 osteosarcoma mice-bearing xenograft model (ED₅₀ = 9.10 mg/

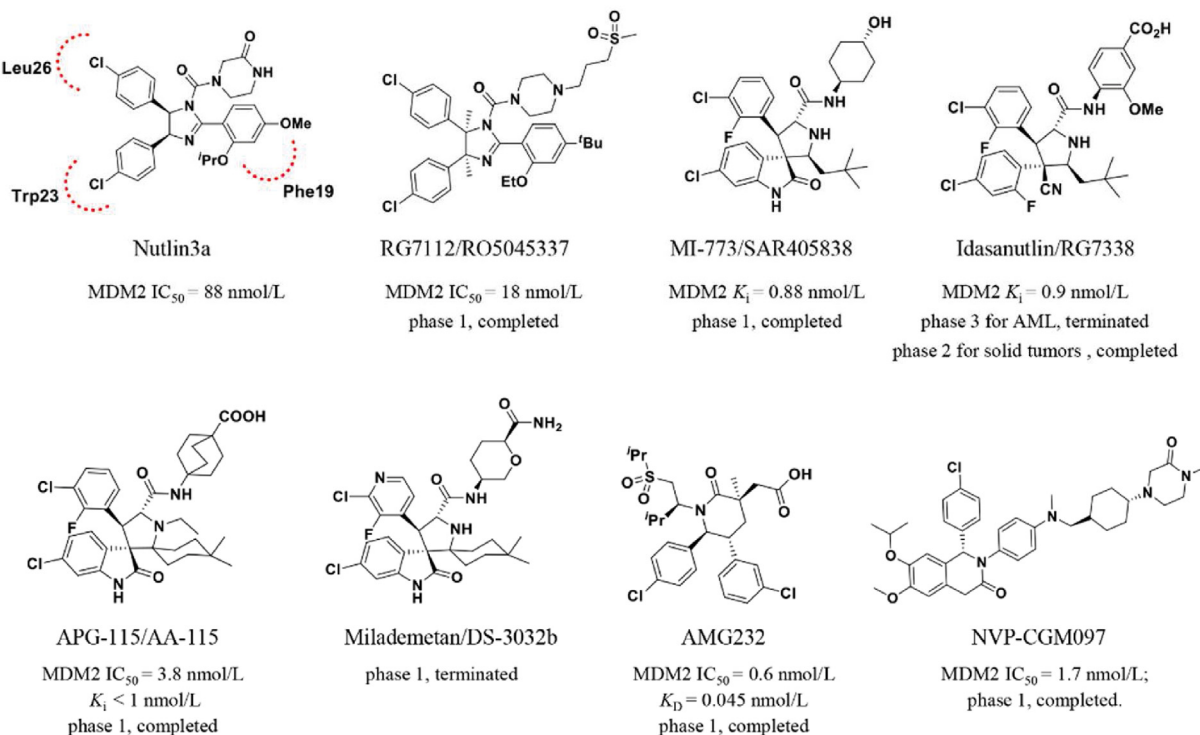


Figure 14 Chemical structures of clinical MDM2 inhibitors.

kg³³¹. Besides, Novartis developed a series of dihydroisoquinolinone p53-MDM2 inhibitors from the virtual screening of 50,000 compounds developed in house³³². Based on the binding pocket of p53-MDM2 by X-ray crystallography and molecular modeling, they identified a clinical candidate, NVP-CGM097³³³.

4.3. Progress and trend in the development of CRL E3 ligases-associated molecule glue degraders

Protein of interest (POI) involves artificially inducing target protein degradation by the UPS, lysosome system, or even autophagy, which represents a R&D breakthrough of PPI to attract huge attention and funding from both academia and the pharmaceutical industry³³⁴. UPS-associated TPD involves two major approaches, PROTAC and MGD. In contrast to PROTACs, MGDs induce the proximity of ligase and POI by matching the protein surface topologies and modulating the binding attitude with ligase and POI. As a result, MGDs display comparable TPD ability while sharing the similar molecular weight and druggable structures with small-molecule agents. Although a rational approach had been reported previously to discover the MGD, largescale discovery of MGDs will require more innovations in screening assays and a deeper understanding of ligase associated PPI readout.

Over the past decades, the bioinformatics revolution has been the beneficiary of a multiomics data explosion, which contributes to improve cancer therapy strategies by extracted enormous useful information. Particularly, the multiomics data, such as genomics, transcriptomics, proteomics and metabolomics data, were generated by high-throughput technologies integrated with drug-response data, provides opportunities for identifying anticancer biomarkers and predicting drug responses. Moreover, multiple biological networks, including PPI network, drug-target network and disease-gene network, are extensively combined with multiomics data to analyze the potency of anticancer targets and facilitate PPI-based drug discovery. In the following, we want to focus on the progress in hijacking CRLs with MGDs, along with the identification of TPD via bioinformatics profiling.

4.3.1. Outline of CRL E3 ligases-associated molecule glue degraders

CRLs ubiquitinate diverse substrate proteins when brought into direct proximity to the ligase³³⁵, including CRL4^{CRBN} and several other substrates of the CRL4 family, such as CRL4^{DCAF15} and CRL4^{DDB1}, attracting considerable attention from pharmaceutical companies owing to their efficacy in the discovery of MGDs (Table 1). In early 2010, CRBN was identified as an immune-regulated target of thalidomide and pomalidomide^{336,337}. However, the mechanism by which these thalidomide-like IMiDs regulate CRL4^{CRBN}, thereby inducing immunomodulatory and anti-inflammatory effects, remains unknown^{336,337}. Lenalidomide was not identified to selectively exploit the ubiquitination and degradation of two lymphoid transcription factors Ikaros (IKZF1) and Aiolos (IKZF3) till 2014^{191,338}. Celgene identified a potent CRL4^{CRBN} molecular glue, thalidomide-derived CC885, that selectively degraded more GSPT1 than IKZF1/3¹⁸⁹. Conversely, neither pomalidomide nor lenalidomide degraded GSPT1, indicating that specific neosubstrate recruitment characteristics are associated with structural differences across IMiDs. The aryl sulfonamide derivative indisulam is a clinical candidate exhibiting selective anticancer activity³³⁹. Han et al.³³⁹ identified the mechanism underlying the anticancer selectivity of indisulam,

which recruited the pre-mRNA splicing factor RBM39 (RNA-binding motif protein 39) to CRL4^{DCAF15} for proteasomal degradation.

Previously reported molecular glues induce the degradation of specific substrates by binding to the CRL4 substrate receptors than the CRL4 adaptor proteins. Stabicki et al.³⁴⁰ analyzed the sensitivity of 4,518 clinical and preclinical drugs in 578 cancer cell lines via high-content screening alongside their relative E3 ligase component mRNA levels. A CDK12 inhibitor, (R)-CR8, revealed a correlation between cytotoxicity and CRL4^{DDB1} mRNA levels. Further studies showed that (R)-CR8 functions as a molecular glue to regulate protein cyclin K degradation³⁴⁰. X-ray crystallography studies of the DDB1–(R)-CR8–CDK12–cyclin K complex demonstrated that (R)-CR8 binds to the ATP-binding pocket of CDK12, forming a high affinity with the DDB1 domain. Previously, the thiazolyl derivative HQ461 was identified as a potential anticancer small molecule capable of inhibiting Nrf2 activity. To reveal the functional mechanism of HQ461, Lv et al.³⁴¹ performed a pooled genome-wide CRISPR-Cas9 knockout screening in lung cancer cells A549 by targeting 19,114 genes with 4 individual sgRNAs per gene. According to the findings, HQ461 converts CDK12 into CRL4^{DDB1} to initiate polyubiquitination and subsequent degradation of the partner protein cyclin K of CDK12. Mayor-Ruiz et al.³⁴² screened a library of >2000 small molecules in either wildtype or UBE2M^{mut} KBM7 cells and found that dCeMM1/2/3/4 displayed a correlation between cytotoxicity and UBE2M-associated cullin4 levels via scalable chemical profiling. Further studies revealed that dCeMM2/3/4 analogs regulated the ubiquitination-mediated degradation of cyclin K by prompting the interaction of CDK12 and cyclin K.

4.3.2. Multi-omics approaches empower the identification of CRL E3 ligases-associated molecule glue degraders

Interestingly, the majority of reported CRL-associated molecular glues are subordinate to CRL4 substrate receptors or adaptors, including CRBN, DCAF15, and DDB1. Notably, cell-based phenotypic assays have provided the richest source for MGD identification. It is hypothesized that numerous screening models were initially established using cell viability-based phenotypes, leading to the identification of hit compounds that interacted with CRL4 substrate receptors and adaptors. However, the traditional MDG discovery approaches face challenges in evaluating the relationship of CRL4 and cell-viability-based assay. These studies still heavily rely on the cell-viability-associated readouts to promote their MDG design, which results in the limitation that the targeted regulators are limited to those with an essential function in cell viability, such as CRL4 in possible. To overcome these limitations, it is crucial to advance phenotypic screens that can be measured, quantified, interpreted, and predicted, enabling a better understanding of MDG discovery. Modern high-throughput screening technologies, such as microarray and next-generation sequencing, have generated vast amounts of biological data that can be integrated in multiomics studies to explore the functional and mechanistic complexity of ubiquitin (Ub)-associated TPD.

Numerous existing data resources, including cancer-gene databases like Online Mendelian Inheritance in Man (OMIM) and Genetic Association Database (GAD), patient omics data from The Cancer Genome Atlas (TCGA) and Gene Expression Omnibus (GEO), and cancer-associated Kyoto Encyclopedia of Genes and Genomes (KEGG), along with drug-gene databases such as DrugBank, Therapeutic Target, and Clinical Trials, serve as foundational resources for bioinformatics analyses of PPI

Table 1 List of representative anticancer small molecules by targeting E2s, CRLs or DUBs.

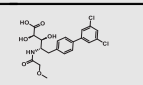
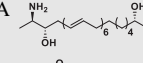
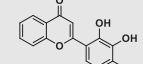
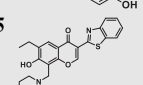
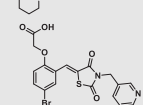
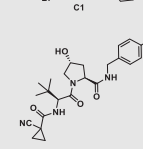
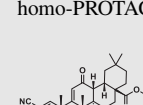
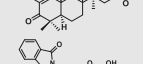
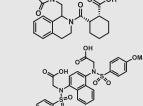
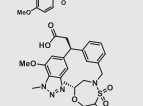
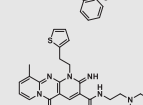
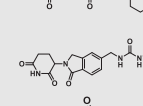
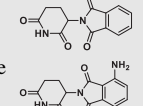
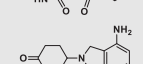
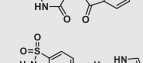
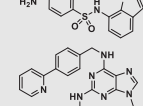
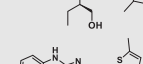
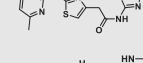
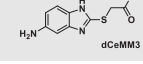
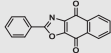
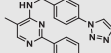
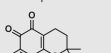
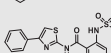
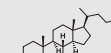
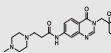
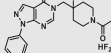
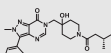
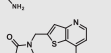
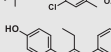
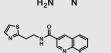
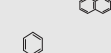
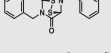
Name	Structure	Target	In vitro	In cells	Cell viability, Cancer cell lines Ref. IC ₅₀
CC0651		Cdc34	IC ₅₀ (FP) = 2.5 μmol/L	p27 deubiquitination @ 30 μmol/L	HCT116 280,281
Leucettamol A		Ubc13	105 μmol/L		282
2D-08		Ubc9	IC ₅₀ = 6 μmol/L	100 μmol/L	BT-474 283
Compound 25		CRL1 ^{Skp2}	>80% inhibition@5 μmol/L	p21, p27 deubiquitination @ 5 μmol/L	<10 μmol/L PC-3, LNCaP 293
C1, C2, C16, C20			>80% inhibition@10 μmol/L	p21, p27 deubiquitination @ 10 μmol/L	MCF-7, TD47, LNCaP 294
VH298		CRL2 ^{VHL}	IC ₅₀ (FP) = 80 nmol/L; @ 50 μmol/L <i>K</i> _d (ITC) = 90 nmol/L	HIF-1α destabilization	No cytotoxic HeLa 299
CM11	homo-PROTAC		<i>K</i> _d (ITC) = 25 nmol/L @ 1 μmol/L	HIF-1α destabilization	HeLa 300
CDDO-Me		CRL3 ^{Keap1}	58.9%@0.1 μmol/L	50 –160 nmol/L	MCF-7 302
ML334			<i>K</i> _d = ~ 1 μmol/L	EC ₅₀ = 18 μmol/L	U2OS 303
Compound 2			EC ₅₀ = 28.6 nmol/L	Nrf2–ARE induction@10 μmol/L	HepG2-ARE-C8 304
KI696			<i>K</i> _d (ITC) = 1.3 nmol/L		305
6lc		CRL3 ^{SP0P}	<i>K</i> _D = 30 μmol/L 15 μmol/L	PTEN deubiquitination @ 2.1 –3.5 μmol/L	A498, OS-RC-2 308,309
CC885		CRL4 ^{CRBN}		GSPT1 degradation @ 1 nmol/L	NB4 189
Thalidomide					336
Pomalidomide					337
Lenalidomide				IKZF1 and IKZF3 degradation @ 1 μmol/L	MM1S 191,338
Indisulam		CRL4 ^{DCAF15}		RBM39 degradation @ 2 μmol/L	HCT116 339
CR8				Cyclin K degradation @ 1 μmol/L	HCT116 340
HQ461			DC ₅₀ = 0.13 μmol/L	1.5 μmol/L	A549 341
dCeMM2/3/4			Cyclin K degradation @ 2.5 μmol/L		KBM7 342

Table 1 (continued)

Name	Structure	Target	In vitro	In cells	Cell viability, Cancer cell lines Ref. IC_{50}		
SJB2-043		USP1	0.54 $\mu\text{mol/L}$	>80% inhibition @ 1 $\mu\text{mol/L}$	1.1 $\mu\text{mol/L}$	K562	347
ML323			76 nmol/L	PCNA deubiquitination @ 20 $\mu\text{mol/L}$	3 $\mu\text{mol/L}$	H1299	348
Q29		USP2	82% inhibition @ 0.5 $\mu\text{mol/L}$	NA	4.7 $\mu\text{mol/L}$	DU145	350
ML364			1.1–1.7 $\mu\text{mol/L}$	cyclin D1 destabilization @ 0.97 $\mu\text{mol/L}$	3 $\mu\text{mol/L}$	HCT116	351
LCAHA			9.7 $\mu\text{mol/L}$	cyclin D1 destabilization @ 20 $\mu\text{mol/L}$	0.9 $\mu\text{mol/L}$	HCT116	352
XL188		USP7	90 nmol/L	p53 accumulation @ 5 $\mu\text{mol/L}$		MM.1S, MCF7	357
FT671			52 nmol/L	p53 accumulation @ 10 $\mu\text{mol/L}$	33 nmol/L	HCT116, MM.1S, MCF7	358
Compound 4			6 nmol/L	p53 accumulation @ 1 $\mu\text{mol/L}$	2–29 nmol/L	HCT116	359
Compound 41			0.44 nmol/L	p53 accumulation @ 25 nmol/L	0.09–0.45 $\mu\text{mol/L}$	MM.1S, H526	360
GNE6640			0.75 $\mu\text{mol/L}$	p53 accumulation @ 10 $\mu\text{mol/L}$	>50% inhibition @ 5 $\mu\text{mol/L}$	HCT116, MCF7, EOL-1	361
Capzimin		Rpn11	0.39 $\mu\text{mol/L}$	Deubiquitination @ 2–10 $\mu\text{mol/L}$	2.1–3.8 $\mu\text{mol/L}$	293T, A549, HCT116	364
SOP11			1.3/0.6 $\mu\text{mol/L}$	Deubiquitination @ 10 $\mu\text{mol/L}$	$IC_{50} = 4.7 \mu\text{mol/L}$	HCT116	365
VLX1570		USP14/ UCH37	8.1/14 $\mu\text{mol/L}$	>80% inhibition @ 25 mmol/L	43–126 nmol/L	RPMI8226, KMS11, OPM-2	366

networks and biological pathways. Based on the databases, mass spectrometry (MS)-based proteomics data analysis has emerged as a key approach for identifying the E3 ligands. Quantitative expression proteomics combined with correlative transcriptomics were employed to examine the mechanisms of action (MoA) of specific MGDs, such as CR8 and dCeMM2-4. In particular, drug-affinity enrichment and MS-based chemoproteomics, such as activity-based protein profiling (ABPP) and drug affinity-responsive target stability (DARTS), have successfully been conducted to discover potential RNF114 small-molecule ligand, natural product nimbolide³⁴³. These approaches have also facilitated the identification of specific fragment–protein interactions, such as E3 covalent engaging ligands^{344,345}. Moreover, advancement in imaging technology and precise visual analysis, such as cellular high-content imaging and small-molecule fluorescence probe, have provided additional insights into the MoA of ligases and ligands, when combined with the bioinformation profiling.

4.4. Deubiquitinases (DUBs) inhibitors

Most of the reported DUB inhibitors primarily target the proteins USP1, USP2, USP7, Rpn11, and USP14. Herein, we thus focused

on novel DUB inhibitors developed between 2013 and 2021 and their potential for cancer therapy (Table 1). Among the human USP family of DUBs, USP1 has been implicated in the DNA damage response, which is responsible for deubiquitinating and stabilizing two crucial DNA repair proteins, PCNA and FANCD2 (fanconi anemia group D2)³⁴⁶. Chen et al.³⁴⁶ employed a self-established ubiquitin–rhodamine-based high-throughput screening method to identify a series of FDA-approved drugs and clinical candidates as potential USP1 inhibitors, including pimozide, GW7647, and flupenthixol. Utilizing a similar ubiquitin–rhodamine-based screening approach, Mistry et al.³⁴⁷ identified several USP1 inhibitors and determined their therapeutic potential for leukemia. Representative SJB2-043, derived from the hit compound C527, promotes the degradation of ID1 (a leukemic cell growth activator) and FANCD2 by inhibiting the catalytic activity of USP1 ($IC_{50} = 0.54 \mu\text{mol/L}$), and is currently being used as a positive control to evaluate other potential USP1 inhibitors. Furthermore, Liang et al.³⁴⁸ developed the first selective and potent USP1 inhibitor, ML323, based on the discoveries of pimozide and GW7647. Phenylpyrimidin-derived ML323 inhibits USP1 with a nanomolar affinity ($IC_{50} = 76 \text{ nmol/L}$) and increases the monoubiquitinated PCNA (Ub-PCNA) levels (PCNA

deubiquitination at 20 $\mu\text{mol/L}$ in H1299³⁴⁹. USP2 helps stabilize various tumor-associated substrates, including MDM2, fatty acid synthase, and cyclin D1^{228,231,233}. Hence, numerous human cancer cell lines undergo apoptosis when USP2 is silenced. Ohayon et al.³⁵⁰ screened and identified a series of UCH-L3 inhibitors and found that these compounds inhibited USP2 more effectively than UCH-L3, especially several ortho-quinones analogs. The natural product β -lapachone Q29, a clinical candidate for treating pancreatic cancer, exhibits simultaneous USP1/2 inhibition (82%–92% inhibition at 20 $\mu\text{mol/L}$)³⁵⁰. ML364, another representative small-molecule USP2 inhibitor, accelerates cyclin D1 degradation and induces cell cycle arrest in both Mino and HCT116 cancer cell lines³⁵¹. In addition, a lithocholic acid (LCA) derivative, LCAHA, destabilizes cyclin D1 in an AKT/GSK3 β -independent manner, by suppressing USP2 but maintaining the expression of p27³⁵².

Recently, USP7 has emerged as a star protein of the DUB family for cancer therapy owing to its importance in regulating p53 and MDM2 levels^{353,354}. Several pharmaceutical companies, such as Hybrigenics, Progenra, FORMA Therapeutics, and Genentech, have contributed to the development of USP7 inhibitors³⁵⁵. Considering that a large number of small-molecule USP7 inhibitors have been developed during the past two decades, this review summarizes the progress of representative USP7 inhibitors from 2012 to the present. Early in 2012, Progenra developed several trisubstituted thiophene derivatives, such as P5091 and P22077348, as first-generation USP7 inhibitors³⁵⁶. These inhibitors covalently conjugate with the catalytic domain cysteine223 of USP7 and are applicable in cancer and immunological oncology therapies³⁵⁶; however, pan-deubiquitination and off-target defects limit their efficacy. By optimizing the structure of the lead compound pyrazolo-[3,4-*d*]-pyrimidin-4-one-piperidine (PyrzPPip), Lamberto et al.³⁵⁷ developed the next generation of USP7, subsequently discovering that XL188 is a highly potent and selective USP7 inhibitor ($\text{IC}_{50} = 90 \text{ nmol/L}$). X-ray crystallography of the USP7–XL188 complex revealed that XL188 is a noncovalent USP7 inhibitor. Additionally, the researchers of Hybrigenics have presented a series of PyrzPPip-derived USP7 inhibitors. They first identified a noncovalent USP7 inhibitor, FT671, in the series. FT671 is capable of specifically suppressing enzyme USP7 with high affinity. Unlike other reported inhibitors, FT671 is an allosteric inhibitor that targets a dynamic pocket close to the catalytic position of USP7³⁵⁸. Furthermore, Almac Discovery used the surface plasmon resonance (SPR) to identify new USP7 inhibitors through a fragment-based screen. Hydroxypiperidine-derived Compound 4, the most potent inhibitor of the hit compounds, selectively inhibits USP7 *in vitro* ($\text{IC}_{50} = 6 \text{ nmol/L}$) and in cells ($\text{IC}_{50} = 49 \text{ nmol/L}$) with nanomolar inhibitory IC_{50} values³⁵⁹. Leger et al.³⁶⁰ identified benzofuran-amide as a potential scaffold for USP7 inhibition, revealing that the optimized scaffold has a large succinimide group that serves as a major potency-driving motif. The succinimide group forms two crucial hydrogen bonds in the allosteric position of USP7. The optimal Compound 41 inhibits USP7 with more potency and selectivity than other previously reported deubiquitinases³⁶⁰. In the same year, GeneTech introduced GNE6640, an additional potent allosteric USP7 inhibitor. Structural analyses revealed that GNE6640 noncovalently binds USP7 at a distance of 12 Å from catalytic cysteine and interacts with acidic residues that mediate the hydrogen bond interaction with the Lys48 side chain of ubiquitin³⁶¹.

As outlined above, the proteasome comprises a 19S regulatory particle (RP) and a 20S core particle. Although approved “omibs”

drugs always target the β 5 active site of the 20S core particle, resistance occurs. Rpn11 is a Zn^{2+} -dependent metalloproteidase derived from the JAMM zinc metalloprotease family of DUBs that hydrolyzes ubiquitin from tagged proteins and is a crucial member of the proteasome 19S regulatory particle³⁶². Inactivating the enzymatic active site of Rpn11 by altering zinc-coordinating histidine residues inhibits substrate degradation in cells³⁶³. Recent research has shown that targeting Rpn11 as a potential cancer treatment target not only inhibits the proteasome but also increases the therapeutic efficacy of “omibs” drugs³⁶⁴. Li et al.³⁶⁴ screened 330,000 compounds and selected 8TQ as a promising lead (a thioester derivative). They subsequently optimized the structure of 8TQ using the FBDD approach to summarize SARs and identified the first potent and specific Rpn11 chemical probe, capzimin ($\text{IC}_{50} = \sim 300 \text{ nmol/L}$), which inhibited the proliferation of bortezomib-resistant cancer cells by stabilizing the proteasome substrates and inducing an unfolded protein response. Utilizing the positive capzimin and their inhouse screening system, they discovered an epipolythiodioxopiperazines-derived SOP11 that inhibits proteasomal deubiquitinases, such as Rpn11 and AMSH. In addition to Rpn11, the 19S RP has two more DUBs, the cysteine proteases USP14 and UCHL5 (UCH37)³⁶⁵. VLX1570, the first DUB inhibitor containing a reactive α and β -unsaturated carbonyl group and covalently interacting with the nucleophilic residues of USP14 and UCHL5, recently entered clinical trials³⁶⁶.

5. Conclusions and perspective

Recent and ongoing research demonstrates that Ub and Ubl pathways play crucial roles in tumorigenesis by degrading or activating/deactivating key regulators of tumor growth and death. The increased knowledge supports the idea that targeting aberrant Ub or Ubl pathways is a novel therapeutic strategy for multiple types of tumors. In this regard, the fundamental advances and follow-on target-based drug discoveries have been crucial in providing vital information concerning contemporary translational efforts to develop precise treatment by targeting Ub and Ubl pathways.

However, several challenges of the Ub and Ubl field are required with solution, such as 1) numerous studies have focused on identifying the roles of E1–E2–E3 ligases in tumorigenesis; however, the oncogenic or tumor-suppressive function of these enzymes is influenced by various factors, such as the cellular context (e.g., β -TRCP) and subcellular localization (e.g., SPOP). Therefore, a comprehensive understanding of the regulatory mechanisms of Ub and Ubl enzymes may provide therapeutic alternatives to inactivate/reactivate or upregulate/downregulate these enzymes in various tumors. 2) Although our multiomics analyses decipher the potential roles of particular enzymes, there is a lack of supporting *in vitro* or *in vivo* studies for many Ub- and Ubl-associated enzymes used in anticancer therapy. 3) Targeting E1, E2, or E3 may affect multiple biological processes, resulting in different phenotypes; therefore, a deeper understanding of each enzyme is required to delineate the potential tumor-promoting effects of putative inhibitors of E1–E2–E3 cascades and develop individualized treatments. 4) Some PPI interface may lack such well-defined pocket, which makes it difficult to design selective and potent small-molecule inhibitors. Overall, the present review highlighted the tumor-suppressive or tumor-promoting roles of many Ub- and Ubl-associated enzymes. An ever-growing list of substrates and upstream regulators will help us better understand the roles of these enzymes in tumors and whether they are promising anticancer targets.

Acknowledgments

This work was supported by the following funds: National Natural Science Foundation of China (Grants 81820108022, 82003297 and 22177076), Innovation Program of Shanghai Municipal Education Commission (2019-01-07-00-10-E00056, China), Shanghai Frontiers Science Center of Disease and Syndrome Biology of Inflammatory Cancer Transformation (2021KJ03-12, China), The Scientific and Technological Innovation Action Plan of Science and Technology Commission of Shanghai (20JC1411300, China), ChenGuang project supported by Shanghai Municipal Education Commission and Shanghai Education Development Foundation (19CG49, China).

Author contributions

Yanyu Jiang and Shuaishuai Ni collected the related papers, drafted and revised the manuscript. Biying Xiao collected the related papers. Lijun Jia revised and finalized the manuscript. All authors read and approved the final manuscript.

Conflicts of interest

The authors declare that they have no conflicts of interest.

References

- Hershko A, Ciechanover A, Heller H, Haas AL, Rose IA. Proposed role of ATP in protein breakdown: conjugation of protein with multiple chains of the polypeptide of ATP-dependent proteolysis. *Proc Natl Acad Sci U S A* 1980;77:1783–6.
- Ciechanover A, Heller H, Elias S, Haas AL, Hershko A. ATP-dependent conjugation of reticulocyte proteins with the polypeptide required for protein degradation. *Proc Natl Acad Sci U S A* 1980;77:1365–8.
- Deng L, Meng T, Chen L, Wei W, Wang P. The role of ubiquitination in tumorigenesis and targeted drug discovery. *Signal Transduct Targeted Ther* 2020;5:11.
- Cappadocia L, Lima CD. Ubiquitin-like protein conjugation: structures, chemistry, and mechanism. *Chem Rev* 2018;118:889–918.
- Bernassola F, Chillemi G, Melino G. HECT-type E3 ubiquitin ligases in cancer. *Trends Biochem Sci* 2019;44:1057–75.
- Wang P, Dai X, Jiang W, Li Y, Wei W. RBR E3 ubiquitin ligases in tumorigenesis. *Semin Cancer Biol* 2020;67:131–44.
- Cai Z, Moten A, Peng D, Hsu CC, Pan BS, Manne R, et al. The Skp2 pathway: a critical target for cancer therapy. *Semin Cancer Biol* 2020;67:16–33.
- Harrigan JA, Jacq X, Martin NM, Jackson SP. Deubiquitylating enzymes and drug discovery: emerging opportunities. *Nat Rev Drug Discov* 2018;17:57–78.
- Ciechanover A, Heller H, Katz-Etzion R, Hershko A. Activation of the heat-stable polypeptide of the ATP-dependent proteolytic system. *Proc Natl Acad Sci U S A* 1981;78:761–5.
- Barghout SH, Schimmer AD. E1 enzymes as therapeutic targets in cancer. *Pharmacol Rev* 2021;73:1–58.
- Hyer ML, Milhollen MA, Ciavarri J, Fleming P, Traore T, Sappal D, et al. A small-molecule inhibitor of the ubiquitin activating enzyme for cancer treatment. *Nat Med* 2018;24:186–93.
- Jin J, Li X, Gygi SP, Harper JW. Dual E1 activation systems for ubiquitin differentially regulate E2 enzyme charging. *Nature* 2007;447:1135–8.
- Li L, Wang M, Yu G, Chen P, Li H, Wei D, et al. Overactivated neddylation pathway as a therapeutic target in lung cancer. *J Natl Cancer Inst* 2014;106:dju083.
- Li Y, Wang C, Xu T, Pan P, Yu Q, Xu L, et al. Discovery of a small molecule inhibitor of cullin neddylation that triggers ER stress to induce autophagy. *Acta Pharm Sin B* 2021;11:3567–84.
- Zhou L, Zhang W, Sun Y, Jia L. Protein neddylation and its alterations in human cancers for targeted therapy. *Cell Signal* 2018;44:92–102.
- Chen P, Hu T, Liang Y, Li P, Chen X, Zhang J, et al. Neddylation inhibition activates the extrinsic apoptosis pathway through ATF4–CHOP–DR5 axis in human esophageal cancer cells. *Clin Cancer Res* 2016;22:4145–57.
- Zhou W, Xu J, Li H, Xu M, Chen ZJ, Wei W, et al. Neddylation E2 UBE2F promotes the survival of lung cancer cells by activating CRL5 to degrade NOXA via the K11 linkage. *Clin Cancer Res* 2017;23:1104–16.
- Liu X, Jiang Y, Wu J, Zhang W, Liang Y, Jia L, et al. NEDD8-activating enzyme inhibitor, MLN4924 (Pevonedistat) induces NOXA-dependent apoptosis through up-regulation of ATF-4. *Biochem Biophys Res Commun* 2017;488:1–5.
- Wang J, Wang S, Zhang W, Wang X, Liu X, Liu L, et al. Targeting neddylation pathway with MLN4924 (Pevonedistat) induces NOXA-dependent apoptosis in renal cell carcinoma. *Biochem Biophys Res Commun* 2017;490:1183–8.
- Milhollen MA, Traore T, Adams-Duffy J, Thomas MP, Berger AJ, Dang L, et al. MLN4924, a NEDD8-activating enzyme inhibitor, is active in diffuse large B-cell lymphoma models: rationale for treatment of NF-κB-dependent lymphoma. *Blood* 2010;116:1515–23.
- Godbersen JC, Humphries LA, Danilova OV, Kebbekus PE, Brown JR, Eastman A, et al. The Nedd8-activating enzyme inhibitor MLN4924 thwarts microenvironment-driven NF-κappaB activation and induces apoptosis in chronic lymphocytic leukemia B cells. *Clin Cancer Res* 2014;20:1576–89.
- Pan Y, Xu H, Liu R, Jia L. Induction of cell senescence by targeting to Cullin-RING ligases (CRLs) for effective cancer therapy. *Int J Biochem Mol Biol* 2012;3:273–81.
- Jia L, Li H, Sun Y. Induction of p21-dependent senescence by an NAE inhibitor, MLN4924, as a mechanism of growth suppression. *Neoplasia* 2011;13:561–9.
- Wang Y, Luo Z, Pan Y, Wang W, Zhou X, Jeong LS, et al. Targeting protein neddylation with an NEDD8-activating enzyme inhibitor MLN4924 induced apoptosis or senescence in human lymphoma cells. *Cancer Biol Ther* 2015;16:420–9.
- Jiang Y, Liang Y, Li L, Zhou L, Cheng W, Yang X, et al. Targeting neddylation inhibits intravascular survival and extravasation of cancer cells to prevent lung-cancer metastasis. *Cell Biol Toxicol* 2019;35:233–45.
- Mackintosh C, Garcia-Dominguez DJ, Ordonez JL, Ginel-Picardo A, Smith PG, Sacristan MP, et al. WEE1 accumulation and deregulation of S-phase proteins mediate MLN4924 potent inhibitory effect on Ewing sarcoma cells. *Oncogene* 2013;32:1441–51.
- Jiang Y, Cheng W, Li L, Zhou L, Liang Y, Zhang W, et al. Effective targeting of the ubiquitin-like modifier NEDD8 for lung adenocarcinoma treatment. *Cell Biol Toxicol* 2020;36:349–64.
- Milhollen MA, Narayanan U, Soucy TA, Veiby PO, Smith PG, Amidon B. Inhibition of NEDD8-activating enzyme induces re-replication and apoptosis in human tumor cells consistent with deregulating CDT1 turnover. *Cancer Res* 2011;71:3042–51.
- Pan WW, Zhou JJ, Yu C, Xu Y, Guo LJ, Zhang HY, et al. Ubiquitin E3 ligase CRL4^{CDT2/DCAF2} as a potential chemotherapeutic target for ovarian surface epithelial cancer. *J Biol Chem* 2013;288:29680–91.
- Li L, Liu B, Dong T, Lee HW, Yu J, Zheng Y, et al. Neddylation pathway regulates the proliferation and survival of macrophages. *Biochem Biophys Res Commun* 2013;432:494–8.
- Liu Y, Zhang W, Wang S, Cai L, Jiang Y, Pan Y, et al. Cullin3-TNFAIP1 E3 ligase controls inflammatory response in hepatocellular carcinoma cells via ubiquitination of RhoB. *Front Cell Dev Biol* 2021;9:617134.
- Zhou L, Jiang Y, Liu X, Li L, Yang X, Dong C, et al. Promotion of tumor-associated macrophages infiltration by elevated neddylation

- pathway via NF-kappaB–CCL2 signaling in lung cancer. *Oncogene* 2019;38:5792–804.
33. Zhou L, Jiang Y, Luo Q, Li L, Jia L. Neddylation: a novel modulator of the tumor microenvironment. *Mol Cancer* 2019;18:77.
 34. Jiang Y, Li L, Li Y, Liu G, Hoffman RM, Jia L. Neddylation regulates macrophages and implications for cancer therapy. *Front Cell Dev Biol* 2021;9:681186.
 35. Yao WT, Wu JF, Yu GY, Wang R, Wang K, Li LH, et al. Suppression of tumor angiogenesis by targeting the protein neddylation pathway. *Cell Death Dis* 2014;5:e1059.
 36. Luo Z, Yu G, Lee HW, Li L, Wang L, Yang D, et al. The Nedd8-activating enzyme inhibitor MLN4924 induces autophagy and apoptosis to suppress liver cancer cell growth. *Cancer Res* 2012;72:3360–71.
 37. Zhao Y, Xiong X, Jia L, Sun Y. Targeting Cullin-RING ligases by MLN4924 induces autophagy via modulating the HIF1–REDD1–TSC1–mTORC1–DEPTOR axis. *Cell Death Dis* 2012;3:e386.
 38. Liang Y, Jiang Y, Jin X, Chen P, Heng Y, Cai L, et al. Neddylation inhibition activates the protective autophagy through NF-kappaB–catalase–ATF3 axis in human esophageal cancer cells. *Cell Commun Signal* 2020;18:72.
 39. Stewart MD, Ritterhoff T, Klevit RE, Brzovic PS. E2 enzymes: more than just middle men. *Cell Res* 2016;26:423–40.
 40. Martinez-Chacin RC, Bodrug T, Bolhuis DL, Kedziora KM, Bonacci T, Ordureau A, et al. Ubiquitin chain-elongating enzyme UBE2S activates the RING E3 ligase APC/C for substrate priming. *Nat Struct Mol Biol* 2020;27:550–60.
 41. Garnett MJ, Mansfeld J, Godwin C, Matsusaka T, Wu J, Russell P, et al. UBE2S elongates ubiquitin chains on APC/C substrates to promote mitotic exit. *Nat Cell Biol* 2009;11:1363–9.
 42. Williamson A, Wickliffe KE, Mellone BG, Song L, Karpen GH, Rape M. Identification of a physiological E2 module for the human anaphase-promoting complex. *Proc Natl Acad Sci U S A* 2009;106:18213–8.
 43. Wu T, Merbl Y, Huo Y, Gallop JL, Tzur A, Kirschner MW. UBE2S drives elongation of K11-linked ubiquitin chains by the anaphase-promoting complex. *Proc Natl Acad Sci U S A* 2010;107:1355–60.
 44. Chong RA, Wu K, Spratt DE, Yang Y, Lee C, Nayak J, et al. Pivotal role for the ubiquitin Y59-E51 loop in lysine 48 polyubiquitination. *Proc Natl Acad Sci U S A* 2014;111:8434–9.
 45. Wu K, Kovacev J, Pan ZQ. Priming and extending: a UbcH5/Cdc34 E2 handoff mechanism for polyubiquitination on a SCF substrate. *Mol Cell* 2010;37:784–96.
 46. van Ree JH, Jegannathan KB, Malureanu L, van Deursen JM. Overexpression of the E2 ubiquitin-conjugating enzyme UbcH10 causes chromosome missegregation and tumor formation. *J Cell Biol* 2010;188:83–100.
 47. Dastsooz H, Cereda M, Donna D, Oliviero S. A comprehensive bioinformatics analysis of UBE2C in cancers. *Int J Mol Sci* 2019;20:2228.
 48. Okamoto Y, Ozaki T, Miyazaki K, Aoyama M, Miyazaki M, Nakagawa A. UbcH10 is the cancer-related E2 ubiquitin-conjugating enzyme. *Cancer Res* 2003;63:4167–73.
 49. Presta I, Novellino F, Donato A, La Torre D, Palleria C, Russo E, et al. UbcH10 a major actor in cancerogenesis and a potential tool for diagnosis and therapy. *Int J Mol Sci* 2020;21:2041.
 50. Liu Y, Zhao R, Chi S, Zhang W, Xiao C, Zhou X, et al. UBE2C is upregulated by estrogen and promotes epithelial-mesenchymal transition via p53 in endometrial cancer. *Mol Cancer Res* 2020;18:204–15.
 51. Zhang RY, Liu ZK, Wei D, Yong YL, Lin P, Li H, et al. UBE2S interacting with TRIM28 in the nucleus accelerates cell cycle by ubiquitination of p27 to promote hepatocellular carcinoma development. *Signal Transduct Targeted Ther* 2021;6:64.
 52. Bajaj S, Alam SK, Roy KS, Datta A, Nath S, Roychoudhury S. E2 Ubiquitin-conjugating enzyme, UBE2C gene, is reciprocally regulated by wild-type and gain-of-function mutant p53. *J Biol Chem* 2016;291:14231–47.
 53. Hu L, Li X, Liu Q, Xu J, Ge H, Wang Z, et al. UBE2S, a novel substrate of Akt1, associates with Ku70 and regulates DNA repair and glioblastoma multiforme resistance to chemotherapy. *Oncogene* 2017;36:1145–56.
 54. Wang W, Kirschner MW. Emi1 preferentially inhibits ubiquitin chain elongation by the anaphase-promoting complex. *Nat Cell Biol* 2013;15:797–806.
 55. Zhang S, You X, Zheng Y, Shen Y, Xiong X, Sun Y. The UBE2C/CDH1/DEPTOR axis is an oncogene and tumor suppressor cascade in lung cancer cells. *J Clin Invest* 2023;133:e162434.
 56. Zhao XC, Wang GZ, Wen ZS, Zhou YC, Hu Q, Zhang B, et al. Systematic identification of CDC34 that functions to stabilize EGFR and promote lung carcinogenesis. *EBioMedicine* 2020;53:102689.
 57. Hou L, Li Y, Wang Y, Xu D, Cui H, Xu X, et al. UBE2D1 RNA expression was an independent unfavorable prognostic indicator in lung adenocarcinoma, but not in lung squamous cell carcinoma. *Dis Markers* 2018;2018:4108919.
 58. Tanaka K, Kondoh N, Shuda M, Matsubara O, Imazeki N, Ryo A, et al. Enhanced expression of mRNAs of antisecretory factor-1, gp96, DAD1 and CDC34 in human hepatocellular carcinomas. *Biochim Biophys Acta* 2001;1536:1–12.
 59. Zhou C, Bi F, Yuan J, Yang F, Sun S. Gain of UBE2D1 facilitates hepatocellular carcinoma progression and is associated with DNA damage caused by continuous IL-6. *J Exp Clin Cancer Res* 2018;37:290.
 60. Chauhan D, Li G, Hideshima T, Podar K, Shringarpure R, Mitsiades C, et al. Blockade of ubiquitin-conjugating enzyme CDC34 enhances anti-myeloma activity of bortezomib/proteasome inhibitor PS-341. *Oncogene* 2004;23:3597–602.
 61. Zhang S, Sun Y. Targeting CDC34 E2 ubiquitin conjugating enzyme for lung cancer therapy. *EBioMedicine* 2020;54:102718.
 62. Sandoval D, Hill S, Ziembra A, Lewis S, Kuhlman B, Kleiger G. Ubiquitin-conjugating enzyme Cdc34 and ubiquitin ligase Skp1–cullin–F-box ligase (SCF) interact through multiple conformations. *J Biol Chem* 2015;290:1106–18.
 63. Liu HT, Liu S, Liu L, Ma RR, Gao P. EGR1-mediated transcription of lncRNA–HNF1A–AS1 promotes cell-cycle progression in gastric cancer. *Cancer Res* 2018;78:5877–90.
 64. Wang S, Xian J, Li L, Jiang Y, Liu Y, Cai L, et al. NEDD8-conjugating enzyme UBC12 as a novel therapeutic target in esophageal squamous cell carcinoma. *Signal Transduct Targeted Ther* 2020;5:123.
 65. Li L, Kang J, Zhang W, Cai L, Wang S, Liang Y, et al. Validation of NEDD8-conjugating enzyme UBC12 as a new therapeutic target in lung cancer. *EBioMedicine* 2019;45:81–91.
 66. Zhou W, Xu J, Tan M, Li H, Li H, Wei W, et al. UBE2M is a stress-inducible dual E2 for neddylation and ubiquitylation that promotes targeted degradation of UBE2F. *Mol Cell* 2018;70:1008–10024.e6.
 67. Sun Y. Targeting E3 ubiquitin ligases for cancer therapy. *Cancer Biol Ther* 2003;2:623–9.
 68. Zhao Y, Sun Y. Cullin-RING ligases as attractive anti-cancer targets. *Curr Pharmaceut Des* 2013;19:3215–25.
 69. Wang Z, Liu P, Inuzuka H, Wei W. Roles of F-box proteins in cancer. *Nat Rev Cancer* 2014;14:233–47.
 70. Jin J, Cardozo T, Lovering RC, Elledge SJ, Pagano M, Harper JW. Systematic analysis and nomenclature of mammalian F-box proteins. *Genes Dev* 2004;18:2573–80.
 71. Zhang H, Kobayashi R, Galaktionov K, Beach D. p19Skp1 and p45Skp2 are essential elements of the cyclin A–CDK2 S phase kinase. *Cell* 1995;82:915–25.
 72. Zhu CQ, Blackhall FH, Pintilie M, Iyengar P, Liu N, Ho J, et al. Skp2 gene copy number aberrations are common in non-small cell lung carcinoma, and its overexpression in tumors with ras mutation is a poor prognostic marker. *Clin Cancer Res* 2004;10:1984–91.
 73. Yu X, Wang R, Zhang Y, Zhou L, Wang W, Liu H, et al. Skp2-mediated ubiquitination and mitochondrial localization of Akt drive tumor growth and chemoresistance to cisplatin. *Oncogene* 2019;38:7457–72.

74. Lu M, Ma J, Xue W, Cheng C, Wang Y, Zhao Y, et al. The expression and prognosis of FOXO3a and Skp2 in human hepatocellular carcinoma. *Pathol Oncol Res* 2009;15:679–87.
75. Masuda TA, Inoue H, Sonoda H, Mine S, Yoshikawa Y, Nakayama K, et al. Clinical and biological significance of S-phase kinase-associated protein 2 (Skp2) gene expression in gastric carcinoma: modulation of malignant phenotype by Skp2 overexpression, possibly via p27 proteolysis. *Cancer Res* 2002;62:3819–25.
76. Yu ZK, Gervais JL, Zhang H. Human CUL-1 associates with the SKP1/SKP2 complex and regulates p21^{CIP1/WAF1} and cyclin D proteins. *Proc Natl Acad Sci U S A* 1998;95:11324–9.
77. Carrano AC, Eytan E, Hershko A, Pagano M. SKP2 is required for ubiquitin-mediated degradation of the CDK inhibitor p27. *Nat Cell Biol* 1999;1:193–9.
78. Kamura T, Hara T, Kotoshiba S, Yada M, Ishida N, Imaki H, et al. Degradation of p57kip2 mediated by SCFSkp2-dependent ubiquitylation. *Proc Natl Acad Sci U S A* 2003;100:10231–6.
79. Nishitani H, Sugimoto N, Roukos V, Nakanishi Y, Saijo M, Obuse C, et al. Two E3 ubiquitin ligases, SCF-Skp2 and DDB1-Cul4, target human Cdt1 for proteolysis. *EMBO J* 2006;25:1126–36.
80. Mendez J, Zou-Yang XH, Kim SY, Hidaka M, Tansey WP, Stillman B. Human origin recognition complex large subunit is degraded by ubiquitin-mediated proteolysis after initiation of DNA replication. *Mol Cell* 2002;9:481–91.
81. Huang H, Regan KM, Wang F, Wang D, Smith DI, van Deursen JM, et al. Skp2 inhibits FOXO1 in tumor suppression through ubiquitin-mediated degradation. *Proc Natl Acad Sci U S A* 2005;102:1649–54.
82. Chan CH, Li CF, Yang WL, Gao Y, Lee SW, Feng Z, et al. The Skp2-SCF E3 ligase regulates Akt ubiquitination, glycolysis, herceptin sensitivity, and tumorigenesis. *Cell* 2012;149:1098–111.
83. Yao F, Zhou Z, Kim J, Hang Q, Xiao Z, Ton BN, et al. SKP2- and OTUD1-regulated non-proteolytic ubiquitination of YAP promotes YAP nuclear localization and activity. *Nat Commun* 2018;9:2269.
84. Wang JY, Liu GZ, Wilmott JS, La T, Feng YC, Yari H, et al. Skp2-mediated stabilization of MTH1 promotes survival of melanoma cells upon oxidative stress. *Cancer Res* 2017;77:6226–39.
85. Lee SW, Li CF, Jin G, Cai Z, Han F, Chan CH, et al. Skp2-dependent ubiquitination and activation of LKB1 is essential for cancer cell survival under energy stress. *Mol Cell* 2015;57:1022–33.
86. Wu J, Zhang X, Zhang L, Wu CY, Rezaeian AH, Chan CH, et al. Skp2 E3 ligase integrates ATM activation and homologous recombination repair by ubiquitinating NBS1. *Mol Cell* 2012;46:351–61.
87. Ruan D, He J, Li CF, Lee HJ, Liu J, Lin HK, et al. Skp2 deficiency restricts the progression and stem cell features of castration-resistant prostate cancer by destabilizing Twist. *Oncogene* 2017;36:4299–310.
88. Finkin S, Aylon Y, Anzi S, Oren M, Shaulian E. Fbw7 regulates the activity of endoreduplication mediators and the p53 pathway to prevent drug-induced polyploidy. *Oncogene* 2008;27:4411–21.
89. Kwon YW, Kim IJ, Wu D, Lu J, Stock Jr WA, Liu Y, et al. Pten regulates Aurora-A and cooperates with Fbw7 in modulating radiation-induced tumor development. *Mol Cancer Res* 2012;10:834–44.
90. Yeh CH, Bellon M, Wang F, Zhang H, Fu L, Nicot C. Loss of FBXW7-mediated degradation of BRAF elicits resistance to BET inhibitors in adult T cell leukemia cells. *Mol Cancer* 2020;19:139.
91. Nateri AS, Riera-Sans L, Da Costa C, Behrens A. The ubiquitin ligase SCFFbw7 antagonizes apoptotic JNK signaling. *Science* 2004;303:1374–8.
92. Wei W, Jin J, Schlissio S, Harper JW, Kaelin Jr WG. The v-Jun point mutation allows c-Jun to escape GSK3-dependent recognition and destruction by the Fbw7 ubiquitin ligase. *Cancer Cell* 2005;8:25–33.
93. Yada M, Hatakeyama S, Kamura T, Nishiyama M, Tsunematsu R, Imaki H, et al. Phosphorylation-dependent degradation of c-Myc is mediated by the F-box protein Fbw7. *EMBO J* 2004;23:2116–25.
94. Welcker M, Orian A, Jin J, Grim JE, Harper JW, Eisenman RN, et al. The Fbw7 tumor suppressor regulates glycogen synthase kinase 3 phosphorylation-dependent c-Myc protein degradation. *Proc Natl Acad Sci U S A* 2004;101:9085–90.
95. Kuai X, Li L, Chen R, Wang K, Chen M, Cui B, et al. SCF(FBXW7)/GSK3beta-mediated GFI1 degradation suppresses proliferation of gastric cancer cells. *Cancer Res* 2019;79:4387–98.
96. Cassavaugh JM, Hale SA, Wellman TL, Howe AK, Wong C, Lounsbury KM. Negative regulation of HIF-1alpha by an FBW7-mediated degradation pathway during hypoxia. *J Cell Biochem* 2011;112:3882–90.
97. Flugel D, Gorlach A, Kietzmann T. GSK-3beta regulates cell growth, migration, and angiogenesis via Fbw7 and USP28-dependent degradation of HIF-1alpha. *Blood* 2012;119:1292–301.
98. Xie CM, Tan M, Lin XT, Wu D, Jiang Y, Tan Y, et al. The FBXW7–SHOC2–Raptor axis controls the cross-talks between the RAS–ERK and mTORC1 signaling pathways. *Cell Rep* 2019;26:3037–3050.e4.
99. Zhao D, Zheng HQ, Zhou Z, Chen C. The Fbw7 tumor suppressor targets KLF5 for ubiquitin-mediated degradation and suppresses breast cell proliferation. *Cancer Res* 2010;70:4728–38.
100. Liu N, Li H, Li S, Shen M, Xiao N, Chen Y, et al. The Fbw7/human CDC4 tumor suppressor targets proproliferative factor KLF5 for ubiquitination and degradation through multiple phosphodegron motifs. *J Biol Chem* 2010;285:18858–67.
101. Tong J, Tan S, Zou F, Yu J, Zhang L. FBW7 mutations mediate resistance of colorectal cancer to targeted therapies by blocking Mcl-1 degradation. *Oncogene* 2017;36:787–96.
102. Inuzuka H, Shaik S, Onoyama I, Gao D, Tseng A, Maser RS, et al. SCF^{Fbw7} regulates cellular apoptosis by targeting MCL1 for ubiquitylation and destruction. *Nature* 2011;471:104–9.
103. Wu G, Lyapina S, Das I, Li J, Gurney M, Pauley A, et al. SEL-10 is an inhibitor of notch signaling that targets notch for ubiquitin-mediated protein degradation. *Mol Cell Biol* 2001;21:7403–15.
104. Gupta-Rossi N, Le Bail O, Gonén H, Brou C, Logeat F, Six E, et al. Functional interaction between SEL-10, an F-box protein, and the nuclear form of activated Notch1 receptor. *J Biol Chem* 2001;276:34371–8.
105. Fryer CJ, White JB, Jones KA. Mastermind recruits CycC:CDK8 to phosphorylate the Notch ICD and coordinate activation with turnover. *Mol Cell* 2004;16:509–20.
106. Liao SY, Chiang CW, Hsu CH, Chen YT, Jen J, Juan HF, et al. CK1delta/GSK3beta/FBXW7alpha axis promotes degradation of the ZNF322A oncoprotein to suppress lung cancer progression. *Oncogene* 2017;36:5722–33.
107. Yumimoto K, Nakayama KI. Recent insight into the role of FBXW7 as a tumor suppressor. *Semin Cancer Biol* 2020;67:1–15.
108. Matsumoto A, Onoyama I, Nakayama KI. Expression of mouse Fbxw7 isoforms is regulated in a cell cycle- or p53-dependent manner. *Biochem Biophys Res Commun* 2006;350:114–9.
109. Cui D, Xiong X, Shu J, Dai X, Sun Y, Zhao Y. FBXW7 confers radiation survival by targeting p53 for degradation. *Cell Rep* 2020;30:497–509.e4.
110. Ye M, Zhang Y, Zhang X, Zhang J, Jing P, Cao L, et al. Targeting FBW7 as a strategy to overcome resistance to targeted therapy in non-small cell lung cancer. *Cancer Res* 2017;77:3527–39.
111. Mao JH, Perez-Losada J, Wu D, Delrosario R, Tsunematsu R, Nakayama KI, et al. Fbxw7/Cdc4 is a p53-dependent, haploinsufficient tumour suppressor gene. *Nature* 2004;432:775–9.
112. Zhao J, Hu C, Chi J, Li J, Peng C, Yun X, et al. miR-24 promotes the proliferation, migration and invasion in human tongue squamous cell carcinoma by targeting FBXW7. *Oncol Rep* 2016;36:1143–9.
113. Spruck C. miR-27a regulation of SCF^{Fbw7} in cell division control and cancer. *Cell Cycle* 2011;10:3232–3.
114. Xia W, Zhou J, Luo H, Liu Y, Peng C, Zheng W, et al. MicroRNA-32 promotes cell proliferation, migration and suppresses apoptosis in breast cancer cells by targeting FBXW7. *Cancer Cell Int* 2017;17:14.
115. Xu Y, Sengupta T, Kukreja L, Minella AC. MicroRNA-223 regulates cyclin E activity by modulating expression of F-box and WD-40 domain protein 7. *J Biol Chem* 2010;285:34439–46.
116. Xu J, Wu W, Wang J, Huang C, Wen W, Zhao F, et al. miR-367 promotes the proliferation and invasion of non-small cell lung cancer via targeting FBXW7. *Oncol Rep* 2017;37:1052–8.

117. Yaron A, Hatzubai A, Davis M, Lavon I, Amit S, Manning AM, et al. Identification of the receptor component of the *IκBα*-ubiquitin ligase. *Nature* 1998;396:590–4.
118. Zhang B, Zhang Z, Li L, Qin YR, Liu H, Jiang C, et al. TSPAN15 interacts with BTTC to promote oesophageal squamous cell carcinoma metastasis via activating NF- κ B signaling. *Nat Commun* 2018;9:1423.
119. Watanabe N, Arai H, Nishihara Y, Taniguchi M, Watanabe N, Hunter T, et al. M-phase kinases induce phospho-dependent ubiquitination of somatic Wee1 by SCFbeta-TrCP. *Proc Natl Acad Sci U S A* 2004;101:4419–24.
120. Xia Y, Padre RC, De Mendoza TH, Bottero V, Tergaonkar VB, Verma IM. Phosphorylation of p53 by IκB kinase 2 promotes its degradation by beta-TrCP. *Proc Natl Acad Sci U S A* 2009;106:2629–34.
121. Zhao Y, Xiong X, Sun Y. DEPTOR, an mTOR inhibitor, is a physiological substrate of SCF(βTrCP) E3 ubiquitin ligase and regulates survival and autophagy. *Mol Cell* 2011;44:304–16.
122. Xu J, Zhou W, Yang F, Chen G, Li H, Zhao Y, et al. The β-TrCP–FBXW2–SKP2 axis regulates lung cancer cell growth with FBXW2 acting as a tumour suppressor. *Nat Commun* 2017;8:14002.
123. Dehan E, Bassermann F, Guardavaccaro D, Vasiliver-Shamis G, Cohen M, Lowes KN, et al. betaTrCP- and Rsk1/2-mediated degradation of BimEL inhibits apoptosis. *Mol Cell* 2009;33:109–16.
124. Huang Y, Hu K, Zhang S, Dong X, Yin Z, Meng R, et al. S6K1 phosphorylation-dependent degradation of Mxi1 by β-Trep ubiquitin ligase promotes Myc activation and radioresistance in lung cancer. *Theranostics* 2018;8:1286–300.
125. Dorrello NV, Peschiaroli A, Guardavaccaro D, Colburn NH, Sherman NE, Pagano M. S6K1- and βTRCP-mediated degradation of PDCD4 promotes protein translation and cell growth. *Science* 2006;314:467–71.
126. Tan M, Gallegos JR, Gu Q, Huang Y, Li J, Jin Y, et al. SAG/ROC-SCF β-TrCP E3 ubiquitin ligase promotes pro-caspase-3 degradation as a mechanism of apoptosis protection. *Neoplasia* 2006;8:1042–54.
127. Wang HM, Xu YF, Ning SL, Yang DX, Li Y, Du YJ, et al. The catalytic region and PEST domain of PTPN18 distinctly regulate the HER2 phosphorylation and ubiquitination barcodes. *Cell Res* 2014;24:1067–90.
128. Zhao B, Li L, Tumaneng K, Wang CY, Guan KL. A coordinated phosphorylation by Lats and CK1 regulates YAP stability through SCF^β-TrCP. *Genes Dev* 2010;24:72–85.
129. Inuzuka H, Tseng A, Gao D, Zhai B, Zhang Q, Shaik S, et al. Phosphorylation by casein kinase I promotes the turnover of the Mdm2 oncoprotein via the SCF^β-TrCP ubiquitin ligase. *Cancer Cell* 2010;18:147–59.
130. Li CW, Lim SO, Xia W, Lee HH, Chan LC, Kuo CW, et al. Glycosylation and stabilization of programmed death ligand-1 suppresses T-cell activity. *Nat Commun* 2016;7:12632.
131. Ding Q, He X, Hsu JM, Xia W, Chen CT, Li LY, et al. Degradation of Mcl-1 by β-TrCP mediates glycogen synthase kinase 3-induced tumor suppression and chemosensitization. *Mol Cell Biol* 2007;27:4006–17.
132. Ougolkov A, Zhang B, Yamashita K, Bilim V, Mai M, Fuchs SY, et al. Associations among β-TrCP, an E3 ubiquitin ligase receptor, β-catenin, and NF- κ B in colorectal cancer. *J Natl Cancer Inst* 2004;96:1161–70.
133. Koch A, Waha A, Hartmann W, Hrychyk A, Schuller U, Waha A, et al. Elevated expression of Wnt antagonists is a common event in hepatoblastomas. *Clin Cancer Res* 2005;11:4295–304.
134. Kim CJ, Song JH, Cho YG, Kim YS, Kim SY, Nam SW, et al. Somatic mutations of the beta-TrCP gene in gastric cancer. *APMIS* 2007;115:127–33.
135. Gerstein AV, Almeida TA, Zhao G, Chess E, Shih Ie M, Buhler K, et al. APC/CTNNB1 (β-catenin) pathway alterations in human prostate cancers. *Genes Chromosomes Cancer* 2002;34:9–16.
136. Liu X, Zurlo G, Zhang Q. The roles of Cullin-2 E3 ubiquitin ligase complex in cancer. *Adv Exp Med Biol* 2020;1217:173–86.
137. Latif F, Tory K, Gnarra J, Yao M, Duh FM, Orcutt ML, et al. Identification of the von Hippel-Lindau disease tumor suppressor gene. *Science* 1993;260:1317–20.
138. Gnarra JR, Tory K, Weng Y, Schmidt L, Wei MH, Li H, et al. Mutations of the VHL tumour suppressor gene in renal carcinoma. *Nat Genet* 1994;7:85–90.
139. Semenza GL. Targeting HIF-1 for cancer therapy. *Nat Rev Cancer* 2003;3:721–32.
140. Kim WY, Kaelin WG. Role of VHL gene mutation in human cancer. *J Clin Oncol* 2004;22:4991–5004.
141. Sato Y, Yoshizato T, Shiraishi Y, Maekawa S, Okuno Y, Kamura T, et al. Integrated molecular analysis of clear-cell renal cell carcinoma. *Nat Genet* 2013;45:860–7.
142. Hsieh JJ, Purdue MP, Signoretti S, Swanton C, Albiges L, Schmidinger M, et al. Renal cell carcinoma. *Nat Rev Dis Prim* 2017;3:17009.
143. Gossage L, Eisen T, Maher ER. VHL, the story of a tumour suppressor gene. *Nat Rev Cancer* 2015;15:55–64.
144. Zhang J, Wu T, Simon J, Takada M, Saito R, Fan C, et al. VHL substrate transcription factor ZHX2 as an oncogenic driver in clear cell renal cell carcinoma. *Science* 2018;361:290–5.
145. Okuda H, Saitoh K, Hirai S, Iwai K, Takaki Y, Baba M, et al. The von Hippel-Lindau tumor suppressor protein mediates ubiquitination of activated atypical protein kinase C. *J Biol Chem* 2001;276:43611–7.
146. Xie L, Xiao K, Whalen EJ, Forrester MT, Freeman RS, Fong G, et al. Oxygen-regulated β₂-adrenergic receptor hydroxylation by EGLN3 and ubiquitylation by pVHL. *Sci Signal* 2009;2:ra33.
147. Na X, Duan HO, Messing EM, Schoen SR, Ryan CK, di Sant’Agnese PA, et al. Identification of the RNA polymerase II subunit hsRPB7 as a novel target of the von Hippel-Lindau protein. *EMBO J* 2003;22:4249–59.
148. Wang P, Song J, Ye D. CRL3s: the BTB–CUL3–RING E3 ubiquitin ligases. *Adv Exp Med Biol* 2020;1217:211–23.
149. Menegon S, Columbano A, Giordano S. The dual roles of NRF2 in cancer. *Trends Mol Med* 2016;22:578–93.
150. Romero R, Sayin VI, Davidson SM, Bauer MR, Singh SX, LeBoeuf SE, et al. Keap1 loss promotes Kras-driven lung cancer and results in dependence on glutaminolysis. *Nat Med* 2017;23:1362–8.
151. Khor TO, Huang MT, Prawan A, Liu Y, Hao X, Yu S, et al. Increased susceptibility of Nrf2 knockout mice to colitis-associated colorectal cancer. *Cancer Prev Res* 2008;1:187–91.
152. Luo J, Bao YC, Ji XX, Chen B, Deng QF, Zhou SW. SPOP promotes SIRT2 degradation and suppresses non-small cell lung cancer cell growth. *Biochem Biophys Res Commun* 2017;483:880–4.
153. Dai X, Gan W, Li X, Wang S, Zhang W, Huang L, et al. Prostate cancer-associated SPOP mutations confer resistance to BET inhibitors through stabilization of BRD4. *Nat Med* 2017;23:1063–71.
154. Zhang P, Wang D, Zhao Y, Ren S, Gao K, Ye Z, et al. Intrinsic BET inhibitor resistance in SPOP-mutated prostate cancer is mediated by BET protein stabilization and AKT–mTORC1 activation. *Nat Med* 2017;23:1055–62.
155. Janouskova H, El Tekle G, Bellini E, Udeshi ND, Rinaldi A, Ulbricht A, et al. Opposing effects of cancer-type-specific SPOP mutants on BET protein degradation and sensitivity to BET inhibitors. *Nat Med* 2017;23:1046–54.
156. Gan W, Dai X, Lunardi A, Li Z, Inuzuka H, Liu P, et al. SPOP promotes ubiquitination and degradation of the ERG oncoprotein to suppress prostate cancer progression. *Mol Cell* 2015;59:917–30.
157. Li G, Ci W, Karmakar S, Chen K, Dhar R, Fan Z, et al. SPOP promotes tumorigenesis by acting as a key regulatory hub in kidney cancer. *Cancer Cell* 2014;25:455–68.
158. Adelaiye-Ogala R, Damayanti NP, Orillion AR, Arisa S, Chintala S, Titus MA, et al. Therapeutic targeting of sunitinib-induced AR phosphorylation in renal cell carcinoma. *Cancer Res* 2018;78:2886–96.
159. Zhang P, Gao K, Jin X, Ma J, Peng J, Wumaier R, et al. Endometrial cancer-associated mutants of SPOP are defective in regulating estrogen receptor-α protein turnover. *Cell Death Dis* 2015;6:e1687.

160. Kim B, Nam HJ, Pyo KE, Jang MJ, Kim IS, Kim D, et al. Breast cancer metastasis suppressor 1 (BRMS1) is destabilized by the Cul3–SPOP E3 ubiquitin ligase complex. *Biochem Biophys Res Commun* 2011;415:720–6.
161. Zhang J, Bu X, Wang H, Zhu Y, Geng Y, Nihira NT, et al. Cyclin D–CDK4 kinase destabilizes PD-L1 via cullin 3–SPOP to control cancer immune surveillance. *Nature* 2018;553:91–5.
162. Ju LG, Zhu Y, Long QY, Li XJ, Lin X, Tang SB, et al. SPOP suppresses prostate cancer through regulation of CYCLIN E1 stability. *Cell Death Differ* 2019;26:1156–68.
163. Ma J, Chang K, Peng J, Shi Q, Gan H, Gao K, et al. SPOP promotes ATF2 ubiquitination and degradation to suppress prostate cancer progression. *J Exp Clin Cancer Res* 2018;37:145.
164. Geng C, Kaochar S, Li M, Rajapakshe K, Fiskus W, Dong J, et al. SPOP regulates prostate epithelial cell proliferation and promotes ubiquitination and turnover of c-MYC oncprotein. *Oncogene* 2017;36:4767–77.
165. Geng C, Rajapakshe K, Shah SS, Shou J, Eedunuri VK, Foley C, et al. Androgen receptor is the key transcriptional mediator of the tumor suppressor SPOP in prostate cancer. *Cancer Res* 2014;74:5631–43.
166. Geng C, He B, Xu L, Barbieri CE, Eedunuri VK, Chew SA, et al. Prostate cancer-associated mutations in speckle-type POZ protein (SPOP) regulate steroid receptor coactivator 3 protein turnover. *Proc Natl Acad Sci U S A* 2013;110:6997–7002.
167. Wang Z, Song Y, Ye M, Dai X, Zhu X, Wei W. The diverse roles of SPOP in prostate cancer and kidney cancer. *Nat Rev Urol* 2020;17:339–50.
168. Nagai Y, Kojima T, Muro Y, Hachiya T, Nishizawa Y, Wakabayashi T, et al. Identification of a novel nuclear speckle-type protein, SPOP. *FEBS Lett* 1997;418:23–6.
169. Lee J, Zhou P. DCAF₅, the missing link of the CUL4–DDB1 ubiquitin ligase. *Mol Cell* 2007;26:775–80.
170. He YJ, McCall CM, Hu J, Zeng Y, Xiong Y. DDB1 functions as a linker to recruit receptor WD40 proteins to CUL4–ROC1 ubiquitin ligases. *Genes Dev* 2006;20:2949–54.
171. Kapetanaki MG, Guerrero-Santoro J, Bisi DC, Hsieh CL, Rapic-Otrin V, Levine AS. The DDB1–CUL4A^{DDB2} ubiquitin ligase is deficient in xeroderma pigmentosum group E and targets histone H2A at UV-damaged DNA sites. *Proc Natl Acad Sci U S A* 2006;103:2588–93.
172. Wang H, Zhai L, Xu J, Joo HY, Jackson S, Erdjument-Bromage H, et al. Histone H3 and H4 ubiquitylation by the CUL4–DDB–ROC1 ubiquitin ligase facilitates cellular response to DNA damage. *Mol Cell* 2006;22:383–94.
173. Cazzalini O, Perucca P, Mocchi R, Sommatisi S, Prosperi E, Stivala LA. DDB2 association with PCNA is required for its degradation after UV-induced DNA damage. *Cell Cycle* 2014;13:240–8.
174. El-Mahdy MA, Zhu Q, Wang QE, Wani G, Praetorius-Ibba M, Wani AA. Cullin 4A-mediated proteolysis of DDB2 protein at DNA damage sites regulates *in vivo* lesion recognition by XPC. *J Biol Chem* 2006;281:13404–11.
175. Ribeiro-Silva C, Sabatella M, Helffricht A, Marteijn JA, Theil AF, Vermeulen W, et al. Ubiquitin and TFIH-stimulated DDB2 dissociation drives DNA damage handover in nucleotide excision repair. *Nat Commun* 2020;11:4868.
176. Yoon T, Chakraborty A, Franks R, Valli T, Kiyokawa H, Raychaudhuri P. Tumor-prone phenotype of the DDB2-deficient mice. *Oncogene* 2005;24:469–78.
177. Alekseev S, Kool H, Rebel H, Fousteri M, Moser J, Backendorf C, et al. Enhanced DDB2 expression protects mice from carcinogenic effects of chronic UV-B irradiation. *Cancer Res* 2005;65:10298–306.
178. Huang S, Fantini D, Merrill BJ, Bagchi S, Guzman G, Raychaudhuri P. DDB2 is a novel regulator of Wnt signaling in colon cancer. *Cancer Res* 2017;77:6562–75.
179. Bommi PV, Chand V, Mukhopadhyay NK, Raychaudhuri P, Bagchi S. NER-factor DDB2 regulates HIF1α and hypoxia-response genes in HNSCC. *Oncogene* 2020;39:1784–96.
180. Cui T, Srivastava AK, Han C, Wu D, Wani N, Liu L, et al. DDB2 represses ovarian cancer cell dedifferentiation by suppressing ALDH1A1. *Cell Death Dis* 2018;9:561.
181. Bommi PV, Ravindran S, Raychaudhuri P, Bagchi S. DDB2 regulates epithelial-to-mesenchymal transition (EMT) in oral/head and neck squamous cell carcinoma. *Oncotarget* 2018;9:34708–18.
182. Havens CG, Walter JC. Mechanism of CRL4^{Cdt2}, a PCNA-dependent E3 ubiquitin ligase. *Genes Dev* 2011;25:1568–82.
183. Panagopoulos A, Taraviras S, Nishitani H, Lygerou Z. CRL4^{Cdt2}: coupling genome stability to ubiquitination. *Trends Cell Biol* 2020;30:290–302.
184. Jin J, Arias EE, Chen J, Harper JW, Walter JC. A family of diverse Cul4–Ddb1-interacting proteins includes Cdt2, which is required for S phase destruction of the replication factor Cdt1. *Mol Cell* 2006;23:709–21.
185. Abbas T, Sivaprasad U, Terai K, Amador V, Pagano M, Dutta A. PCNA-dependent regulation of p21 ubiquitylation and degradation via the CRL4^{Cdt2} ubiquitin ligase complex. *Genes Dev* 2008;22:2496–506.
186. Abbas T, Shibata E, Park J, Jha S, Karnani N, Dutta A. CRL4^{Cdt2} regulates cell proliferation and histone gene expression by targeting PR-Set7/Set8 for degradation. *Mol Cell* 2010;40:9–21.
187. Huh J, Piwnica-Worms H. CRL4^{CDT2} targets CHK1 for PCNA-independent destruction. *Mol Cell Biol* 2013;33:213–26.
188. Lontos M, Koutsami M, Sideridou M, Evangelou K, Kletsas D, Levy B, et al. Dereregulated overexpression of hCdt1 and hCdc6 promotes malignant behavior. *Cancer Res* 2007;67:10899–909.
189. Matyskiela ME, Lu G, Ito T, Pagarigan B, Lu CC, Miller K, et al. A novel cereblon modulator recruits GSPT1 to the CRL4^{CRBN} ubiquitin ligase. *Nature* 2016;535:252–7.
190. Sievers QL, Petzold G, Bunker RD, Renneville A, Slabicki M, Liddicoat BJ, et al. Defining the human C2H2 zinc finger degrome targeted by thalidomide analogs through CRBN. *Science* 2018;362:eaat0572.
191. Lu G, Middleton RE, Sun H, Naniong M, Ott CJ, Mitsiades CS, et al. The myeloma drug lenalidomide promotes the cereblon-dependent destruction of Ikaros proteins. *Science* 2014;343:305–9.
192. Yamamoto J, Suwa T, Murase Y, Tateno S, Mizutome H, Asatsuma-Okumura T, et al. ARID2 is a pomalidomide-dependent CRL4^{CRBN} substrate in multiple myeloma cells. *Nat Chem Biol* 2020;16:1208–17.
193. Eichner R, Heider M, Fernandez-Saiz V, van Bebber F, Garz AK, Lemeer S, et al. Immunomodulatory drugs disrupt the cereblon–CD147–MCT1 axis to exert antitumor activity and teratogenicity. *Nat Med* 2016;22:735–43.
194. Heider M, Eichner R, Stroh J, Morath V, Kuisl A, Zecha J, et al. The IMiD target CRBN determines HSP90 activity toward transmembrane proteins essential in multiple myeloma. *Mol Cell* 2021;81:1170–86, e10.
195. Zhao Y, Xiong X, Sun Y. Cullin-RING ligase 5: functional characterization and its role in human cancers. *Semin Cancer Biol* 2020;67:61–79.
196. Hashimoto M, Ayada T, Kinjyo I, Hiwatashi K, Yoshida H, Okada Y, et al. Silencing of SOCS1 in macrophages suppresses tumor development by enhancing antitumor inflammation. *Cancer Sci* 2009;100:730–6.
197. Shen L, Evel-Kabler K, Strube R, Chen SY. Silencing of SOCS1 enhances antigen presentation by dendritic cells and antigen-specific anti-tumor immunity. *Nat Biotechnol* 2004;22:1546–53.
198. Zhao G, Gong L, Su D, Jin Y, Guo C, Yue M, et al. Cullin5 deficiency promotes small-cell lung cancer metastasis by stabilizing integrin beta1. *J Clin Invest* 2019;129:972–87.
199. Zhang CX, Ye SB, Ni JJ, Cai TT, Liu YN, Huang DJ, et al. STING signaling remodels the tumor microenvironment by antagonizing myeloid-derived suppressor cell expansion. *Cell Death Differ* 2019;26:2314–28.
200. Yoneda T, Kunimura N, Kitagawa K, Fukui Y, Saito H, Narikiyo K, et al. Overexpression of SOCS3 mediated by adenovirus vector in

- mouse and human castration-resistant prostate cancer cells increases the sensitivity to NK cells *in vitro* and *in vivo*. *Cancer Gene Ther* 2019;26:388–99.
201. Sasi W, Jiang WG, Sharma A, Mokbel K. Higher expression levels of SOCS 1,3,4,7 are associated with earlier tumour stage and better clinical outcome in human breast cancer. *BMC Cancer* 2010;10:178.
 202. Lewis RS, Kolesnik TB, Kuang Z, D'Cruz AA, Blewitt ME, Masters SL, et al. TLR regulation of SPSB1 controls inducible nitric oxide synthase induction. *J Immunol* 2011;187:3798–805.
 203. Nishiyama T, Matsumoto K, Maekawa S, Kajita E, Horinouchi T, Fujimuro M, et al. Regulation of inducible nitric-oxide synthase by the SPRY domain- and SOCS box-containing proteins. *J Biol Chem* 2011;286:9009–19.
 204. Vannini F, Kashfi K, Nath N. The dual role of iNOS in cancer. *Redox Biol* 2015;6:334–43.
 205. Kim HJ, Kim HJ, Kim MK, Bae MK, Sung HY, Ahn JH, et al. SPSB1 enhances ovarian cancer cell survival by destabilizing p21. *Biochem Biophys Res Commun* 2019;510:364–9.
 206. Feng Y, Pan TC, Pant DK, Chakrabarti KR, Alvarez JV, Ruth JR, et al. SPSB1 promotes breast cancer recurrence by potentiating c-MET signaling. *Cancer Discov* 2014;4:790–803.
 207. Kumar S, Tomooka Y, Noda M. Identification of a set of genes with developmentally down-regulated expression in the mouse brain. *Biochem Biophys Res Commun* 1992;185:1155–61.
 208. Wang X, Trotman LC, Kopkie T, Alimonti A, Chen Z, Gao Z, et al. NEDD4-1 is a proto-oncogenic ubiquitin ligase for PTEN. *Cell* 2007;128:129–39.
 209. Cai J, Li R, Xu X, Zhang L, Lian R, Fang L, et al. CK1alpha suppresses lung tumour growth by stabilizing PTEN and inducing autophagy. *Nat Cell Biol* 2018;20:465–78.
 210. Xu C, Fan CD, Wang X. Regulation of Mdm2 protein stability and the p53 response by NEDD4-1 E3 ligase. *Oncogene* 2015;34:281–9.
 211. Yang Y, Luo M, Zhang K, Zhang J, Gao T, Connell DO, et al. Nedd4 ubiquitylates VDAC2/3 to suppress erastin-induced ferroptosis in melanoma. *Nat Commun* 2020;11:433.
 212. Cao XR, Lill NL, Boase N, Shi PP, Croucher DR, Shan H, et al. Nedd4 controls animal growth by regulating IGF-1 signaling. *Sci Signal* 2008;1:ra5.
 213. Jing W, Wang G, Cui Z, Xiong G, Jiang X, Li Y, et al. FGFR3 destabilizes PD-L1 via NEDD4 to control T-cell-mediated bladder cancer immune surveillance. *Cancer Res* 2022;82:114–29.
 214. Zhou W, Xu J, Zhao Y, Sun Y. SAG/RBX2 is a novel substrate of NEDD4-1 E3 ubiquitin ligase and mediates NEDD4-1 induced chemosensitization. *Oncotarget* 2014;5:6746–55.
 215. Walden H, Rittinger K. RBR ligase-mediated ubiquitin transfer: a tale with many twists and turns. *Nat Struct Mol Biol* 2018;25:440–5.
 216. Bernardini JP, Lazarou M, Dewson G. Parkin and mitophagy in cancer. *Oncogene* 2017;36:1315–27.
 217. Liu J, Zhang C, Zhao Y, Yue X, Wu H, Huang S, et al. Parkin targets HIF-1alpha for ubiquitination and degradation to inhibit breast tumor progression. *Nat Commun* 2017;8:1823.
 218. Gupta A, Anjomani-Virmouni S, Koundouros N, Dimitriadi M, Choo-Wing R, Valle A, et al. PARK2 depletion connects energy and oxidative stress to PI3K/Akt activation via PTEN S-nitrosylation. *Mol Cell* 2017;65:999–1013.e7.
 219. Yeo CW, Ng FS, Chai C, Tan JM, Koh GR, Chong YK, et al. Parkin pathway activation mitigates glioma cell proliferation and predicts patient survival. *Cancer Res* 2012;72:2543–53.
 220. Fujiwara M, Marusawa H, Wang HQ, Iwai A, Ikeuchi K, Imai Y, et al. Parkin as a tumor suppressor gene for hepatocellular carcinoma. *Oncogene* 2008;27:6002–11.
 221. Carroll RG, Hollville E, Martin SJ. Parkin sensitizes toward apoptosis induced by mitochondrial depolarization through promoting degradation of Mcl-1. *Cell Rep* 2014;9:1538–53.
 222. Li C, Zhang Y, Cheng X, Yuan H, Zhu S, Liu J, et al. PINK1 and PARK2 suppress pancreatic tumorigenesis through control of mitochondrial iron-mediated immunometabolism. *Dev Cell* 2018;46:441–55.e8.
 223. Liu J, Zhang C, Wu H, Sun XX, Li Y, Huang S, et al. Parkin ubiquitinates phosphoglycerate dehydrogenase to suppress serine synthesis and tumor progression. *J Clin Invest* 2020;130:3253–69.
 224. Lee SB, Kim JJ, Han SA, Fan Y, Guo LS, Aziz K, et al. The AMPK–Parkin axis negatively regulates necroptosis and tumorigenesis by inhibiting the necrosome. *Nat Cell Biol* 2019;21:940–51.
 225. Mevissen TET, Komander D. Mechanisms of deubiquitinase specificity and regulation. *Annu Rev Biochem* 2017;86:159–92.
 226. Zhang F, Zhao Y, Sun Y. USP2 is an SKP2 deubiquitylase that stabilizes both SKP2 and its substrates. *J Biol Chem* 2021;297:101109.
 227. He J, Lee HJ, Saha S, Ruan D, Guo H, Chan CH. Inhibition of USP2 eliminates cancer stem cells and enhances TNBC responsiveness to chemotherapy. *Cell Death Dis* 2019;10:285.
 228. Stevenson LF, Sparks A, Allende-Vega N, Xirodimas DP, Lane DP, Saville MK. The deubiquitinating enzyme USP2a regulates the p53 pathway by targeting Mdm2. *EMBO J* 2007;26:976–86.
 229. Allende-Vega N, Sparks A, Lane DP, Saville MK. MdmX is a substrate for the deubiquitinating enzyme USP2a. *Oncogene* 2010;29:432–41.
 230. Zhao Y, Wang X, Wang Q, Deng Y, Li K, Zhang M, et al. USP2a supports metastasis by tuning TGF-beta signaling. *Cell Rep* 2018;22:2442–54.
 231. Graner E, Tang D, Rossi S, Baron A, Migita T, Weinstein LJ, et al. The isopeptidase USP2a regulates the stability of fatty acid synthase in prostate cancer. *Cancer Cell* 2004;5:253–61.
 232. Wang Z, Kang W, Li O, Qi F, Wang J, You Y, et al. Abrogation of USP7 is an alternative strategy to downregulate PD-L1 and sensitize gastric cancer cells to T cells killing. *Acta Pharm Sin B* 2021;11:694–707.
 233. Shan J, Zhao W, Gu W. Suppression of cancer cell growth by promoting cyclin D1 degradation. *Mol Cell* 2009;36:469–76.
 234. Zheng N, Chu M, Lin M, He Y, Wang Z. USP7 stabilizes EZH2 and enhances cancer malignant progression. *Am J Cancer Res* 2020;10:299–313.
 235. Wang Q, Ma S, Song N, Li X, Liu L, Yang S, et al. Stabilization of histone demethylase PHF8 by USP7 promotes breast carcinogenesis. *J Clin Invest* 2016;126:2205–20.
 236. Li M, Brooks CL, Kon N, Gu W. A dynamic role of HAUSP in the p53–Mdm2 pathway. *Mol Cell* 2004;13:879–86.
 237. Yi L, Cui Y, Xu Q, Jiang Y. Stabilization of LSD1 by deubiquitinating enzyme USP7 promotes glioblastoma cell tumorigenesis and metastasis through suppression of the p53 signaling pathway. *Oncol Rep* 2016;36:2935–45.
 238. Novellasdemunt L, Foglizzo V, Cuadrado L, Antas P, Kucharska A, Encheva V, et al. USP7 is a tumor-specific WNT activator for APC-mutated colorectal cancer by mediating beta-catenin deubiquitination. *Cell Rep* 2017;21:612–27.
 239. Cheng J, Yang H, Fang J, Ma L, Gong R, Wang P, et al. Molecular mechanism for USP7-mediated DNMT1 stabilization by acetylation. *Nat Commun* 2015;6:7023.
 240. Du Z, Song J, Wang Y, Zhao Y, Guda K, Yang S, et al. DNMT1 stability is regulated by proteins coordinating deubiquitination and acetylation-driven ubiquitination. *Sci Signal* 2010;3:ra80.
 241. Watanabe K, Yokoyama S, Kaneto N, Hori T, Iwakami Y, Kato S, et al. COP9 signalosome subunit 5 regulates cancer metastasis by deubiquitinating SNAIL. *Oncotarget* 2018;9:20670–80.
 242. Zhang S, Hong Z, Chai Y, Liu Z, Du Y, Li Q, et al. CSN5 promotes renal cell carcinoma metastasis and EMT by inhibiting ZEB1 degradation. *Biochem Biophys Res Commun* 2017;488:101–8.
 243. Li J, Li Y, Wang B, Ma Y, Chen P. CSN5/Jab1 facilitates non-small cell lung cancer cell growth through stabilizing survivin. *Biochem Biophys Res Commun* 2018;500:132–8.
 244. Mao L, Le S, Jin X, Liu G, Chen J, Hu J. CSN5 promotes the invasion and metastasis of pancreatic cancer by stabilization of FOXM1. *Exp Cell Res* 2019;374:274–81.
 245. Lim SO, Li CW, Xia W, Cha JH, Chan LC, Wu Y, et al. Deubiquitination and stabilization of PD-L1 by CSN5. *Cancer Cell* 2016;30:925–39.

246. Tauriello DV, Haeghebaert A, Kuper I, Edelmann MJ, Henraat M, Cannings-van Dijk MR, et al. Loss of the tumor suppressor CYLD enhances Wnt/beta-catenin signaling through K63-linked ubiquitination of Dvl. *Mol Cell* 2010;37:607–19.
247. Shinriki S, Jono H, Maeshiro M, Nakamura T, Guo J, Li JD, et al. Loss of CYLD promotes cell invasion via ALK5 stabilization in oral squamous cell carcinoma. *J Pathol* 2018;244:367–79.
248. Zhang Z, Fan Y, Xie F, Zhou H, Jin K, Shao L, et al. Breast cancer metastasis suppressor OTUD1 deubiquitinates SMAD7. *Nat Commun* 2017;8:2116.
249. Piao S, Pei HZ, Huang B, Baek SH. Ovarian tumor domain-containing protein 1 deubiquitinates and stabilizes p53. *Cell Signal* 2017;33:22–9.
250. Yuan L, Lv Y, Li H, Gao H, Song S, Zhang Y, et al. Deubiquitylase OTUD3 regulates PTEN stability and suppresses tumorigenesis. *Nat Cell Biol* 2015;17:1169–81.
251. Du T, Li H, Fan Y, Yuan L, Guo X, Zhu Q, et al. The deubiquitylase OTUD3 stabilizes GRP78 and promotes lung tumorigenesis. *Nat Commun* 2019;10:2914.
252. Yuan J, Luo K, Zhang L, Cheville JC, Lou Z. USP10 regulates p53 localization and stability by deubiquitinating p53. *Cell* 2010;140:384–96.
253. Sun J, Li T, Zhao Y, Huang L, Sun H, Wu H, et al. USP10 inhibits lung cancer cell growth and invasion by upregulating PTEN. *Mol Cell Biochem* 2018;441:1–7.
254. Wang X, Xia S, Li H, Wang X, Li C, Chao Y, et al. The deubiquitinase USP10 regulates KLF4 stability and suppresses lung tumorigenesis. *Cell Death Differ* 2020;27:1747–64.
255. Lin Z, Yang H, Tan C, Li J, Liu Z, Quan Q, et al. USP10 antagonizes c-Myc transcriptional activation through SIRT6 stabilization to suppress tumor formation. *Cell Rep* 2013;5:1639–49.
256. Weisberg EL, Schauer NJ, Yang J, Lamberto I, Doherty L, Bhatt S, et al. Inhibition of USP10 induces degradation of oncogenic FLT3. *Nat Chem Biol* 2017;13:1207–15.
257. Liao Y, Liu N, Xia X, Guo Z, Li Y, Jiang L, et al. USP10 modulates the SKP2/Bcr-Abl axis via stabilizing SKP2 in chronic myeloid leukemia. *Cell Discov* 2019;5:24.
258. Zhu H, Yan F, Yuan T, Qian M, Zhou T, Dai X, et al. USP10 promotes proliferation of hepatocellular carcinoma by deubiquitinating and stabilizing YAP/TAZ. *Cancer Res* 2020;80:2204–16.
259. Lu C, Ning Z, Wang A, Chen D, Liu X, Xia T, et al. USP10 suppresses tumor progression by inhibiting mTOR activation in hepatocellular carcinoma. *Cancer Lett* 2018;436:139–48.
260. Chandrashekhar DS, Karthikeyan SK, Korla PK, Patel H, Shovon AR, Athar M, et al. UALCAN: an update to the integrated cancer data analysis platform. *Neoplasia* 2022;25:18–27.
261. Chandrashekhar DS, Bashel B, Balasubramanya SAH, Creighton CJ, Ponce-Rodriguez I, Chakravarthi B, et al. UALCAN: a portal for facilitating tumor subgroup gene expression and survival analyses. *Neoplasia* 2017;19:649–58.
262. Majeed S, Aparnathi MK, Nixon KCJ, Venkatasubramanian V, Rahman F, Song L, et al. Targeting the ubiquitin-proteasome system using the UBA1 inhibitor TAK-243 is a potential therapeutic strategy for small-cell lung cancer. *Clin Cancer Res* 2022;28:1966–78.
263. Best S, Hashiguchi T, Kittai A, Bruss N, Paiva C, Okada C, et al. Targeting ubiquitin-activating enzyme induces ER stress-mediated apoptosis in B-cell lymphoma cells. *Blood Adv* 2019;3:51–62.
264. Barghout SH, Aman A, Nouri K, Blatman Z, Arevalo K, Thomas GE, et al. A genome-wide CRISPR/Cas9 screen in acute myeloid leukemia cells identifies regulators of TAK-243 sensitivity. *JCI Insight* 2021;6:e141518.
265. Shan Y, Yang G, Huang H, Zhou Y, Hu X, Lu Q, et al. Ubiquitin-like modifier activating enzyme 1 as a novel diagnostic and prognostic indicator that correlates with ferroptosis and the malignant phenotypes of liver cancer cells. *Front Oncol* 2020;10:592413.
266. Zhuang J, Shirazi F, Singh RK, Kuiatse I, Wang H, Lee HC, et al. Ubiquitin-activating enzyme inhibition induces an unfolded protein response and overcomes drug resistance in myeloma. *Blood* 2019;133:1572–84.
267. Kim SJ, Hyoeng Lee T, Hee Nam S, Kim JH, Oh S, Sook Cho Y, et al. Association of Uba6-specific-E2 (USE1) with lung tumorigenesis. *J Natl Cancer Inst* 2017;109:1–11.
268. Osoegawa A, Yoshino I, Tanaka S, Sugio K, Kameyama T, Yamaguchi M, et al. Regulation of p27 by S-phase kinase-associated protein 2 is associated with aggressiveness in non-small-cell lung cancer. *J Clin Oncol* 2004;22:4165–73.
269. Richter KT, Kschonsak YT, Vodickska B, Hoffmann I. FBXO45-MYCBP2 regulates mitotic cell fate by targeting FBXW7 for degradation. *Cell Death Differ* 2020;27:758–72.
270. Schweiggert J, Habeck G, Hess S, Mikus F, Beloshistov R, Meese K, et al. SCF^{Fbxw5} targets kinesin-13 proteins to facilitate ciliogenesis. *EMBO J* 2021;40:e107735.
271. Yao Y, Liu Z, Huang S, Huang C, Cao Y, Li L, et al. The E3 ubiquitin ligase, FBXW5, promotes the migration and invasion of gastric cancer through the dysregulation of the Hippo pathway. *Cell Death Dis* 2022;8:79.
272. Yang F, Xu J, Li H, Tan M, Xiong X, Sun Y. FBXW2 suppresses migration and invasion of lung cancer cells via promoting beta-catenin ubiquitylation and degradation. *Nat Commun* 2019;10:1382.
273. Shimizu K, Nihira NT, Inuzuka H, Wei W. Physiological functions of FBXW7 in cancer and metabolism. *Cell Signal* 2018;46:15–22.
274. Wilkinson KD, Smith SE, O'Connor L, Sternberg E, Taggart JJ, Berge DA, et al. A specific inhibitor of the ubiquitin activating enzyme: synthesis and characterization of adenosyl-phospho-ubiquitinol, a nonhydrolyzable ubiquitin adenylate analogue. *Biochemistry* 1990;29:7373–80.
275. Yu Q, Jiang Y, Sun Y. Anticancer drug discovery by targeting cullin neddylation. *Acta Pharm Sin B* 2020;10:746–65.
276. Soucy TA, Smith PG, Milhollen MA, Berger AJ, Gavin JM, Adhikari S, et al. An inhibitor of NEDD8-activating enzyme as a new approach to treat cancer. *Nature* 2009;458:732–6.
277. Brownell JE, Sintchak MD, Gavin JM, Liao H, Buzzese FJ, Bump NJ, et al. Substrate-assisted inhibition of ubiquitin-like protein-activating enzymes: the NEDD8 E1 inhibitor MLN4924 forms a NEDD8-AMP mimetic *in situ*. *Mol Cell* 2010;37:102–11.
278. Chen JJ, Tsu CA, Gavin JM, Milhollen MA, Buzzese FJ, Mallender WD, et al. Mechanistic studies of substrate-assisted inhibition of ubiquitin-activating enzyme by adenosine sulfamate analogues. *J Biol Chem* 2011;286:40867–77.
279. Langston SP, Grossman S, England D, Afroze R, Bence N, Bowman D, et al. Discovery of TAK-981, a first-in-class inhibitor of SUMO-activating enzyme for the treatment of cancer. *J Med Chem* 2021;64:2501–20.
280. Ceccarelli DF, Tang X, Pelletier B, Orlicky S, Xie W, Plantevin V, et al. An allosteric inhibitor of the human Cdc34 ubiquitin-conjugating enzyme. *Cell* 2011;145:1075–87.
281. Huang H, Ceccarelli DF, Orlicky S, St-Cyr DJ, Ziemb A, Garg P, et al. E2 enzyme inhibition by stabilization of a low-affinity interface with ubiquitin. *Nat Chem Biol* 2014;10:156–63.
282. Tsukamoto S. Search for inhibitors of the ubiquitin-proteasome system from natural sources for cancer therapy. *Chem Pharm Bull (Tokyo)* 2016;64:112–8.
283. Kim YS, Nagy K, Keyser S, Schneekloth Jr JS. An electrophoretic mobility shift assay identifies a mechanistically unique inhibitor of protein sumoylation. *Chem Biol* 2013;20:604–13.
284. Blaquierre N, Villemure E, Staben ST. Medicinal chemistry of inhibiting RING-type E3 ubiquitin ligases. *J Med Chem* 2020;63:7957–85.
285. Duran-Frigola M, Cigler M, Winter GE. Advancing targeted protein degradation via multiomics profiling and artificial intelligence. *J Am Chem Soc* 2023;145:2711–32.
286. Chamberlain PP, Hamann LG. Development of targeted protein degradation therapeutics. *Nat Chem Biol* 2019;15:937–44.
287. Wang Y, Jiang X, Feng F, Liu W, Sun H. Degradation of proteins by PROTACs and other strategies. *Acta Pharm Sin B* 2020;10:207–38.

288. Li Z, Lin Y, Song H, Qin X, Yu Z, Zhang Z, et al. First small-molecule PROTACs for G protein-coupled receptors: inducing α_1A -adrenergic receptor degradation. *Acta Pharm Sin B* 2020;10:1669–79.
289. Lu B, Ye J. Commentary: PROTACs make undruggable targets druggable: challenge and opportunity. *Acta Pharm Sin B* 2021;11:3335–6.
290. Diehl CJ, Ciulli A. Discovery of small molecule ligands for the von Hippel-Lindau (VHL) E3 ligase and their use as inhibitors and PROTAC degraders. *Chem Soc Rev* 2022;51:8216–57.
291. He S, Ma J, Fang Y, Liu Y, Wu S, Dong G, et al. Homo-PROTAC mediated suicide of MDM2 to treat non-small cell lung cancer. *Acta Pharm Sin B* 2021;11:1617–28.
292. Luo G, Li Z, Lin X, Li X, Chen Y, Xi K, et al. Discovery of an orally active VHL-recruiting PROTAC that achieves robust HMGCR degradation and potent hypolipidemic activity *in vivo*. *Acta Pharm Sin B* 2021;11:1300–14.
293. Chan CH, Morrow JK, Li CF, Gao Y, Jin G, Moten A, et al. Pharmacological inactivation of Skp2 SCF ubiquitin ligase restricts cancer stem cell traits and cancer progression. *Cell* 2013;154:556–68.
294. Wu L, Grigoryan AV, Li Y, Hao B, Pagano M, Cardozo TJ. Specific small molecule inhibitors of Skp2-mediated p27 degradation. *Chem Biol* 2012;19:1515–24.
295. Hon WC, Wilson MI, Harlos K, Claridge TD, Schofield CJ, Pugh CW, et al. Structural basis for the recognition of hydroxyproline in HIF-1 alpha by pVHL. *Nature* 2002;417:975–8.
296. Min JH, Yang H, Ivan M, Gertler F, Kaelin Jr WG, Pavletich NP. Structure of an HIF-1alpha-pVHL complex: hydroxyproline recognition in signaling. *Science* 2002;296:1886–9.
297. Buckley DL, Van Molle I, Gareiss PC, Tae HS, Michel J, Noblin DJ, et al. Targeting the von Hippel-Lindau E3 ubiquitin ligase using small molecules to disrupt the VHL/HIF-1alpha interaction. *J Am Chem Soc* 2012;134:4465–8.
298. Buckley DL, Gustafson JL, Van Molle I, Roth AG, Tae HS, Gareiss PC, et al. Small-molecule inhibitors of the interaction between the E3 ligase VHL and HIF1alpha. *Angew Chem Int Ed Engl* 2012;51:11463–7.
299. Soares P, Gadd MS, Frost J, Galdeano C, Ellis L, Epemolu O, et al. Group-based optimization of potent and cell-active inhibitors of the von Hippel-Lindau (VHL) E3 ubiquitin ligase: structure–activity relationships leading to the chemical probe (2S,4R)-1-((S)-2-(1-cyanocyclopropanecarboxamido)-3,3-dimethylbutanoyl)-4-hydroxy-N-(4-(4-methylthiazol-5-yl)benzyl)pyrrolidine-2-carboxamide (VH298). *J Med Chem* 2018;61:599–618.
300. Maniaci C, Hughes SJ, Testa A, Chen W, Lamont DJ, Rocha S, et al. Homo-PROTACs: bivalent small-molecule dimerizers of the VHL E3 ubiquitin ligase to induce self-degradation. *Nat Commun* 2017;8:830.
301. Ma B, Lucas B, Capacci A, Lin EY, Jones JH, Dechantsreiter M, et al. Design, synthesis and identification of novel, orally bioavailable non-covalent Nrf2 activators. *Bioorg Med Chem Lett* 2020;30:126852.
302. Cleasby A, Yon J, Day PJ, Richardson C, Tickle JJ, Williams PA, et al. Structure of the BTB domain of Keap1 and its interaction with the triterpenoid antagonist CDDO. *PLoS One* 2014;9:e98896.
303. Hu L, Magesh S, Chen L, Wang L, Lewis TA, Chen Y, et al. Discovery of a small-molecule inhibitor and cellular probe of Keap1–Nrf2 protein–protein interaction. *Bioorg Med Chem Lett* 2013;23:3039–43.
304. Jiang ZY, Lu MC, Xu LL, Yang TT, Xi MY, Xu XL, et al. Discovery of potent Keap1–Nrf2 protein–protein interaction inhibitor based on molecular binding determinants analysis. *J Med Chem* 2014;57:2736–45.
305. Heightman TD, Callahan JF, Chiarparin E, Coyle JE, Griffiths-Jones C, Lakdawala AS, et al. Structure–activity and structure-conformation relationships of aryl propionic acid inhibitors of the Kelch-like ECH-associated protein 1/nuclear factor erythroid 2-related factor 2 (KEAP1/NRF2) protein–protein interaction. *J Med Chem* 2019;62:4683–702.
306. Pintard L, Willis JH, Willems A, Johnson JL, Srivastava M, Kurz T, et al. The BTB protein MEL-26 is a substrate-specific adaptor of the CUL-3 ubiquitin-ligase. *Nature* 2003;425:311–6.
307. Zhuang M, Calabrese MF, Liu J, Waddell MB, Nourse A, Hammel M, et al. Structures of SPOP-substrate complexes: insights into molecular architectures of BTB-Cul3 ubiquitin ligases. *Mol Cell* 2009;36:39–50.
308. Dong Z, Wang Z, Guo ZQ, Gong S, Zhang T, Liu J, et al. Correction to structure–activity relationship of SPOP inhibitors against kidney cancer. *J Med Chem* 2021;64:905.
309. Guo ZQ, Zheng T, Chen B, Luo C, Ouyang S, Gong S, et al. Small-molecule targeting of E3 ligase adaptor SPOP in kidney cancer. *Cancer Cell* 2016;30:474–84.
310. Lopez J, John SW, Tenev T, Rautureau GJ, Hinds MG, Francalanci F, et al. CARD-mediated autoinhibition of cIAP1's E3 ligase activity suppresses cell proliferation and migration. *Mol Cell* 2011;42:569–83.
311. Varfolomeev E, Blankenship JW, Wayson SM, Fedorova AV, Kayagaki N, Garg P, et al. IAP antagonists induce autoubiquitination of c-IAPs, NF-kappaB activation, and TNFalpha-dependent apoptosis. *Cell* 2007;131:669–81.
312. Du C, Fang M, Li Y, Li L, Wang X. Smac, a mitochondrial protein that promotes cytochrome c-dependent caspase activation by eliminating IAP inhibition. *Cell* 2000;102:33–42.
313. Wu G, Chai J, Suber TL, Wu JW, Du C, Wang X, et al. Structural basis of IAP recognition by Smac/DIABLO. *Nature* 2000;408:1008–12.
314. Flygare JA, Beresini M, Budha N, Chan H, Chan IT, Cheeti S, et al. Discovery of a potent small-molecule antagonist of inhibitor of apoptosis (IAP) proteins and clinical candidate for the treatment of cancer (GDC-0152). *J Med Chem* 2012;55:4101–13.
315. Peng Y, Sun H, Nikolovska-Coleska Z, Qiu S, Yang CY, Lu J, et al. Potent, orally bioavailable diazabicyclic small-molecule mimetics of second mitochondria-derived activator of caspases. *J Med Chem* 2008;51:8158–62.
316. Baggio C, Gambini L, Udompholkul P, Salem AF, Aronson A, Dona A, et al. Design of potent pan-IAP and Lys-covalent XIAP selective inhibitors using a thermodynamics driven approach. *J Med Chem* 2018;61:6350–63.
317. Sun H, Nikolovska-Coleska Z, Lu J, Meagher JL, Yang CY, Qiu S, et al. Design, synthesis, and characterization of a potent, nonpeptide, cell-permeable, bivalent Smac mimetic that concurrently targets both the BIR2 and BIR3 domains in XIAP. *J Am Chem Soc* 2007;129:15279–94.
318. Eckelman BP, Salvesen GS, Scott FL. Human inhibitor of apoptosis proteins: why XIAP is the black sheep of the family. *EMBO Rep* 2006;7:988–94.
319. Li L, Thomas RM, Suzuki H, De Brabander JK, Wang X, Harran PG. A small molecule Smac mimic potentiates TRAIL- and TNFalpha-mediated cell death. *Science* 2004;305:1471–4.
320. Li N, Feng L, Han HQ, Yuan J, Qi XK, Lian YF, et al. A novel Smac mimetic APG-1387 demonstrates potent antitumor activity in nasopharyngeal carcinoma cells by inducing apoptosis. *Cancer Lett* 2016;381:14–22.
321. Condon SM, Mitsuuchi Y, Deng Y, LaPorte MG, Rippin SR, Haimowitz T, et al. Birinapant, a smac-mimetic with improved tolerability for the treatment of solid tumors and hematological malignancies. *J Med Chem* 2014;57:3666–77.
322. Johnson CN, Ahn JS, Buck IM, Chiarparin E, Day JEH, Hopkins A, et al. A fragment-derived clinical candidate for antagonism of X-linked and cellular inhibitor of apoptosis proteins: 1-(6-[4-fluorophenyl]methyl)-5-(hydroxymethyl)-3,3-dimethyl-1H,2H,3H-pyrrolo[3,2-b]pyridin-1-yl)-2-[(2R,5R)-5-methyl-2-((3R)-3-methylmorpholin-4-yl)methyl]piperazin-1-yl]ethan-1-one (ASTX660). *J Med Chem* 2018;61:7314–29.

323. Fang Y, Liao G, Yu B. Small-molecule MDM2/X inhibitors and PROTAC degraders for cancer therapy: advances and perspectives. *Acta Pharm Sin B* 2020;10:1253–78.
324. Vassilev LT, Vu BT, Graves B, Carvajal D, Podlaski F, Filipovic Z, et al. *In vivo* activation of the p53 pathway by small-molecule antagonists of MDM2. *Science* 2004;303:844–8.
325. Vu B, Wovkulich P, Pizzolato G, Lovey A, Ding Q, Jiang N, et al. Discovery of RG7112: a small-molecule MDM2 inhibitor in clinical development. *ACS Med Chem Lett* 2013;4:466–9.
326. Ding K, Lu Y, Nikolovska-Coleska Z, Qiu S, Ding Y, Gao W, et al. Structure-based design of potent non-peptide MDM2 inhibitors. *J Am Chem Soc* 2005;127:10130–1.
327. Aguilar A, Lu J, Liu L, Du D, Bernard D, McEachern D, et al. Discovery of 4-(3'R,4'S,5'R)-6''-chloro-4'-(3-chloro-2-fluorophenyl)-1'-ethyl-2''-oxodispiro[cyclohexane-1,2'-pyrrolidine-3',3''-indoline]-5'-carboxamido)bicyclo[2.2.2]octane-1-carboxylic acid (AA-115/APG-115): a potent and orally active murine double minute 2 (MDM2) inhibitor in clinical development. *J Med Chem* 2017;60:2819–39.
328. Wang S, Sun W, Zhao Y, McEachern D, Meaux I, Barriere C, et al. SAR405838: an optimized inhibitor of MDM2–p53 interaction that induces complete and durable tumor regression. *Cancer Res* 2014;74:5855–65.
329. Ishizawa J, Nakamaru K, Seki T, Tazaki K, Kojima K, Chachad D, et al. Predictive gene signatures determine tumor sensitivity to MDM2 inhibition. *Cancer Res* 2018;78:2721–31.
330. Chessari G, Hardcastle IR, Ahn JS, Anil B, Anscombe E, Bawn RH, et al. Structure-based design of potent and orally active isoindolinone inhibitors of MDM2–p53 protein–protein interaction. *J Med Chem* 2021;64:4071–88.
331. Sun D, Li Z, Rew Y, Gribble M, Bartberger MD, Beck HP, et al. Discovery of AMG 232, a potent, selective, and orally bioavailable MDM2–p53 inhibitor in clinical development. *J Med Chem* 2014;57:1454–72.
332. Gessier F, Kallen J, Jacoby E, Chene P, Stachyra-Valat T, Ruetz S, et al. Discovery of dihydroisoquinolinone derivatives as novel inhibitors of the p53–MDM2 interaction with a distinct binding mode. *Bioorg Med Chem Lett* 2015;25:3621–5.
333. Holzer P, Masuya K, Furet P, Kallen J, Valat-Stachyra T, Ferretti S, et al. Discovery of a dihydroisoquinolinone derivative (NVP-CGM097): a highly potent and selective MDM2 inhibitor undergoing phase 1 clinical trials in p53wt tumors. *J Med Chem* 2015;58:6348–58.
334. Yang Z, Sun Y, Ni Z, Yang C, Tong Y, Liu Y, et al. Merging PROTAC and molecular glue for degrading BTK and GSPT1 proteins concurrently. *Cell Res* 2021;31:1315–8.
335. Kozicka Z, Thoma NH. Haven't got a glue: protein surface variation for the design of molecular glue degraders. *Cell Chem Biol* 2021;28:1032–47.
336. Ito T, Ando H, Suzuki T, Ogura T, Hotta K, Imamura Y, et al. Identification of a primary target of thalidomide teratogenicity. *Science* 2010;327:1345–50.
337. Zhu YX, Braggio E, Shi CX, Bruins LA, Schmidt JE, Van Wier S, et al. Cereblon expression is required for the antimyeloma activity of lenalidomide and pomalidomide. *Blood* 2011;118:4771–9.
338. Kronke J, Udeshi ND, Narla A, Grauman P, Hurst SN, McConkey M, et al. Lenalidomide causes selective degradation of IKZF1 and IKZF3 in multiple myeloma cells. *Science* 2014;343:301–5.
339. Han T, Goralski M, Gaskell N, Capota E, Kim J, Ting TC, et al. Anticancer sulfonamides target splicing by inducing RBM39 degradation via recruitment to DCAF15. *Science* 2017;356:eaal3755.
340. Slabicki M, Kozicka Z, Petzold G, Li YD, Manojkumar M, Bunker RD, et al. The CDK inhibitor CR8 acts as a molecular glue degrader that depletes cyclin K. *Nature* 2020;585:293–7.
341. Lv L, Chen P, Cao L, Li Y, Zeng Z, Cui Y, et al. Discovery of a molecular glue promoting CDK12–DDB1 interaction to trigger cyclin K degradation. *Elife* 2020;9:e59994.
342. Mayor-Ruiz C, Bauer S, Brand M, Kozicka Z, Siklos M, Imrichova H, et al. Rational discovery of molecular glue degraders via scalable chemical profiling. *Nat Chem Biol* 2020;16:1199–207.
343. Spradlin JN, Hu X, Ward CC, Brittain SM, Jones MD, Ou L, et al. Harnessing the anti-cancer natural product nimbolide for targeted protein degradation. *Nat Chem Biol* 2019;15:747–55.
344. Henning NJ, Manford AG, Spradlin JN, Brittain SM, Zhang E, McKenna JM, et al. Discovery of a covalent FEM1B recruiter for targeted protein degradation applications. *J Am Chem Soc* 2022;144:701–8.
345. Backus KM, Correia BE, Lum KM, Forli S, Horning BD, Gonzalez-Paez GE, et al. Proteome-wide covalent ligand discovery in native biological systems. *Nature* 2016;534:570–4.
346. Chen J, Dexheimer TS, Ai Y, Liang Q, Villamil MA, Inglese J, et al. Selective and cell-active inhibitors of the USP1/UAF1 deubiquitinase complex reverse cisplatin resistance in non-small cell lung cancer cells. *Chem Biol* 2011;18:1390–400.
347. Mistry H, Hsieh G, Buhrlage SJ, Huang M, Park E, Cuny GD, et al. Small-molecule inhibitors of USP1 target ID1 degradation in leukemic cells. *Mol Cancer Therapeut* 2013;12:2651–62.
348. Liang Q, Dexheimer TS, Zhang P, Rosenthal AS, Villamil MA, You C, et al. A selective USP1–UAF1 inhibitor links deubiquitination to DNA damage responses. *Nat Chem Biol* 2014;10:298–304.
349. Dexheimer TS, Rosenthal AS, Luci DK, Liang Q, Villamil MA, Chen J, et al. Synthesis and structure-activity relationship studies of *N*-benzyl-2-phenylpyrimidin-4-amine derivatives as potent USP1/UAF1 deubiquitinase inhibitors with anticancer activity against nonsmall cell lung cancer. *J Med Chem* 2014;57:8099–110.
350. Ohayon S, Refua M, Hendler A, Aharoni A, Brik A. Harnessing the oxidation susceptibility of deubiquitinases for inhibition with small molecules. *Angew Chem Int Ed Engl* 2015;54:599–603.
351. Davis MI, Pragani R, Fox JT, Shen M, Parmar K, Gaudiano EF, et al. Small molecule inhibition of the ubiquitin-specific protease USP2 accelerates cyclin D1 degradation and leads to cell cycle arrest in colorectal cancer and mantle cell lymphoma models. *J Biol Chem* 2016;291:24628–40.
352. Magiera K, Tomala M, Kubica K, De Cesare V, Trost M, Zieba BJ, et al. Lithocholic acid hydroxyamide destabilizes Cyclin D1 and induces G0/G1 arrest by inhibiting deubiquitinase USP2a. *Cell Chem Biol* 2017;24:458–70. e18.
353. Tavana O, Gu W. Modulation of the p53/MDM2 interplay by HAUSP inhibitors. *J Mol Cell Biol* 2017;9:45–52.
354. Zhang L, Ye B, Chen Z, Chen ZS. Progress in the studies on the molecular mechanisms associated with multidrug resistance in cancers. *Acta Pharm Sin B* 2023;13:982–97.
355. Wu J, Kumar S, Wang F, Wang H, Chen L, Arsenault P, et al. Chemical approaches to intervening in ubiquitin specific protease 7 (USP7) function for oncology and immune oncology therapies. *J Med Chem* 2018;61:422–43.
356. Chauhan D, Tian Z, Nicholson B, Kumar KG, Zhou B, Carrasco R, et al. A small molecule inhibitor of ubiquitin-specific protease-7 induces apoptosis in multiple myeloma cells and overcomes bortezomib resistance. *Cancer Cell* 2012;22:345–58.
357. Lamberto I, Liu X, Seo HS, Schauer NJ, Iacob RE, Hu W, et al. Structure-guided development of a potent and selective non-covalent active-site inhibitor of USP7. *Cell Chem Biol* 2017;24:1490–500. e11.
358. Turnbull AP, Ioannidis S, Krajewski WW, Pinto-Fernandez A, Heride C, Martin ACL, et al. Molecular basis of USP7 inhibition by selective small-molecule inhibitors. *Nature* 2017;550:481–6.
359. Gavory G, O'Dowd CR, Helm MD, Flasz J, Arkoudis E, Dossang A, et al. Discovery and characterization of highly potent and selective allosteric USP7 inhibitors. *Nat Chem Biol* 2018;14:118–25.

360. Leger PR, Hu DX, Biannic B, Bui M, Han X, Karbarz E, et al. Discovery of potent, selective, and orally bioavailable inhibitors of USP7 with *in vivo* antitumor activity. *J Med Chem* 2020;63:5398–420.
361. Kategaya L, Di Lello P, Rouge L, Pastor R, Clark KR, Drummond J, et al. USP7 small-molecule inhibitors interfere with ubiquitin binding. *Nature* 2017;550:534–8.
362. Verma R, Aravind L, Oania R, McDonald WH, Yates JR 3rd, Koonin EV, et al. Role of Rpn11 metalloprotease in deubiquitination and degradation by the 26S proteasome. *Science* 2002;298:611–5.
363. Sherman DJ, Li J. Proteasome inhibitors: harnessing proteostasis to combat disease. *Molecules* 2020;25:671.
364. Li J, Yakushi T, Parlati F, Mackinnon AL, Perez C, Ma Y, et al. Capzimin is a potent and specific inhibitor of proteasome isopeptidase Rpn11. *Nat Chem Biol* 2017;13:486–93.
365. Li J, Zhang Y, Da Silva Sil Dos Santos B, Wang F, Ma Y, Perez C, et al. Epidithiodiketopiperazines inhibit protein degradation by targeting proteasome deubiquitinase Rpn11. *Cell Chem Biol* 2018;25:1350–8.e9.
366. Ward JA, Pinto-Fernandez A, Cornelissen L, Bonham S, Diaz-Saez L, Riant O, et al. Re-evaluating the mechanism of action of α,β -unsaturated carbonyl DUB inhibitors b-AP15 and VLX1570: a paradigmatic example of unspecific protein cross-linking with Michael acceptor motif-containing drugs. *J Med Chem* 2020;63:3756–62.